COMPARISON OF FACTOR OF SAFETY OBTAINED FROM LIMIT EQUILIBRIUM
METHODS WITH STRENGTH REDUCTION FACTORS IN FINITE ELEMENT MODELING

A THESIS SUBMITTED TO
THE GRADUATE SCHOOL OF NATURAL AND APPLIED SCIENCES
OF
MIDDLE EAST TECHNICAL UNIVERSITY

BY

VOLKAN ENGİN

IN PARTIAL FULFILLMENT OF THE REQUIREMENTS
FOR
THE DEGREE OF MASTER OF SCIENCE
IN
CIVIL ENGINEERING

FEBRUARY 2012

Approval of the thesis:

COMPARISON OF FACTOR OF SAFETY OBTAINED FROM LIMIT EQUILIBRIUM METHODS WITH STRENGTH REDUCTION FACTORS IN FINITE ELEMENT MODELING

submitted by **Volkan ENGİN** in partial fulfillment of the requirements for the degree of **Master of Science in Civil Engineering Department, Middle East Technical University** by,

Prof. Dr. Canan Özgen

Dean, Graduate School of **Natural and Applied Sciences**   _____

Prof.Dr. Güney ÖZCEBE

Head of Department, **Civil Engineering**   _____

Inst. Dr. N. Kartal TOKER

Supervisor, **Civil Engineering Dept., METU**   _____

Prof.Dr. Orhan EROL

Co-Supervisor, **Civil Engineering Dept., METU**   _____

Examining Committee Members:

Prof. Dr. Ufuk ERGUN

Civil Engineering Department, METU   _____

Instr. Dr. N. Kartal TOKER

Civil Engineering Department, METU   _____

Prof. Dr. Orhan EROL

Civil Engineering Department, METU   _____

Prof. Dr. Kemal Önder ÇETİN

Civil Engineering Department, METU   _____

Dr. Aslı Özkeskin ÇEVİK

SONAR Drilling & Geological Research Center   _____

Date : 08.02.2012

I hereby declare that all information in this document has been obtained and presented in accordance with academic rules and ethical conduct. I also declare that, as required by these rules and conduct, I have fully cited and referenced all material and results that are not original to this work.

Name, Last Name   :   Volkan Engin

Signature   :

ABSTRACT

COMPARISON OF FACTOR OF SAFETY OBTAINED FROM LIMIT EQUILIBRIUM METHODS WITH STRENGTH REDUCTION FACTORS IN FINITE ELEMENT MODELING

ENGİN, Volkan

M.Sc., Civil Engineering Department

Supervisor: Inst. Dr. N. Kartal TOKER

Co-Supervisor: Prof. Dr. Orhan EROL

February 2012, 122 pages

Designing with Limit Equilibrium Methods involve a factor of safety (FS) in order to maintain the stability and to keep the resisting structure away from limit state on the safe side. Finite Element Program (such as Plaxis) on the other hand, instead of an FS, reduces the shear strength of the soil by introducing a reduction factor that is applied to $\tan\phi$ & c values, resulting in different analysis results compared with Limit Equilibrium Methods results.

This study aims to associate $\tan\phi$ & c reduction factors with the FS value obtained from Limit Equilibrium Methods. The conventional value obtained by Limit Equilibrium Method will be assumed as the true FS, and $\tan\phi$ & c reduction factors will be correlated with this value. The expected result of this thesis is to obtain a relation or a factor between assumed true FS value obtained from Limit Equilibrium Methods and $\tan\phi$ & c reduction factors derived from the software model.

Keywords: safety factor, limit equilibrum, retaining walls, finite element

ÖZ

LİMİT DENGE METODU İLE ELDE EDİLEN GÜVENLİK KATSAYISININ SONLU ELEMANLAR YÖNTEMİNDE KULLANILAN DAYANIM AZALTMA KATSAYISI İLE KARŞILAŞTIRILMASI

ENGİN, Volkan

Yüksek Lisans, İnşaat Mühendisliği Bölümü

Tez Yöneticisi: Öğr. Gör. Dr. Kartal TOKER

Ortak Tez Yöneticisi: Prof. Dr. Orhan EROL

Şubat 2012, 122 sayfa

Limit Denge Yöntemleri dayanma yapısının stabilitesini sağlamak ve bu dayanma yapısını denge durumundan güvenli tarafta tutabilmek için tasarımda bir güvenlik katsayısı kullanırlar. Diğer yandan, Sonlu Elemanlar Programları (Plaxis vb.) genel bir güvenlik katsayısı kullanmak yerine, tanϕ & c değerlerine uygulanan bir azaltma katsayısı kullanırlar, bu da elde edilen sonuçların Limit Denge Yöntemlerinden elde edilen sonuçlarla farklılıklar göstermesine sebep olur.

Bu çalışmada Limit Denge Yöntemlerinden elde edilerek kullanılan klasik güvenlik katsayıları doğru kabul edilerek Sonlu Elemanlar Yöntemlerinde kullanılan tanϕ & c azaltma katsayıları ile aralarındaki farklılıklar araştırılacaktır. Bu tezden elde edilmesi beklenen sonuç bilgisayar modelinde kullanılan katsayılar ile Limit Denge Yöntemlerinde kullanılan güvenlik katsayıları arasında bir ilişki veya katsayı elde etmektir.

Anahtar Kelimeler: güvenlik katsayısı, limit denge, istinat duvarları, sonlu elemanlar

TO MY FAMILY,

ACKNOWLEDGEMENTS

I would hereby like to express my deepest gratitude to my advisor Inst. Dr. N. Kartal TOKER for his guidance, advice, criticism, encouragements, unlimited patience and positive attitude throughout the whole phases of this research. Without his valuable support, the completion of this study would be nearly impossible.

I am also thankful Prof. Dr. Orhan EROL for his valuable suggestions and comments.

I would sincerely like to thank to my family, Zerrin Engin and Korcan Engin, for their valuable support, enthusiasm and encouragement. It was them who motivated me at the very beginning and throughout the process.

To my little sister - angel, Yasemen Engin; beside all your help, support and trust in my success, I would like to thank you for your smile, it is the most valuable thing for me, and helps me to keep up even in the most troubled times.

Sincere thanks to all my friends and all the people that have helped me with this thesis.

TABLE OF CONTENTS

LIST OF FIGURES

LIST OF TABLES

LIST OF SYMBOLS

H: Retaining Height

D: Embedment Depth

ϕ: Internal Friction Angle

c_u: Undrained Shear Strength

E: Modulus of Elasticity

K_0: In Situ Lateral Earth Pressure Coefficient

K_a: Limiting Active Earth Pressure Coefficient

K_p: Limiting Passive Earth Pressure Coefficient

ϕ_w: Wall - Soil Interface Friction Angle

α : Inclination of Wall from Vertical

ß : Inclination of Ground Surface Above the Wall

z_p: Depth from Excavation Level to Rotational Point, "O"

x (z): Distance from Pile Toe to Rotational Point, "O"

R^2: Coefficient of Determination

LE: Limit Equilibrium

FEM: Finite Element Modeling

γ: Unit Weight of Soil

CHAPTER 1

INTRODUCTION

1.1 General

In todays developing world, increasing populations in metropolitan cities bring the need for complex solutions in geotechnical engineering problems, which results in high dependency to computer aided design (CAD) softwares because of rapid, accurate and feasible solutions compared to a conventional solution procedure followed by an engineer. As the softwares get more complex and closer to the real situation, most of the daily users' insight towards them decreases. Results derived from conventional solutions and software outputs need to be associated to each other in order to create a transition between these results.

One of the most common geotechnical fields that are involving these type of problems are retaining walls. Traditional analysis methods for these structures are presented in various codes. Also, these structures can be modelled with recent softwares using numerical modeling, results of which can be compared with traditional methods and correlations can be obtained between these two approaches.

An embedded retaining wall is a relatively thin geotechnical structure that is inserted into (steel sheet piles) or constructed in (reinforced concrete piles) the ground and designed to withstand forces due to soil surface elevation difference from one side to the other or due to dredging, backfilling, pore pressures and surcharges. The wall may withstand these forces either by passive earth pressures only (cantilever retaining walls) or in addition to passive earth pressures, structural supports such as anchors and struts may be used (anchored – propped retaining walls).

As requirements of design increase and become more sophisticated in modern engineering practice, the procedures that have been used for a long time (such as allowable stress design and load & resistance factor design) are being replaced with concepts that are

scientifically advanced and able to satisfy the needs (limit equilibrium concept for instance, serviceability limit state and ultimate limit state).

Today, numerous calculation methods for retaining walls exist from classical limit equilibrium methods (conventional methods of limit equilibrium; Serviceability Limit State and Ultimate Limit State with reference to Eurocode 7) to most developed numerical modelling methods (Reaction Modulus, Finite Differences or Finite Elements Methods).

PLAXIS is one of the most common geotechnical modelling softwares used in today's practice. It is a non-linear finite element computation software used for two or three dimensional analysis of deformation and stability in geotechnical engineering. In this thesis, PLAXIS is used for modeling the sections and obtain earth pressures in order to derive and compare FS values.

1.2   Research Goals

Classical limit equilibrium methods involve fully mobilized active and passive earth pressure diagrams (which, for most cases, can not be satisfied, i.e., soil can not reach to its limiting active and passive earth pressure values) with an FS value, resulting in oversafe designs compared with FS values obtained from numerical modeling methods. Aim of this study is to compare these FS values calculated and analysed for an embedded retaining wall from Limit Equilibrium Methods and 2D Finite Element Modeling, and finally, obtain relations between them.

1.3   Scope of Work

In this thesis, cantilever and single level strut supported retaining wall models are analyzed with various limit equilibrium methods provided in geotechnical codes (such as U.S.S. Steel Sheet Piling Design Manual and California Trenching and Shoring Manual) for various parameters such as retained height of the wall (H), internal friction angle (ϕ) and undrained shear strength (c_u). Also PLAXIS is used for deriving and developing FS values. In addition to safety factor provided by PLAXIS as ΣMsf, additional methodologies are developed involving outputs of numerical analysis, and presented for these models. In addition to the parameters mentioned above, Modulus of elasticity of soil (E) and soil model (Mohr-Coulomb Model & Hardening Soil Model) were varied in PLAXIS solutions as well. Range of models generated for these parameters are listed in tables 1.1 & 1.2.

Table 1. 1; Parameters used in analyses (height intervals are 1m)

Cohesionless Soil with Cantilever Wall				
ϕ	30˚	35˚	37.5˚	40˚
H	5m to 7m	5m to 8m	8m	5m to 10m
Cohesive Soil with Cantilever Wall				
c	50 kPa	75 kPa	100 kPa	150 kPa
H	6m to 10m	6m to 12m	6m to 12m	6m
Cohesionless Soil with Wall Supported by One Level of Struts				
ϕ	30˚	35˚	40˚	
H	8m to 12m	8m to 12m	8m to 12m	
Cohesive Soil with Wall Supported by One Level of Struts				
c	50 kPa	75 kPa	100 kPa	
H	8m to 12m	8m to 12m	8m to 12m	

Table 1. 2; Additional Parameters (Elasticity Modulus increments are 10Mpa)

Soil	H	c	ϕ	E
Cohesionless	5m	0kPa	35˚	30MPa to 60MPa
Cohesive	6m	50kPa	0˚	30MPa to 60MPa

FS values obtained from these analyses are compared and results are used in least squares fit regression to obtain correlations between these values whenever possible.

1.4 Outline of Thesis

In addition to information on some basic concepts such as retaining walls and earth pressures, Chapter 2 provides theoretical background on conventional limit equilibrium methods, definition of safety factor and how it changes with Eurocode 7. Also, some information about PLAXIS is presented with notes on modeling.

Chapter 3 describes the methodology used in calculating safety factors for each method. Developing limit equilibrium calculations of conventional solutions and derivation of safety factors from PLAXIS outputs are presented in this chapter.

Chapter 4 summarizes results obtained from calculations provided in chapter 3, and presents these results in a tabular form. Graphs corresponding to varying parameters are plotted and outputs are discussed regarding these parameters.

Chapter 5 presents the methodology used for correlating FS values calculated in chapter 3. Different curve fittings are explained with corresponding data sets, and resultant correlations are presented in a tabular form. Results obtained from correlations are discussed in this chapter as well.

In Chapter 6, results obtained in chapters 4 & 5 are briefly discussed and outcomes are presented. Also, how results obtained from this thesis can be applied in geotechnical problems is discussed and recommendations for future studies are suggested.

CHAPTER 2

THEORETICAL BACKGROUND

In this chapter, definitions of common geotechnical terms such as brief explanation of earth pressures and definition of FS are presented with reference to Code of Practice CP2, BS EN 1997-1:2004 (Eurocode 7) and CIRIA Report C580. Change in application of FS in Eurocode 7 is described and also, definition of Limit State according to Eurocode 7 and Serviceability & Ultimate Limit State descriptions are presented. Additionally, information on geotechnical finite element analysis software, PLAXIS, and its modules is provided.

2.1   Embedded Retaining Walls

In geotechnical applications, earth retaining structures are used for maintaining elevation differences of ground surface. In highly populated areas, excavating self supporting slopes is not possible most of the time because of lack of empty space around the construction site. It is inevitable to use retaining walls in such cases for vertical excavations.

Eurocode 7 divides retaining structures into 3 categories; gravity walls, embedded walls and composite retaining structures (see table 2.1 for retaining wall types). The definition of embedded retaining wall given in Eurocode 7 is as;

"Relatively thin walls of steel, reinforced concrete or timber, supported by anchorages, struts and/or passive earth pressure. The bending capacity of such walls plays a significant role in the support of the retained material while the role of the weight of the wall is insignificant. Examples of such walls include cantilever steel sheet pile walls, anchored or strutted steel or concrete sheet pile walls and diaphragm walls."

2.1.1   Cantilever Retaining Walls

A cantilever wall "is a sheet pile wall which derives its support solely through interaction with the surrounding soil" (Powrie, 2004), ie, only the net passive resistance below the

excavation depth prevents the cantilever wall from over turning. A cantilever wall should penetrate the soil enough to achieve equilibrium between soil loads and fixity of the toe (see 2.4.5 & 2.4.6, limit equilibrium concept for free and fixed earth support methods). Large penetration depths make this type of retaining walls economic only for relatively small heights.

Table 2. 1; Retaining Wall Types (CIRIA C580, 2003)
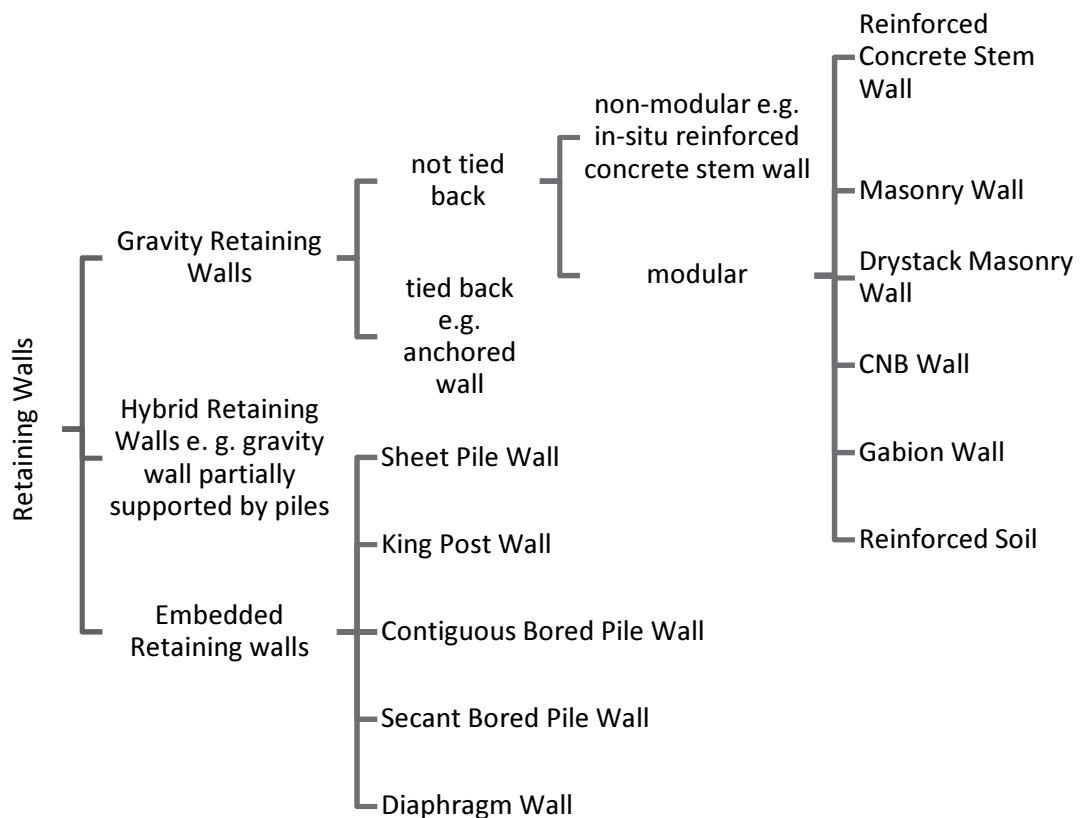
2.1.2 Strutted - Anchored Retaining Walls

These types of retaining walls are fixed at the base just like in cantilever walls but in addition to this fixity, added structural elements (such as struts or anchors) provide extra support and inhibit motion at a point on the wall. Support at pile toe may be analyzed with free or fixed earth support approaches.

For relatively higher retaining heights, these walls are more economical, allow shorter embedment depths and decrease maximum displacements, compared to cantilever walls.

2.2   Lateral Earth Pressures

Lateral Earth Pressures are the pressures that soil exerts on any structure below the ground level. Most of the retaining structures such as retaining walls, dams, tunnels etc. are subjected to lateral earth pressures. In order to determine the stresses on retaining walls due to lateral earth pressures, earth pressure coefficient, K, is used. Earth pressure coefficient is the ratio of horizontal stress to vertical stress in the soil, mostly in terms of effective stresses.

In situ lateral earth pressures are calculated with K value, while soil is in "at rest" conditions. An increase or a decrease in earth pressures (due to an excavation, loading etc.) results in changing of K from K_0 to its limiting values, K_a or K_p; active and passive earth pressure coefficients, respectively.

2.2.1   Concept

In 1776, Coulomb presented the Theory of Earth Pressure. According to Coulomb, in case of a vertical retaining wall, limit equilibrium conditions exist in the retained soil mass. Soil is expected to slide along a plane with an inclination (as a wedge) and the forces on this inclined plane are in a limiting equilibrium condition. Equation 2.1 below presents the formula of active lateral earth pressure coefficient of Coulomb, modified by Tschebotarioff.

$$K_a = \frac{\cos^2(\phi - \alpha)}{\cos^2\alpha * \cos(\phi_w + \alpha)[1 + \sqrt{\frac{(\sin(\phi + \phi_w)\sin(\phi - \beta)}{\cos(\phi_w + \alpha)\cos(\alpha - \beta)}}]^2} \qquad (2.1)$$

Where ϕ_w is the wall - soil interface friction angle (as defined by Coulomb), α is the inclination of wall from vertical, ß is the inclination of ground surface above the wall and ϕ is the angle of internal friction.

Rankine presented his earth pressure theory 80 years after Coulomb, considering that the soil mass is in plastic equilibrium. Static equilibrium of stresses is developed on the plane of failure. Equation 2.2 below is the formula of active lateral earth pressure coefficient presented by Rankine where ß is the inclination of ground surface above the wall and ϕ is the angle of internal friction.

$$K_a = \frac{\cos\beta - \sqrt{\cos^2\beta - \cos^2\phi}}{\cos\beta + \sqrt{\cos^2\beta - \cos^2\phi}}$$

<div align="right">(2.2)</div>

The difference between these two theories is that; solutions obtained by a limit equilibrium analysis, as in Coulomb's Theory, results in failure loads greater than the true failure load; leading to an unsafe solution (upper bound). On the other hand, analysis based on static stress equilibrium, as in Rankine's Theory, provides failure loads smaller than the true failure load; leading to a safe solution (lower bound).

Although Coulomb provides a more realistic model and provides more precise K_a values, addition of wall friction gives higher passive pressures. In order to avoid possible high passive pressure values, neglecting wall friction ($\phi_w=0$) would be appropriate. In engineering problems, for practical purposes, it is convenient to use Rankine's Earth Pressure equations.
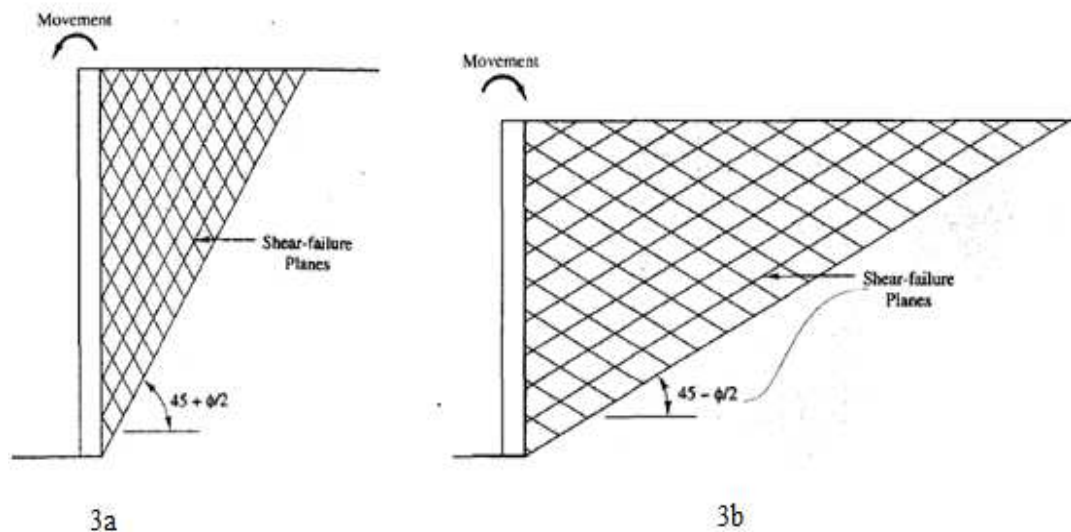
Figure 2. 1; Development of shear failure planes in the soil behind a wall as it transitions from the at-rest condition to the active Condition (3a) and Passive Condition (3b), (Coduto, 1998)

Common assumptions in the analysis of cohesionless and cohesive models, also adhered to in this thesis, are as follows; soil is homogeneous and isotropic (which means c, ϕ & γ have the same values everywhere), the most critical shear surface is a plane, the ground surface is horizontal, the wall is long enough that it can be analyzed for plane strain conditions, (ie., in two dimensions) and wall moves enough to generate active and passive conditions. The

active and passive shear surfaces to be used in shear calculations of cohesionless materials are shown in figure 2.1.

2.2.2   Drained Behavior of Cohesionless Soils

Coarse - grained (cohesionless) materials such as sands and gravels are sufficiently pervious materials, causing no development of excess pore pressures in case of changes in stress state as a result of an excavation. Their shear strength is calculated by the angle of internal friction ϕ, and given by the equation;
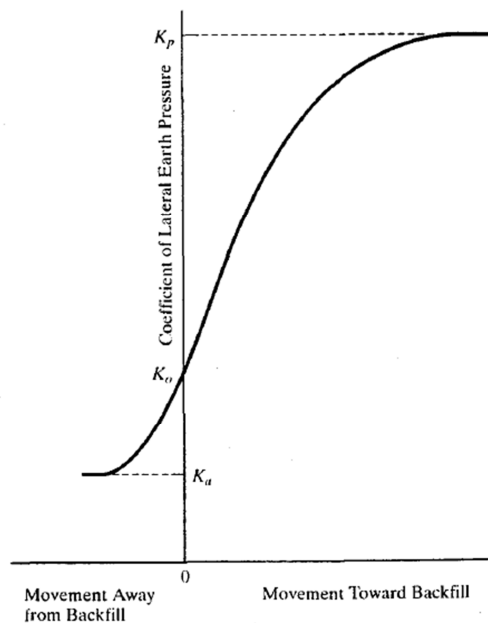
Figure 2. 2; Effect of wall movement on lateral earth pressure coefficient in sand (Coduto, 1998)

$$\tau' = \sigma' \tan \phi' \qquad (2.3)$$

"At-Rest Pressure is the horizontal in situ earth pressure when no displacement of soil occurs" (Powrie, 2004). In case of a retaining wall, before the excavation stage, pressures acting on sides of the wall in horizontal direction are calculated with lateral earth pressure coefficient, K_0. Eurocode suggests that at-rest conditions behind the retaining walls in normally consolidated soils when the horizontal movement of the wall is less than 0,05% of its retained height, is calculated as;

$$K_0 = (1 - \sin \phi) \qquad (2.4)$$

Where ϕ is the internal friction angle of soil.

"Active Earth Pressure is the limiting pressure between the wall and soil, produced when the relative wall/soil motion tends to allow the soil to expand horizontally" (Powrie, 2004). In case of an embedded retaining wall, as the wall starts rotating – translating into the excavated area, soil behind the wall relaxes and K_0 values decrease. The limiting value, K_a (for a horizontal retaining surface) of coefficient of lateral earth pressure is determined by Rankine's Theory as;

$$K_a = \frac{1-\sin\phi}{1+\sin\phi} = \tan^2(45-\frac{\phi}{2}) \qquad (2.5)$$

Figure 2. 3; Change of Active and Passive Lateral Earth Pressures with changing stress states (G. N. Smith & Ian G. N. Smith, 1998)

"Passive Earth Pressure is the limiting pressure between the wall and soil produced when the relative wall/soil motion tends to compress the soil horizontally" (Powrie, 2004). In case of an embedded retaining wall, after the excavation, soil on retained side pushes the wall toward the excavated side – causing increase of lateral earth pressure coefficient – lateral pressures in excavated side below the dredge level. Limiting value of coefficient of lateral earth pressure, K_p, (for a horizontal retaining surface) is calculated with Rankine's Theory as;

$$K_p = \frac{1+\sin\phi}{1-\sin\phi} = \tan^2(45+\frac{\phi}{2}) \qquad (2.6)$$

2.2.3 Undrained Behavior of Cohesive Soils

Fine-grained (cohesive) materials such as silts and clays have lower permeabilities, higher void ratios and their interaction between pore water & soil particles are less, compared to cohesionless materials. In case of an excavation, because of the lower permeability values, pore water is trapped in the soil body if enough time is not allowed for drainage; resulting in undrained behaviour of the soil in short period.

Strength of clay changes with time, so does the lateral earth pressures, accordingly. Immediately after the excavation, the strength of the clay is determined by its undrained strength, with no contribution from internal friction (ϕ = 0, K_a & K_p = 1). Immediately after the excavation, total stresses dominate the stability calculations, where undrained shear strength, c_u is equal to one half of the unconfined compressive strength, q_u. In long term, this conditions change; cohesion decreases to c' (in effective stress calculations, taken as 0 most of the time) and internal friction angle, ϕ, increases to 20 - 30˚. Therefore, an effective stress analysis is required with parameters ϕ' & c' for long term conditions.
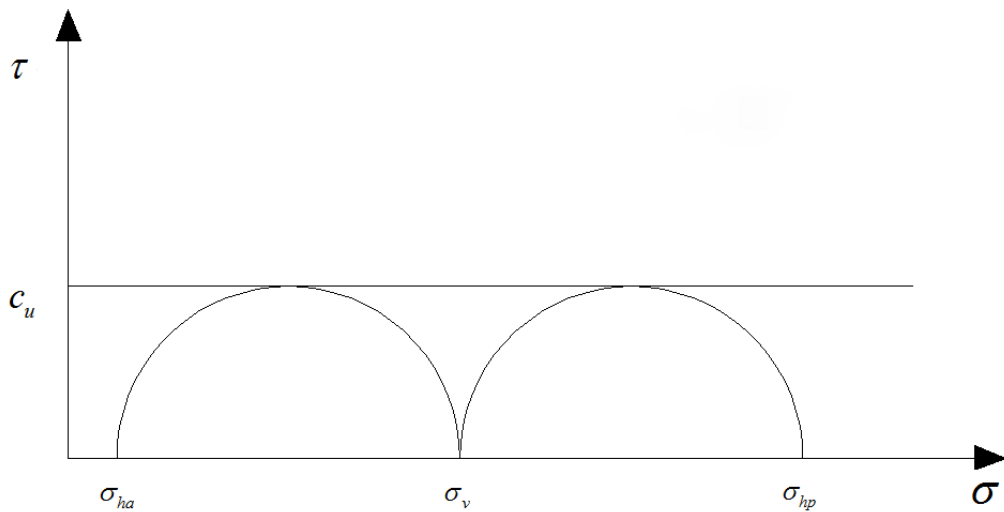
Figure 2. 4; Strength envelope showing active and passive failure

$$\sigma_{ha} = \sigma_v - 2c_u \qquad (2.7)$$

$$\sigma_{hp} = \sigma_v + 2c_u \qquad (2.8)$$

Figure 2.4 shows the undrained stress circles of a cohesive saturated soil in a triaxial test. It can be seen that, with no drainage allowed, ϕ_u = 0, the undrained shear strength of the soil

sample is c_u, σ_v is the vertical stress, σ_{ha} & σ_{hp} are the limiting stress states for active and passive conditions, respectively. Formulations of σ_{ha} & σ_{hp} are presented in equations 2.7 & 2.8.

In the analysis of cohesive models, short term - undrained conditions are investigated and undrained parameters, ie, ϕ_u = 0 and c_u are used in this thesis.

In case of an excavation, undrained conditions are expected initally after the excavation. Undrained conditions are more critical for fine silts and normally consolidated clays. Calculations regarding the undrained parameters are carried out considering this situation. But, after some time, depending on the nature of the soil, shear strength drops down with dissipating negative excess pore water pressure. Drained analysis should be carried out to determine the long term effects and the results of drained analysis may be more critical in excavations, especially for over-consolidated clays and clays with c_u is greater than about 40kPa (effective parameters may not compensate for the undrained strength).

2.3   Factor of Safety

2.3.1   Definition of Safety Factor

Factor of Safety (FS) is the ratio of restoring/resisting moments (or forces) to disturbing moments (or forces) in engineering problems. An appropriate factor is assigned so that the uncertainties including idealizations, approximations and assumptions in design can be compensated. With introduction of Eurocode 7, previous design methods (presented in codes such as Code of Practice, CP2; Earth Retaining Structures, 1951) are replaced with limit state approaches (see section 2.4.4 for Ultimate Limit State and Serviceability Limit State). This change resulted in change of methods regarding the way factor of safety is applied in design approaches.

2.3.2   FS in Traditional Methods

Traditional approaches involve application of an overall safety factor to the calculations in order to prevent the effects of all the unknowns (such as uncertainties in soil properties and loads, construction tolerances, unplanned excavation concept in Eurocode 7, ultimate

limit state design, differences between modelled and actual conditions of pressures etc.) in the design.

FS is applied in following ways;

- A scale factor applied to the depth of embedment, in order to prevent rotational failure, calculated from limit equilibrium methods (1.2-1.4 of calculated embedment depth)

- A reduction factor applied to the theoretical soil strengths

- A factor applied to obtain increased net or gross pressures

2.3.2.1 Working State Design (Allowable Stress Design, ASD)

Allowable Stress Design Method compares the actual stresses that design loads applied to the structure and allowable stress of the system; where allowable stress is the strength divided by the assigned safety factor.

2.3.2.2 Ultimate Strength Design

Load and Resistance Factor Design Method compares the required strength and actual strength. In other words, design loads are increased by load factors, then compared with ultimate load-bearing capacity.

2.3.2.3 Gross Pressure Method

In Gross Pressure Method (Code of Practice, CP2 Method, 1951), an FS value is applied to the area of passive resistance distribution in front of the wall to reduce the resisting passive pressure (figure 2.5b). For simplification of calculations, passive resistance below the rotational point can be taken as a point load (figure2.5d).

2.3.2.4 Net Available Passive Resistance Method

In Net Available Passive Resistance Method (Burland, Potts and Walsh, 1981), a modified pressure distribution is used and a safety factor is applied to the net available passive resistance (figure 2.5e).

(a) Wall geometry

(b) CP2: Theoretical pressure distribution

(c) BS 8002:1994 method

(d) CP2: Distribution assumed for design

(e) Net available passive resistance method

(f) Net total pressure method
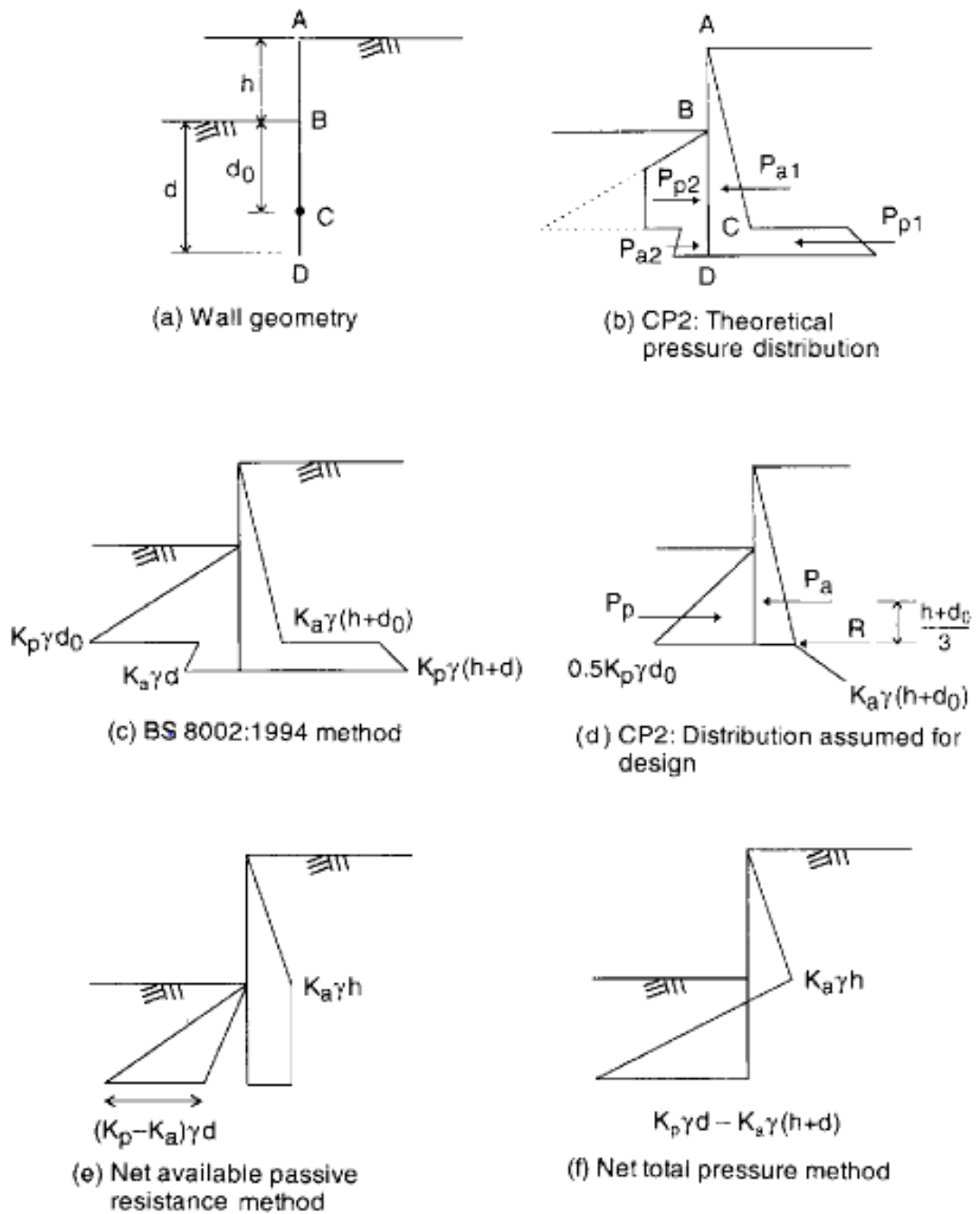
Figure 2. 5; Pressure Distribution on Sheet Pile Walls (Smith, 1998)

2.3.2.5   Strength Factor Method

Strength Factor Method uses the same pressure distribution with the Gross Pressure Method but the safety factor is applied not to the total passive force but to the parameters, c' & ϕ'. This method is used in conventional calculations in this thesis.

$$\tan\phi'_m = \frac{\tan\phi'}{FS} \tag{2.9}$$

$$c'_m = \frac{c'}{FS} \tag{2.10}$$

2.3.2.6 Net Total Pressure Method

In Net Total Pressure Method (used in British Steel Piling Handbook, 1997) factor of safety is applied to the net horizontal pressure distribution diagram which is obtained by subtracting active earth pressures from passive earth pressures at any depth (figure 2.5f).

2.3.3 Factor of Safety in Eurocode 7

In Eurocode 7, instead of an overall safety factor, a limit state design is introduced which involves partial factors applied to actions and ground properties (which is accepted by many of the National Standards such as BS 8002). Partial factors applied to various parameters (grouped as actions and ground properties, such as; loads, surcharges, unexpected excavations, soil properties etc.) enable increasing the unfavourable loads and decrease favourable loads.

Actions mentioned above are classified as shown in table 2.2 (permanent - dead loads, G and variable – imposed loads, Q). These actions include soil weight, stresses in the ground, surcharges, pore water pressures and seepage forces. Further more, unfavourable and favourable concept is added and design approaches with partial factors are considered. Drained and undrained soil strengths are separately factored. Table 2.3 presents the factors to be applied to the calculated values. (Design approaches are presented in 2.3.4)

Advantage of this method is to allow for effects of uncertainties in characteristic parameters individually. Also, in calculations stage, all the components of the analysis are factored by its own, the only task remaining for the engineer is to calculate the depth of embedment for stability.

2.3.4 Design Approaches in Eurocode 7

In EC7, there are 3 different sets of factors to be applied to actions, resistances and material properties. The reason for this is the countries' selection of method of approach in verification of strength; a load and material factor approach or load and resistance approach. Brief information on these approaches is given below, and table 2.3 presents the factors used in these design approaches.

2.3.4.1 Design Approach 1

DA1 is used for designing pile foundations and anchors, factors are applied to resistances instead of material properties. This category includes small and relative simple structures where ground conditions are known and straight forward methods may be used. Negligible risk for property and life is considered.

Partial factor set used in design approach 1/1 considers the effect of active earth pressures, by involving a partial factor of 1.35 in permanent unfavourable loads. Passive earth pressures (permanent favourable loads) are kept unfactored.

DA1/2 assigns the multipliers of permanent loads as 1.00 and applies partial factors to soil strength parameters. This set of partial factors suits well with phi-c reduction calculations in this study, considering models involving undrained clays, but not applicable to models involving drained sands.

<div align="center">Table 2. 2; Types of Actions in Eurocode 7</div>

Type of Action	Symbol	Examples
Permanent	G	Self weight of the structure and permanent loads, water pressure (under normal conditions)
Variable (live)	Q	Traffic, snow, wind, thermal load
Accidental	A	Accidental removal of a strut, impact, fire, seismic load

Table 2. 3; Factors Used in Design Approaches in Eurocode 7

	EC7 DA1/1	EC7 DA1/2	EC7 DA2	EC7 DA3
Permanent Unfavourable Load	1.35	1	1.35	1.0/1.35
Variable Unfavourable Load	1.5	1.3	1.5	1.0/1.5
Permanent Favourable Load	1	1	1	1
c'	1	1.25	1	1.25
$\tan\phi'$	1	1.25	1	1.25
c_u	1	1.4	1	1.4
Resistance	1	1	1.1/1.4	N/A

2.3.4.2 Design Approach 2

DA2 is used for checking foundation's reliability by applying partial factors to actions or action effects and to resistances simultaneously, while ground strengths are left unfactored (Bond & Harris, 2008). Design with this approach requires quantitative geotechnical data and analysis to check for fundamental requirements.

Design approach 2 involves partial factors that are applied to permanent favourable-unfavourable loads and resistances. Similar to DA1/1, factors are applied to passive earth pressures and soil strength parameters are kept constant in this approach.

2.3.4.3 Design Approach 3

In DA3, partial factors are applied to structural actions and material properties simultaneously, geotechnical actions and resistances are left unfactored. DA3 covers design of very large/unusual structures or components involving abnormal risks or unusual ground and loading conditions. Examples of such walls and other structures are; structures retaining/supporting soil or water, spread foundations, raft foundations, piled foundations, excavations, bridge piers, embankments & earth works, ground anchors & tie back systems.

DA3 considers the effects of variable unfavourable loads. Partial factors in DA3 are the same with DA1/2 for this study, since, models to be used are not subjected to these kind of loads.

2.4   Limit Equilibrium Concept

Limiting equilibrium methods are used in designing earth retaining structures to determine the required embedment depth, shear forces & bending moments in retaining wall cross sections and analyzing the stress distributions in collapse conditions (limiting criterion).

An understanding of limit state design can be obtained by comparing it with working state design as; working state design analyzes the expected situation, then applies the safety factors. On the other hand, limit state analyses the unexpected states at which the structure reaches its acceptable limit. Eurocode 7 moves away from working stresses concept and overall factor of safety understanding to limit state design approach, with partial factors. In other words, instead of calculating the collapse load and applying a safety factor, Eurocode 7 recommends to define Actions and Resistances, then check actions ≤ resistances, while applying partial factors to actions, resistances and material properties.

In this section, assumptions, failure modes and design methods for cantilever and one level strutted embedded walls considering limit equilibrium calculations are discussed with reference to manuals such as U.S.S. Steel Sheet Piling Design Manual, California Trenching and Shoring Manual and U.S. Army Corps of Engineers Design of Sheet Pile Walls Manual.

2.4.1   Assumptions

Assumptions are required in order to simplify the complex wall - soil system. The main assumption of limit equilibrium method solutions is that, soil reaches its limiting active and passive earth pressures. This assumption enables using of full passive and active diagrams, but in real situation, active pressures occur even at very little displacement, on the other hand, passive pressures require larger displacements.

A cantilever wall rotates as a rigid body about some point in its embedded length, implying that active pressures occur in retained side and passive pressures occur in excavated side; down to a point of rotation (where zero displacements occur). Below this transition point, passive pressures in retained side and active pressures in excavated side occur.

Another assumption is about displacements at strut – anchor level. It is assumed that struts prevent any displacement at that level, so that rotation occurs at strut level.

2.4.2   Failure Modes

US Army Corps of Engineers' Design of Sheet Pile Wall Manual (1994) classifies system stability failures of embedded retaining walls as;

Deep Seated Failure; This failure mode corresponds to failure of entire soil mass. In cohesive soils, failure of a model in this mode can not be prevented by increasing pile length or changing the position of the anchorage. Example of this failure mode is in figure 2.6.
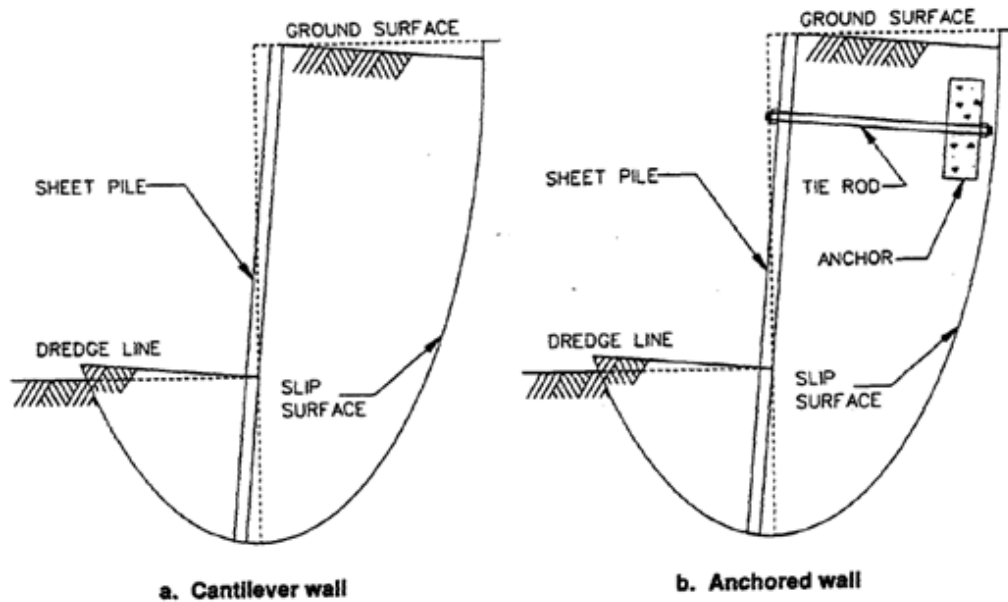
Figure 2. 6; Deep Seated Failure of; a. Cantilever Wall b. Anchored Wall (U.S. Army Corps of Engineers, 1994)

Rotational Failure; The reason for this type of failure is insufficient pile penetration depth. Active earth pressures exerted on the wall can not be compensated by passive earth pressures due to lack of embedment depth. Example of this failure mode is in figure 2.7.

Other failure modes may be due to failure of structural members, such as insufficient moment capacity reinforced concrete piles or tensile capacity of anchors. Examples of these type of failures are in figure 2.8. The structural members can be designed against this mode independently, so this mode is not within the scope of this thesis.
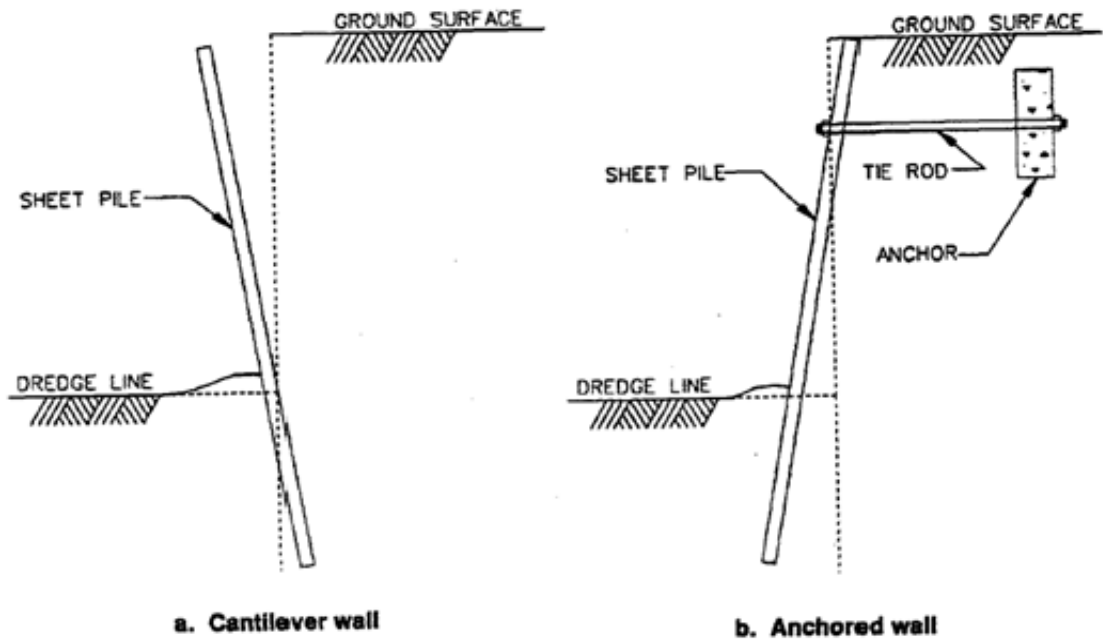
Figure 2. 7; Rotational Failure of; a. Cantilever Wall b. Anchored Wall (U.S. Army Corps of Engineers, 1994)
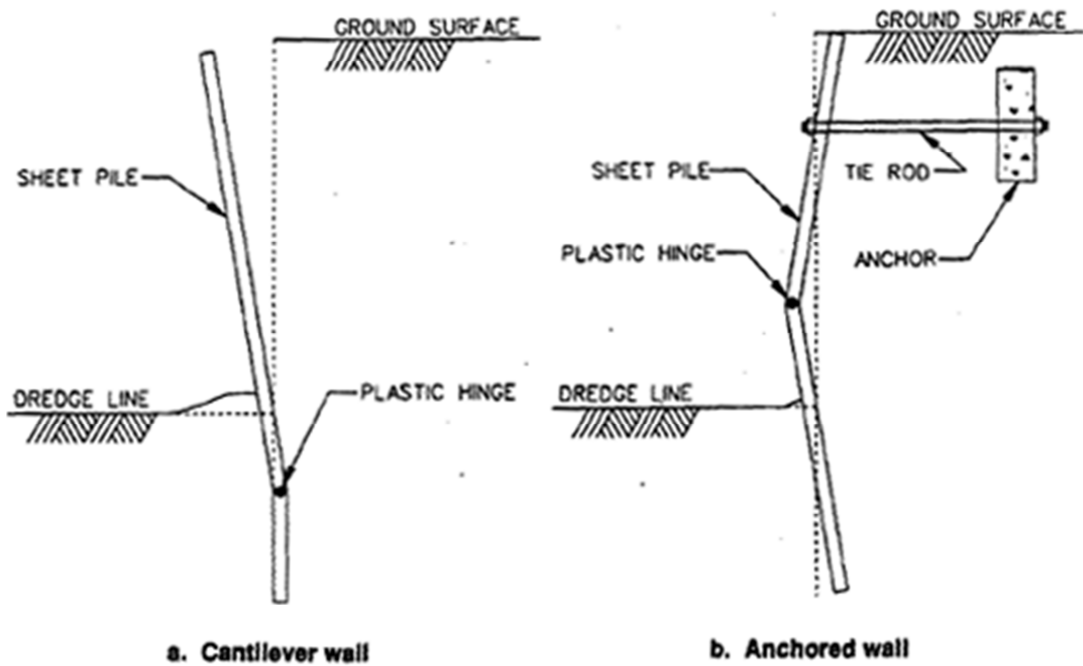
Figure 2. 8; Flexural Failure of; a. Cantilever Wall b. Anchored Wall (U.S. Army Corps of Engineers, 1994)

2.4.3 Design Basics

Sheet pile walls are flexible structures that allow displacement in soil; resulting in reaching limiting values of earth pressures. These structures satisfy equilibrium conditions with passive pressures in ground and/or with help of one or more rows of struts or anchors that provide some fixity. Unless there is a structural failure, the expected failure of an embedded cantilever retaining wall is as shown in figure 2.9a. As can be seen, for a cantilever wall with a depth of penetration d, rotation at a point z_p below the excavation level is expected. Limiting stress distribution consistent with this mode of collapse is illustrated in figure 2.9a following the approach of Bolton (1979). It can be seen that the unknowns d and z_p are determinable from the conditions of horizontal force and moment equilibrium. It is assumed that the materials are plastic and the lateral earth pressures in each zone of soil at failure are given by the active and passive limits.
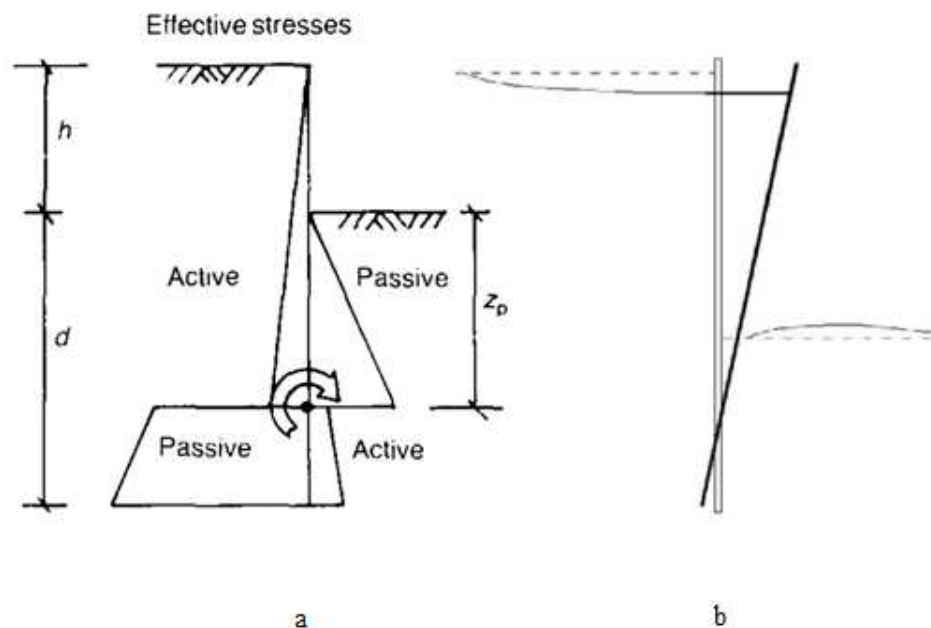
Figure 2. 9; a. Equilibrium Stress Distribution of a Cantilever Retaining Wall at Collapse (Bolton, 1979), b. Example of Failure Mechanism in Limit Mode for Rotational Failure of a Cantilever Embedded Retaining Wall (Sigström, 2010)

2.4.4   Design in Eurocode 7

According to Eurocode 7, limit states to be considered in designing a retaining structure can be listed as following for all types of retaining structures;

-         loss of overall stability,

-         failure of a structural element (such as a wall, anchor, wale or strut) or failure of the connection between such elements,

-         combined failure in ground and in structural element,

-         movements of the retaining structure which may cause collapse or affect the appearance or efficient use of the structure, nearby structures or services which rely on it,

-         unacceptable leakage through or beneath the wall,

-         unacceptable transport of soil grains through or beneath the wall,

-         unacceptable change in flow of groundwater.

In addition to above, the following limit states shall be considered for gravity retaining structures and for composite retaining structures;

-         bearing resistance failure of the soil below the base,

-         failure by sliding at the base of the wall,

-         failure by toppling of the wall,

and for embedded retaining structures;

-         failure by rotation or translation of the wall or parts thereof,

-         failure by lack of vertical equilibrium of the wall. (Eurocode 7)

Limit State definitions emphasized in Eurocode 7 are provided in table 2.4.

2.4.4.1   Ultimate Limit State

"Ultimate limit states are concerned with the safety of people and the structure. Examples of ultimate limit states include loss of equilibrium, excessive deformation, rupture, loss of stability, transformation of the structure into a mechanism, and fatigue." (Bond & Harris, 2008). In other words, safety of people and structure due to a major damage that can occur once in structure's life span, such as; loss of equilibrium, excessive translation and/or rotation of the wall, is the concern of this limit state principle.

Table 2. 4; Eurocode 7 Limit States Definitions, (Wallap Manual, 2010)

Limit State Acronym	Description	Relevant to Embedded Walls
EQU	Loss of equilibrium (eg. Toppling)	No
STR	Failure of structural members by excessive deformation, formation of a mechanism or rupture	Yes. Bending failure of walls. Tensile or pull-out failure of anchors. Strut failure
FAT	Fatigue or creep failure	Maybe. In very stiff clays with high K_0 values, active pressures which have relaxed during excavation may recover to K_0 levels in the long term.
GEO	Failure or excessive deformation of the ground	Yes. Active or passive failure of soil. Ground heave.
UPL	Loss of equilibrium due to uplift by water pressure	Yes
HYD	Hydraulic heave, internal erosion or piping due to hydraulic gradients	Yes

2.4.4.2   Serviceability Limit State

"Serviceability limit states are concerned with the functioning of the structure under normal use, the comfort of people, and the appearance of the construction works. Serviceability limit states may be reversible (e.g. deflection) or irreversible (e.g. yield)." (Bond & Harris, 2008) In other words, in this limit state principle, movement of the ground and deformations of the structure should remain within acceptable limits through life span of the structure, also, maintenance and durability conditions are concerned.

2.4.5   Free Earth Support Method

To design an embedded retaining wall, support conditions to be idealized at toe of the wall should be determined. Wall may be designed with either Free Earth Support Method or Fixed Earth Support Method.

In Free Earth Support Method, wall is considered to be a simply supported vertical beam; built deep enough into the ground in order to prevent horizontal movements, but free to rotate at its toe as if it is a pin support. The other support is provided by a strut or an anchorage near its top. This kind of design allows for shorter embedment depth with lower bending moments.

Free Earth Support Method assumes that rotation occurs at fixity level and displacements are enough to develop full active and passive pressures. Wall is free to rotate and move at its base.
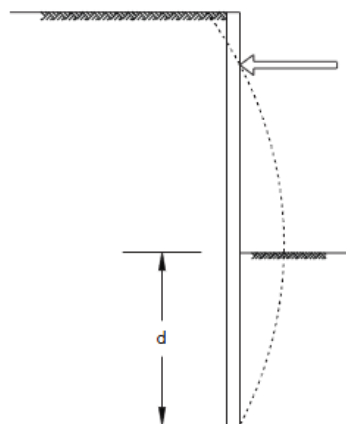
Figure 2. 10; Deflected shape of a one level strutted wall, idealized with free earth support method (Arcelor, 2005)

2.4.6   Fixed Earth Support Method

In Fixed Earth Support Method, wall is penetrated relatively deeper compared to the free earth support method. This brings rotational and lateral restriction to the toe of the wall. In other words, wall can not move or rotate at its toe and acts as a vertical cantilever beam with a pin support near its top. With this method, because of the fixed end, maximum

bending moments are lower compared to free earth support, but the wall length is increased.

The difference between free and fixed earth support method lies in the wall embedment length and bending moments. A cantilever wall requires more penetration depth to obtain equilibrium conditions compared to a retaining wall with a fixity (anchorage or strut) close to top of the wall. In analyses of cantilever retaining walls, fixed earth support method and in analyses of one level strutted retaining walls, free earth support method is used in this thesis.
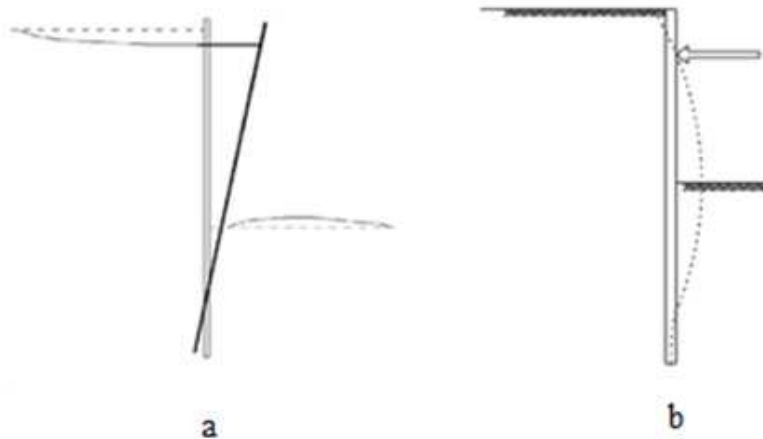
Figure 2. 11; a. Deflected shape of a cantilever wall (Sigström, 2010), b. Deflected shape of a one level strutted wall (Arcelor, 2005)

2.4.7 Cantilever Walls in Cohesionless Soils

In design of cantilever walls, fixed earth support method is used in manuals. Sufficient embedment depth provides a fixed support at the toe of the wall, enabling a rotation at a depth z_p from excavated ground surface level (see figure 2.9a). 2 unknowns, namely; z_p and d, are solved by moment and horizontal force equilibrium equations (Since these equations are non-linear, solution is obtained by trial and error procedure). Conventional pressure distribution is shown in figure 2.9a. As can be seen, above the rotational point z_p, active pressures generated on retained side and passive pressures in excavated side below the excavation level. However, below the rotational point, passive pressures are generated in retained side and active pressures are generated in excavated side due to the movement of soil.

In addition to the pressure diagram shown in figure 2.9a, a simplified pressure distribution can be used. In this pressure distribution, stresses below the level of rotational point are omitted and a force "C" is placed at bottom of the pile in order to replace the omitted forces (figure 2.12).
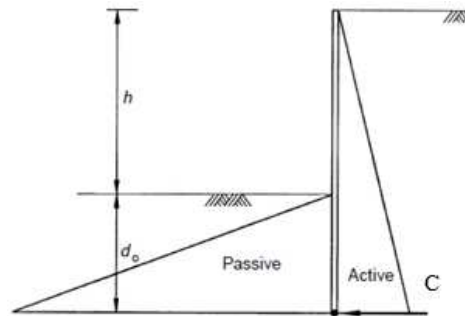
Figure 2. 12; Simplified pressure distribution of a cantilever wall (California Trenching and Shoring Manual, 1995)

This distribution is convenient for initial design of walls. After the calculations, the depth of embedment is increased by %20 to %40 in order to prevent rotation and horizontal movement. Both California Trenching and Shoring Manual and USS Steel Sheet Piling Manual applies this method.
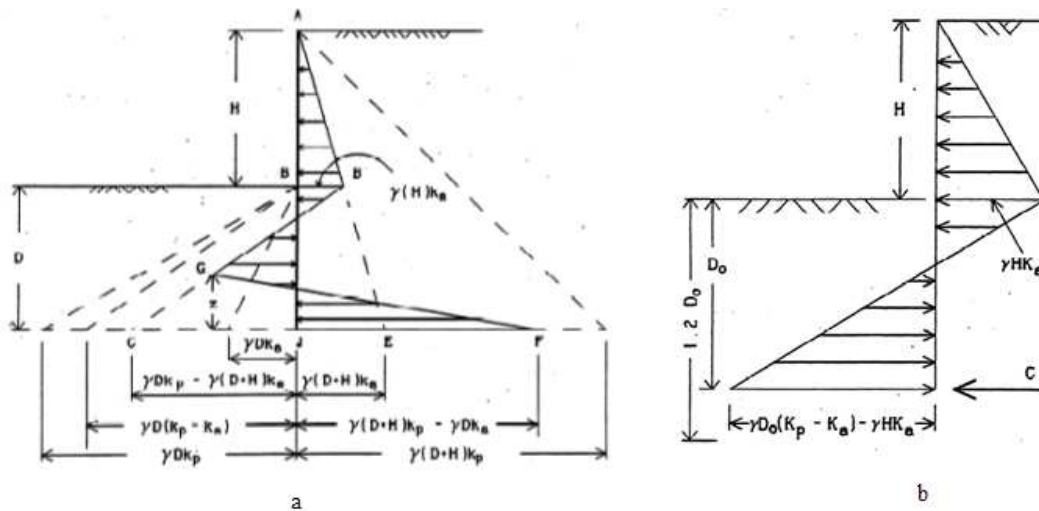
Figure 2. 13; a. Full Method with Superposed Pressures (California Trenching and Shoring Manual, 1995), b. Simplified Method with Superposed Pressures (Ryner, 2001)

In addition to full and simplified pressure distributions, superposed versions of these pressure distributions can also be used for ease of calculations. Resultant distributions are shown in figure 2.13.

2.4.8 Cantilever Walls in Cohesive Soils

Two different situations are considered in U.S.S. Steel Sheet Piling Design Manual for cantilever walls in cohesive soil; either the wall may be entirely in cohesive layer or retained side may be granular. Wall in entirely clay layer is considered in this part.

Figure 2.14 shows the pressure distribution of a cohesive soil immediately after the excavation where undrained conditions occur (ϕ = 0). Dotted line shows the negative pressure zone, but not included in calculations because soil develops tension cracks. Below the dredge line, passive pressure distribution is constant since $K_a = K_p = 1$ down until the rotational point level "b". Below this level, passive pressures are generated in the retained side, as can be seen in figure 2.14a.

Solution procedure is the same as that of a cantilever wall in cohesionless soil; fixed earth support method is applied with 2 unknowns, depth d and depth of rotational point d_0.
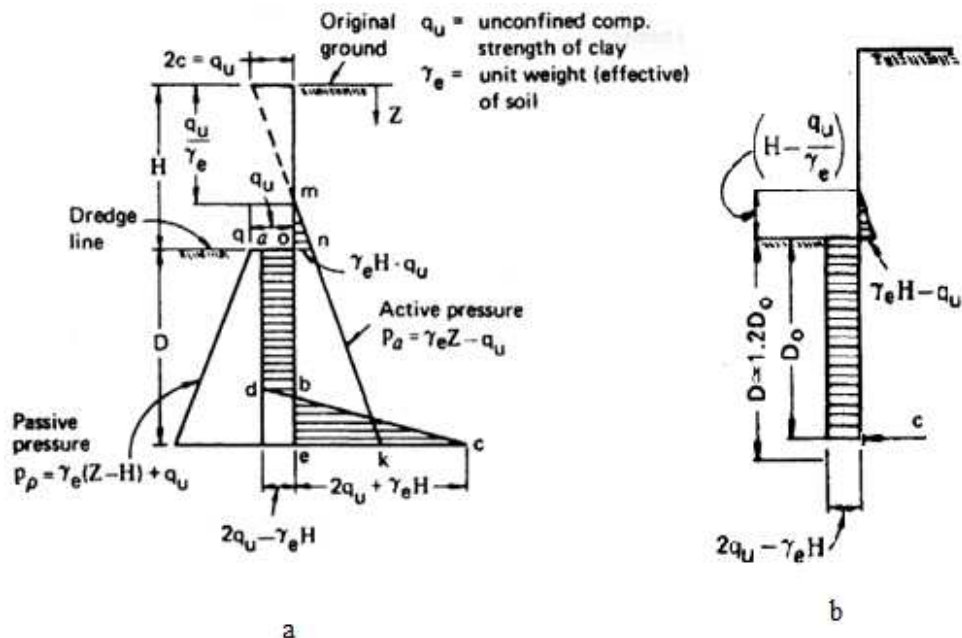
Figure 2. 14; a. Pressure distribution of a cantilever wall retaining clay, full pressure distribution, b. Simplified pressure distribution (U.S.S. Steel Sheet Piling Design Manual, 1984)

Similar to cohesionless soils, the pressure distribution for cantilever walls in cohesive soils can be simplified by changing the passive resistance below the rotational point with a force "C" with a requirement of % 20 to % 40 increase in embedment depth, d, at the end of calculations in analysis. Figure 2.14b shows the simplified pressure distribution.

2.4.9 Strutted Walls in Cohesionless and Cohesive Soils

Free and Fixed Earth Methods can both be applied to strutted walls. Since the wall gains its resistance not only from passive pressure below the excavation level but from the support that is placed at upper elevations of the retained height as well, the analysis can be done with both methods. Analysis with free earth assumption enables horizontal displacements at wall toe level, valid for shorter embedment depths. On the other hand, fixed earth assumption is for deeper embedments but with lower bending moments.

As mentioned in assumptions, the wall is assumed to be rotating as a rigid body around the level of support. Although this results in tendency to produce passive stresses in soil above the support level, it is assumed that wall is subjected to active pressures. The depth of penetration required for stability is calculated by moment equilibrium with respect to level of strut support.
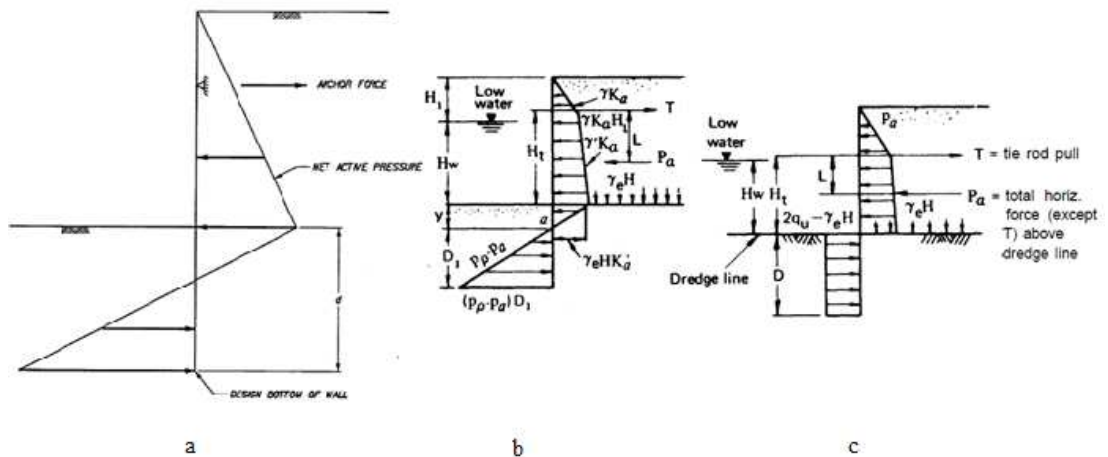
Figure 2. 15; a. Support idealization of strutted walls in cohesionless soils (U.S. Army Corps of Engineers Pile Design Manual, 1994), Superposed pressure distributions of strutted walls, a. Cohesionless, b. Cohesive (U.S.S. Steel Sheet Piling Design Manual, 1984)

U.S.S. Steel Sheet Piling Design Manual recommends a design procedure as follows; calculation of lateral earth pressures, locating the point of zero pressure, calculation of

force above the zero pressure level and below the excavation level; then determination of D_1, depth of wall below the zero pressure level, by solving moment equilibrium.

Figure 2.10 shows the deflected shape of a one level strutted retaining wall. Corresponding superposed pressure distribution is given in figure 2.15. In this thesis, Free Earth Support Method is used for strutted walls.

2.5   Numerical Modeling & PLAXIS

Numerical modeling is an analysis method applied to models where it is very difficult to solve the problem analytically due to several variables of the problem's nature. Today, numerical modeling is applied to wide variety of problems, including geotechnical problems that involve several variables such as material properties, stresses, structural parameters etc. As the complexity of problems increase, solutions involving numerical modeling become the norm in engineering.

Numerical modeling softwares use algorithms in solving partial differential equations that are established with various variables. Complex model is divided into well defined small parts, on which the calculations involving matrices obtained with parameters of the model are carried out. For each individual part, stresses, deformations and other variable dependent results are obtained, and finally, all parts are gathered together.

Finite element modeling (FEM) is a numerical analysis technique that provides approximate solutions to engineering problems. It provides the capability to achieve fast and optimized solutions, with complex and numerous variables including complex boundary and loading conditions, materials with non homogeneous and non linear properties etc. In other words, finite element analysis provides solutions based on actual stress-strain relations and boundary conditions. Finite element modeling differs from limit equilibrium methods where no information can be provided except that the limit conditions.

On the other hand, in order to achieve accurate results, the problematic system should be modelled with care. Required parameters for finite element modeling are more than that of a limit equilibrium solution where, some of the parameters may not be readily available and needs detailed soil investigations and tests. When dealing with geotechnical problems involving finite element analysis, theoretical background knowledge on finite element modeling is required in addition to soil and structural mechanics, in order to generalise and

simplify the problem properly as well as interpret the analysis results. Otherwise, results can lead to non sensible solution domains. Tables 2.5, 2.6 & 2.7 present the differences between limit equilibrium methods and finite element modeling, requirements for solution and requirements for design, respectively.

Table 2. 5; Design requirements satisfied by limit equilibrium analysis and finite element modeling method (Potts and Zdravkovic, 1999) (S: Satisfied, NS: Not Satisfied)

Method of Analysis	Design Requirements						
	Stability			Wall & Support		Adjacent Structures	
	Wall & Support	Base Heave	Overall	Structural Force	Displacement	Structural Force	Displacement
Limit Equilibrium	S	NS	NS	S	NS	NS	NS
Finite Element Method	S	S	S	S	S	S	S

Table 2. 6; Basic solution requirements satisfied by limit equilibrium analysis and finite element modeling method (Potts and Zdravkovic, 1999)

Method of Analysis	Solution Requirements				
	Equilibrium	Compatibility	Constitutive Behaviour	Boundary Conditions	
				Force	Displacement
Limit Equilibrium	S	NS	Rigid with a failure criterion	S	NS
Finite Element Method	S	S	Any	S	S

Table 2. 7; Comparison chart for limit equilibrium and finite element modeling (Powrie, 2003)

Type of Analysis	Advantages	Limitations
Limit Equilibrium	- Needs only the soil strength - Simple and straightforward	- does not model soil structure interaction - does not calculate deformations (hand calculations of deformations possible by relating mobilized strength, soil shear strain and wall rotation; or through empirical databases - statically indeterminate systems (multi propped walls), non uniform surcharges and berms require considerable idealization - can model only drained (effective stress) or undrained (total stress) conditions - two dimensional only for most problems - results take no account of pre-excavation stress state
Finite Element Modeling	- full soil structure interaction analysis is possible, modelling construction sequence etc. - complex soil models can represent variation of stiffness with strain and anisotropy - takes account of pre-excavation stress state - can model complex wall and excavation geometry including structural and support details - wall and ground movements are computed - potentially good representation of pore water response - can model consolidation as soil moves from undrained to drained conditions - can carry out two-dimensional or three dimensional analyses	- can be time consuming to set up and difficult to model certain aspects, e.g. wall installation - quality of results dependent on availability of appropriate stress strain models for the ground - extensive high quality data (e.g. Pre-excavation lateral stresses as well as soil stiffness and strength) needed to obtain most representative results - simple (linear elastic) soil model may give unrealistic ground movements - structural characterization of many geotechnical finite element and finite difference packages may be crude - significant software-specific experience required by user - simplistic representation of pore water response

2.5.1 Brief History of PLAXIS

PLAXIS is a geotechnical finite element analysis software. Development of the software started in late 1970's under supervision of Professor Pieter A. Vermeer in Technical University of Delft. Purpose of the software was estimate – predict possible movements of a Dutch Dam "Oosterschelde-dam" which is protecting a part of Netherlands against flooding. The earlier versions of the software were capable of analyzing elastic-plastic calculations for plane strain problems with high order elements. Today, different versions of the software are capable of analyzing & modeling 3D problems, as well as transient groundwater flows, incorporating a variety of advanced soil models. A 2D version (8.2) is used for all FEM work in this thesis.

2.5.2 Modules in PLAXIS

PLAXIS 2D is composed of several modules, which are arranged in a logical order to model the problem properly. In this topic, modules are explained with references to models used in this thesis.

2.5.2.1 Input Module

Input module of PLAXIS is the module where users define the geometry, layer boundaries of the model and material characteristics. Assignment of material properties to the defined materials as well as soil properties to corresponding clusters determined by the geometrical input takes place in input module. General properties as the units and grid properties to be used in the model, selecting whether the model would be plane strain or axisymmetry and number of nodes in a mesh element (6 or 15) are determined in this part. Walls, beams, anchors, struts, geotextiles etc. with their properties are also defined in this module.

Soil model to be used in the analysis is selected as Mohr Coulomb, Hardening Soil etc. in input module as well. PLAXIS uses various material models which are Linear Elastic Model, Mohr-Coulomb Model, Jointed Rock Model, Hardening Soil Model, Soft Soil Model, Soft Soil Creep Model and User-defined Soil Model. After the model is defined, mesh is to be generated with an element distribution coarseness. Not necessary but, refining the mesh in clusters that are expected to be of greater interest in analysis results (determined by the user) would be useful, if user wishes to avoid slowness of a model in which the entire mesh is fine.

Proceeding with generation of mesh, input module continues with inital stresses and pore pressures generation screen. In this part, users can model steady-state flow conditions by defining phreatic levels in addition to closed flow and consolidation boundaries if applied.
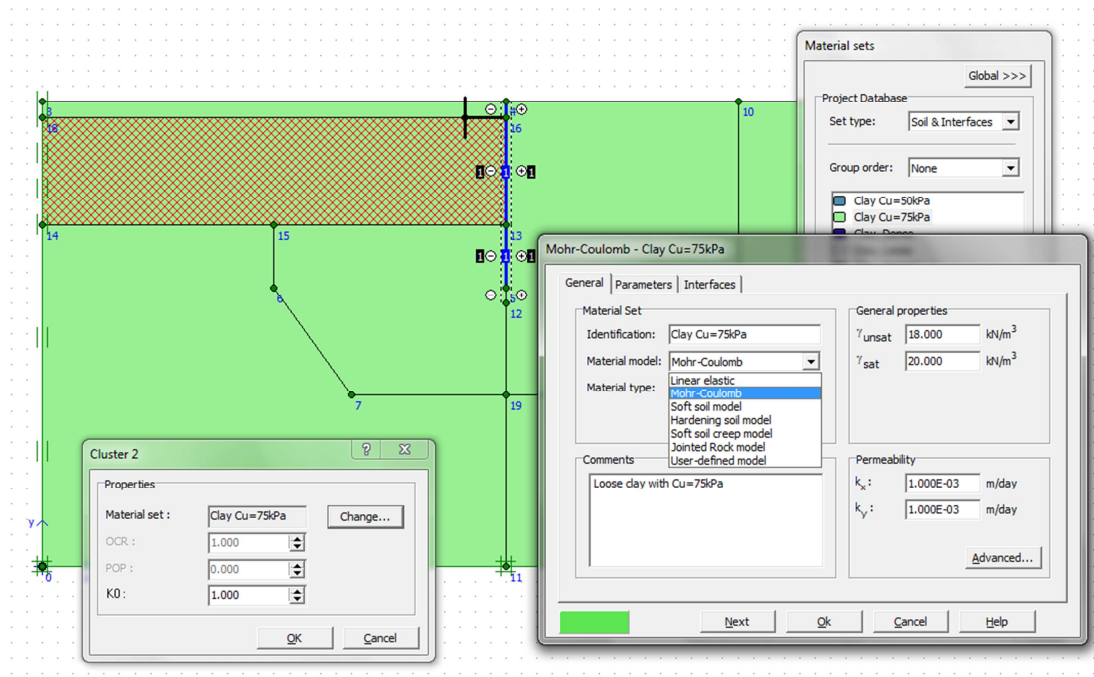
Figure 2. 16; PLAXIS input screen for strut supported clay model

Up to this part, any incorrect parameter - material properties etc. provided to the software input may cause to misleading results in analysis. Figure 2.16 presents an input screen of a strut supported clay model. Red hatched area is selected and properties of this cluster can be seen in lower left corner of the figure. Also, material model set that PLAXIS offers to the users are shown.

2.5.2.2   Calculation Module

Calculation module of the software is the part where analysis methods, numerical analysis parameters, construction stages, change of material properties & water levels are presented. Loading input methods and calculation types are selected in this part. Input methods are incremental multipliers, total multipliers and staged construction; calculation types are plastic, consolidation, phi/c reduction and dynamic analysis in PLAXIS 8.2.

2.5.2.2.1 Loading Input Methods

Loading input method defines the way PLAXIS applies the loads to the model. In total multipliers, user can define the multiplier of current configuration of external loads. The actual applied load at the end of the calculation phase is the product of the input value of the load and corresponding multiplier. In incremental multipliers, the initially applied load increment in the first step of the calculation phase is the product of the input value of the load and the corresponding multiplier. (PLAXIS Manual, 2002)

Staged construction mode of loading input method is used for defining changing geometry, load combinations, stress state, weight and strength or stiffness of elements in the model. For an embedded retaining wall, construction stages are defined individually for each step, using staged construction mode.

A brief order of construction phases of a strut supported retaining wall can be mentioned as; first, pile is placed by activating the plate in "define" menu of staged construction. Next stage, excavation of soil to the depth of strut level takes place by deactivating corresponding cluster. Then, strut is placed and in the final stage, full depth of soil is excavated (to the planned dredge level) by deactivating the corresponding cluster.

2.5.2.2.2 Calculation Types

Plastic calculation uses small deformation theory (Brinkgreve, 2007) which involves elastic/plastic deformations of elements for each node on the element. Staged construction (described above) type of loading input is used with plastic calculations.

Consolidation analysis is used when the dissipating excess pore pressures changing with time are expected to be analyzed.

Phi-c reduction analysis determines an overall safety factor for the model. Safety analysis is performed by reducing strength parameters of soil until failure occurs. Then, the FS value, ΣMsf, is determined from the relation of input strength parameters and strength parameters reached at the end of analysis - where failure occured. Phi-c reduction method uses "incremental multipliers" option as loading input.

$$\Sigma Msf = \frac{\tan \phi_{input}}{\tan \phi_{reduced}} = \frac{c_{input}}{c_{reduced}} \qquad (2.11)$$

Phi-c reduction applies only for soil parameters. Strength parameters of structural elements are not reduced in this analysis method. Safety factors of such structures should be considered seperately considering shear forces and bending moments they are exposed. An example of phi-c reduction results is given in figure 2.17.
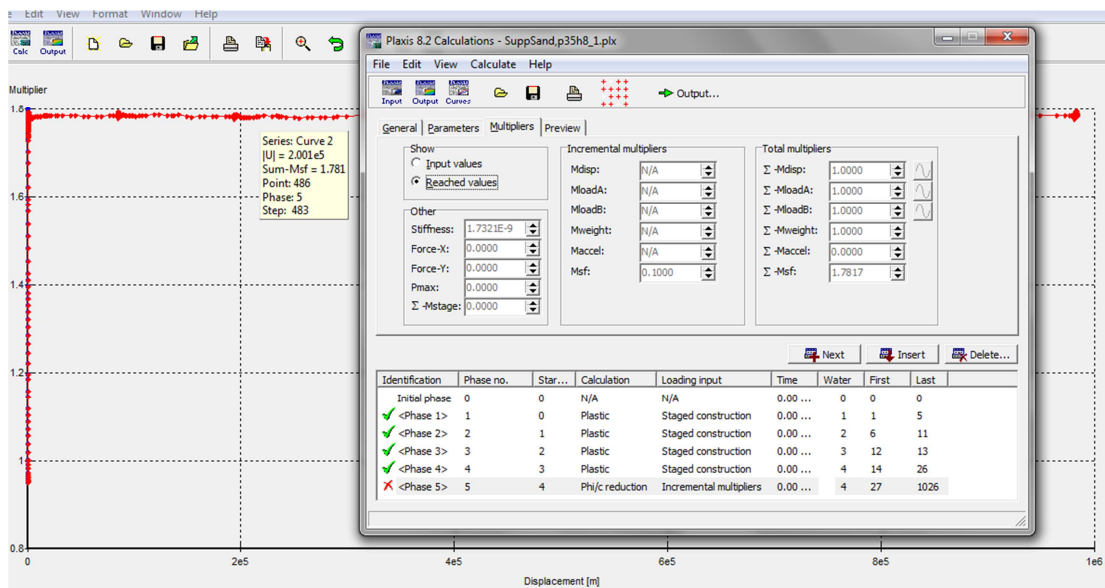
Figure 2. 17; An analysis result of phi-c reduction method, with PLAXIS Curves output of ΣMsf vs Displacement

2.5.2.3   Output Module

Analysis results - outputs of each phase can be examined in output mode. Deformed shape of the model, stresses and strains in soil, axial forces, shear forces and bending moments on plates, forces on struts and anchors, displacements corresponding to the structural elements, displacements of soil and pore pressures are visually and tabularly presented.

2.5.2.4   Curves Module

Curves module can generate load-displacement curves, time-displacement curves, stress paths, displacement vs multipliers and stress-strain diagrams at user-selected points. Load-displacement curves are useful in visualizing the relation between applied loads and resultant displacements.

CHAPTER 3

DEVELOPING THE METHODOLOGY & CALCULATIONS

In this chapter, methodology used for obtaining safety factors by applying limit equilibrium methods described in chapter 2 and numerical analysis methods are presented. Analyses are carried out considering the following parameters provided in table 3.1 (all possible combinations were not analyzed).

Cohesionless soil with internal friction angle, ϕ = 30, 35, 37,5 & 40˚, and cohesive soil with undrained shear strength c_u=50-75-100-150 kPa are analyzed for;

- retaining heights starting from 5m to 12m with 1 meter intervals for each analysis,

- support of wall either cantilever or one level strutted,

- material model either Mohr-Coulomb or Hardening Soil Model, varied for a selected case

- modulus of elasticity for 30, 40, 50 & 60 Mpa, varied for a selected case

- limit equilibrium method; conventional or simplified pressure diagrams

Material model analysis and analysis depending on modulus of elasticity are available for numerical solutions only. Corresponding limit equilibrium analysis results are used with same parameters of H & soil strength for comparing and obtaining FS values. Data sets used and FS factors obtained are presented in detail in chapter 4.

Table 3. 1; Analyzed models

Cantilever Pile Fixed Earth Support Used in Limit Equilibrium Analysis

Cohesionless Material — E (Mpa) = 50

	H (m) = 5			H = 6			H = 7			H = 8			H = 9			H = 10			E = 30	E = 40	E = 60
φ (°)	30	35	40	30	35	40	30	35	40	30	35	40	30	35	40	30	35	40	(H=5, φ=35)		
Traditional	✓	✓	✓	✓	✓	✓	✓	✓	✓	×	✓	✓	×	×	✓	×	×	✓			
Simplified	✓	✓	✓	✓	✓	✓	✓	✓	✓	×	✓	✓	×	×	✓	×	×	✓	×	×	×
Plaxis Analysis	✓	✓	✓	✓	✓	✓	✓	✓	✓	×	✓	✓	×	×	✓	×	×	✓	✓	✓	✓

Cohesive Material — E (Mpa) = 50

	H (m) = 6			H = 7			H = 8			H = 9			H = 10			H = 11			E = 30	E = 40	E = 60
cu (kPa)	50	75	100	50	75	100	50	75	100	50	75	100	50	75	100	50	75	100	(H=6, cu=50)		
Traditional	✓	✓	✓	✓	✓	✓	✓	✓	✓	✓	✓	✓	✓	✓	✓	×	✓	✓	×	×	×
Simplified	✓	✓	✓	✓	✓	✓	✓	✓	✓	✓	✓	✓	✓	✓	✓	×	✓	✓	×	×	×
Plaxis Analysis	✓	✓	✓	✓	✓	✓	✓	✓	✓	✓	✓	✓	✓	✓	✓	×	✓	✓	✓	✓	✓

Strutted Pile Free Earth Support Used in Limit Equilibrium Analysis

Cohesionless Material — E (Mpa) = 50

	H (m) = 8			H = 9			H = 10			H = 11			H = 12		
φ (°)	30	35	40	30	35	40	30	35	40	30	35	40	30	35	40
Traditional	✓	✓	✓	✓	✓	✓	✓	✓	✓	✓	✓	✓	✓	✓	✓
Simplified	✓	✓	✓	✓	✓	✓	✓	✓	✓	✓	✓	✓	✓	✓	✓
Plaxis Analysis	✓	✓	✓	✓	✓	✓	✓	✓	✓	✓	✓	✓	✓	✓	✓

Cohesive Material — E (Mpa) = 50

	H (m) = 8			H = 9			H = 10			H = 11			H = 12		
cu (kPa)	50	75	100	50	75	100	50	75	100	50	75	100	50	75	100
Traditional	✓	✓	✓	✓	✓	✓	✓	✓	✓	✓	✓	✓	✓	✓	✓
Simplified	✓	✓	✓	✓	✓	✓	✓	✓	✓	✓	✓	✓	✓	✓	✓
Plaxis Analysis	✓	✓	✓	✓	✓	✓	✓	✓	✓	✓	✓	✓	✓	✓	✓

3.1 Cantilever Wall Retaining Sand

Four different solution procedures are presented in this section for cantilever walls retaining sand; 2 different procedures are presented for solutions concerning either the simplification (presented in detail in 2.4.7, Cantilever Walls in Cohesionless Soils) applied at pile bottom, or not. Remaining two solutions are following the superposed pressure distribution of the first two solutions. In order to distinguish the difference between pressure distribution procedures, methods are titled as 1a and 1b for full method solution and its superposed pressure distribution solution, 2a and 2b for simplified method solution and its superposed distribution solution, respectively.

3.1.1 LE Solution with Traditional Method, Full Pressure Distribution (1a)

In calculating safety factor from conventional methods, pressure distribution shown in figure 3.1 is used. Pile rotating at point "O" is shown by the dashed line. Distance from pile toe to the point of rotation "O" is denoted as "x". Above the level of rotation (called as "O" from now on), retained side is in active state (1st Area) and excavated side below the dredge level is in passive state (2nd Area). Below the level of "O", 5th & 6th areas are in passive state and 3rd & 4th are in active state due to the rotation of the pile as shown (areas below "O" are divided for ease of calculations).

Forces for areas shown in figure 3.1 are calculated with formulas given in table 3.2.

Table 3. 2; Force & moment formulas

Area	Force Equation	Moment Arm (w.r.t. "O")	Moment Direction (w.r.t. "O")
1	$\gamma_{dry}.(H+D-x).K_a.(H+D-x)/2$	$(H+D-x)/3$	CCW
2	$\gamma_{dry}.(D-x).(K_p/FS).(D-x)/2$	$(D-x)/3$	CW
3	$\gamma_{dry}.K_a.(D-x).x$	$x/2$	CCW
4	$\gamma_{dry}.K_a.(D-(D-x)).x/2$	$2x/3$	CCW
5	$\gamma_{dry}.(K_p/FS).(H+D-x).x$	$x/2$	CW
6	$\gamma_{dry}.(K_p/FS).(H+D-(H+D-x)).x/2$	$2x/3$	CW
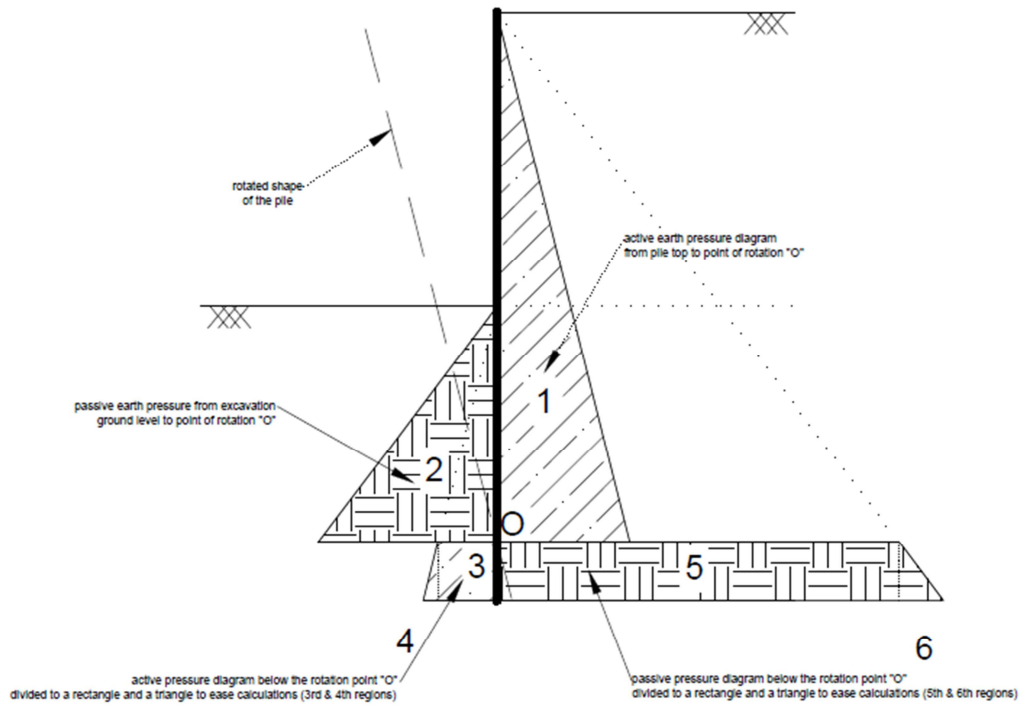
Figure 3. 1; Conventional pressure distribution

As can be seen from table 3.2, solving these equations for horizontal force equilibrium and moment equilibrium simultaneously provides 2 equations with 2 unknowns; x and FS. The equations for force and moment equilibrium (simplified for safety factor) are presented below, respectively.

$$FS = \frac{K_p * \gamma * [\frac{(D-x)^3}{2} + (D-x)*x + \frac{x^2}{2}]}{K_a * \gamma * [\frac{(H+D-x)^2}{2} + (H+D-x)*x + \frac{x^2}{2}]} \tag{3.1}$$

$$FS = \frac{K_p * \gamma * [\frac{(D-x)^3}{6} + (D-x)*\frac{x^2}{2} + \frac{x^3}{3}]}{K_a * \gamma * [\frac{(H+D-x)^3}{6} + (H+D-x)*\frac{x^2}{2} + \frac{x^3}{3}]} \tag{3.2}$$

These 2 equations provide one logical set of x & FS values. A sample graph of these two equations for the parameters ϕ = 30° and H = 5 meters, are in figure 3.2.

Graph of FS Values Calculated From Force & Moment Equations for H = 5m & ϕ = 30˚

$y = -0.0211x^4 + 0.2138x^3 - 0.1087x^2 - 0.1238x + 1.4321$
$R^2 = 1$
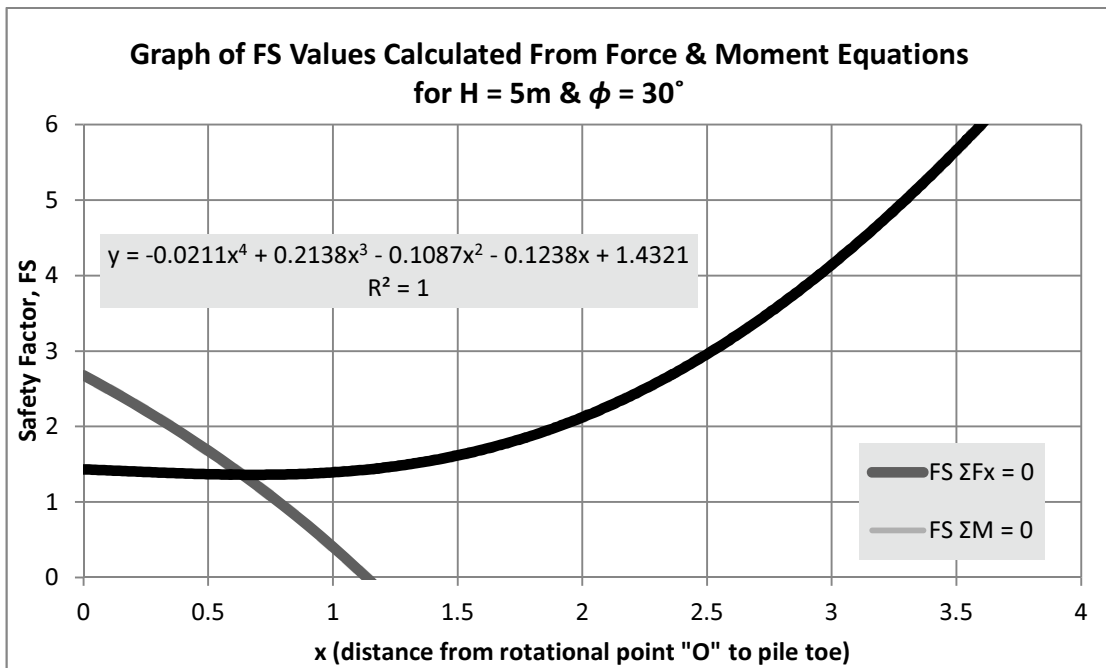
Figure 3. 2; FS Values Calculated from Force & Moment Equations for H = 5m & ϕ = 30˚

Intersection of these two lines is the solution of force and moment equations. The FS value of this model is 1,34 for x = 0,64m from pile toe (Although the quadratic equations have two more solution sets, other two have imaginary solutions, which are discarded).

3.1.2 LE Solution with Traditional Method, Superposed Pressure Distribution (1b)

This solution obtains FS and x values from the superposed form of general pressure diagram. California Trenching Manual and U.S. Steel Sheet Piling Manual apply this diagram in analysis of cantilever piles in granular soils.

In this pressure diagram, direction of net pressure changes at a distance "z" from pile toe. Areas (FBA_2) and (ECJ) generate the over-turning moments, where as (EA_1A_2) generates the restoring moment. Rotational point lies within the height "z" and pile toe.

$$\Delta(EA_1A_2) - \Delta(FBA_2) - \Delta(ECJ) = 0 \tag{3.3}$$

Figure 3. 3; Superposed pressure distribution used in limit equilibrium (U.S.S. Steel Sheet Piling Design Manual, 1984)

To solve the system according to the superposed pressure distribution given in figure 3.3, pressures at points listed in table 3.3 are calculated with corresponding equations, with factor of safety and "z" distance as the two unknowns. After determining pressures in table 3.4, force equations and moment equations are written, as seen in table 3.5.

Table 3. 3; Equations of pressures for the corresponding points presented in figure 3.3

Point	P Formulae
A1	$\gamma_{dry}.K_a.H$
A2	$\gamma_{dry}.K_a.(H+D)$
E	$\gamma_{dry}.D.(K_p/FS)-\gamma_{dry}.(H+D).K_a$
J	$\gamma_{dry}.(H+D).(K_p/FS)-\gamma_{dry}.D.K_a$
C	$\gamma_{dry}.(D-z).(K_p/FS)-\gamma_{dry}.(H+D-z).K_a$

Table 3. 4; Equations of force areas with corresponding moment arms for superposed pressure distribution diagram

Area ID		Formula	Moment Arm (w.r.t. bottom)
EA_1A_2		$(E+A_2)*D/2$	$D/3$
FBA_2		$A_2*(H+D)/2$	$(D+H)/3$
ECJ		$(E+J)*z/2$	$z/3$
BAA_1		$A_1*H/2$	$H/3$
AA_1A_2F		$(A_1+A_2)/2*D$	
	1	A_1*D	$D/2$
	2	$(A_2-A_1)/2*D$	$D/3$

Solving these equations for restoring & over turning moments and forces; the 2 equations for the system of 2 unknowns, factor of safety and "z" distance are obtained and given below in table 3.5 as;

Table 3. 5; Force and moment equations

force equilibrium (ΣFx);	z formula
$\Sigma F = H.P_{A1}/2+(P_{A1}+P_{A2}).D/2+(P_E+P_J).z/2-(P_E+P_{A2}).D/2$	$z = [(P_E+P_{A2}).D-H.P_A-(P_A+P_{A2}).D]/(P_E+P_J)$

moment equilibrium (ΣM wrt bottom);	z formula
$\Sigma M = (H.P_{A1}/2).(H/3+D)+(P_{A1}.D).(D/2)$ $+(P_{A2}-P_{A1}).(D/2).(D/3)$ $+(P_E+P_J).(z/2).(z/3)-(P_E+P_{A2}).(D/2).(D/3)$	$z^2 = [(P_E-2.P_A).D^2-3.H.P_A.(H/3+D)]/(P_E+P_J)$

The simplified form of these two equations are given below and a sample graph taken from the analysis of cantilever wall in sand with parameters ϕ = 30˚ and H = 5m is provided in figure 3.4.

$$\sum F = 0 \rightarrow FS = \frac{K_p * \gamma * [D*z+(H+D)*z-D^2]}{K_a * \gamma * [D*z+(H+D)*z-(H+D)^2]} \qquad (3.4)$$

$$\sum M = 0 \rightarrow FS = \frac{K_p * \gamma * [D^3-(H+D)*z^2-D*z^2]}{K_a * \gamma * [(H+D)^3-(H+D)*z^2-D*z^2]} \qquad (3.5)$$

42
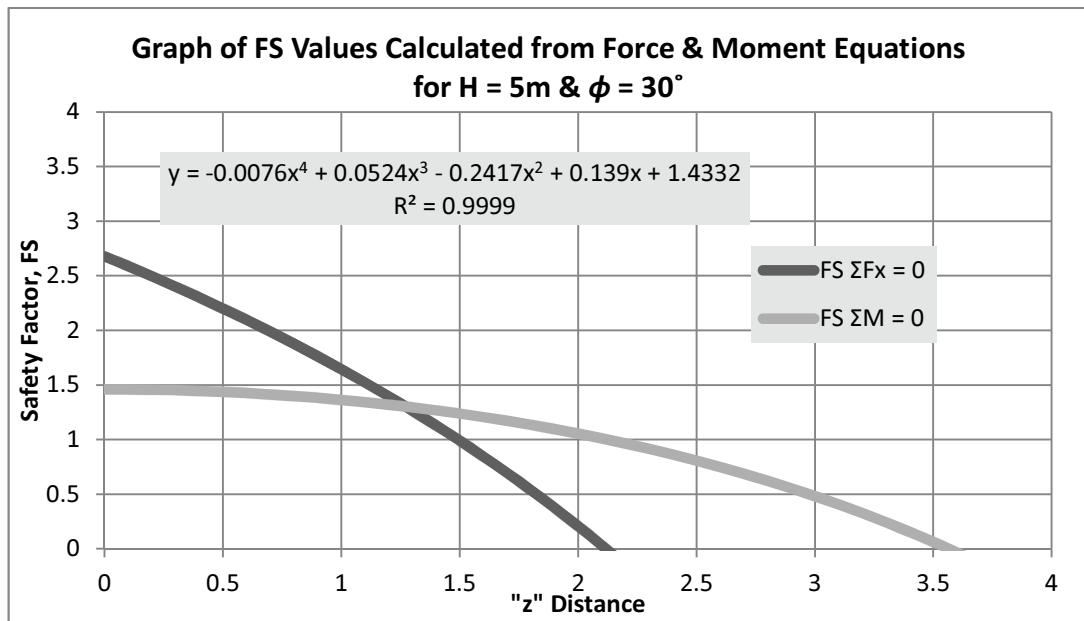
Figure 3. 4; FS vs z graph for moment and force equilibrium

As can be seen from figure 3.4, z & FS couple satisfying both moment and force equilibriums is z = 1,27m from pile bottom for FS = 1,30 and x, distance from pile toe to rotational point "O" is calculated as 0,96m.

3.1.3   LE Solution with Simplified Method, Full Pressure Distribution (2a)

As mentioned in chapter 2, in simplified pressure diagram, forces obtained from pressures below the rotational point level is replaced with a force "C", as can be seen from figure 3.5. Calculations are reduced significantly in simplified pressure distribution if compared with full pressure distribution. FS can be calculated directly by taking moments with respect to "O". Although this method is adviced to be used in preliminary designs only, calculations regarding simplified pressure distribution is included in this thesis in order to observe the difference between full method and simplified method.

Forces are calculated from active and passive lateral earth pressures, as shown in table 3.6. In design manuals, since the embedment depth is unknown, calculations aim to calculate "D" with an increase of % 20 to % 40 at the end. However, in this thesis, embedment depth is predefined as 6 meters. Considering a pile with D=5m results in an embedment depth of 6 meters including the % 20 increase in D. Therefore, limit equilibrium calculations are carried out with 5 meters of embedment depth.
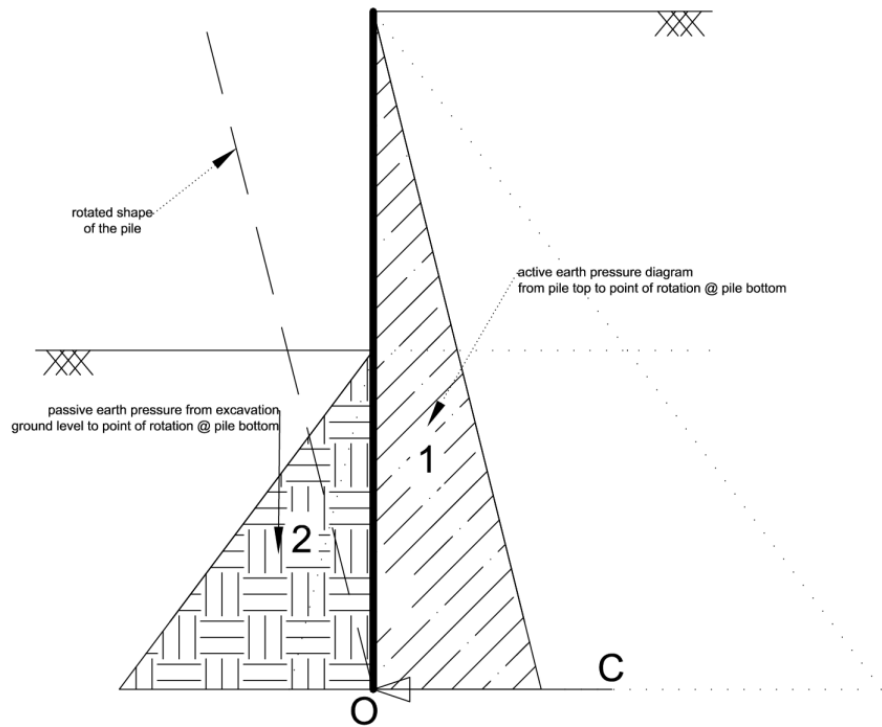
Figure 3. 5; Simplified pressure diagram of cantilever retaining wall retaining sand

Table 3. 6; Simplified method force and moment equations

Area	Force Equation	Moment Arm (w.r.t. bottom)	Direction (wrt bottom)
1	$\gamma_{dry}.(H+D).K_a.(H+D)/2$	$(H+D)/3$	CCW
2	$\gamma_{dry}.(D).(K_p/FS).(D)/2$	$D/3$	CW

$$FS = \frac{K_p * \gamma * [D^2 - (H+D)*z^2 - D*z^2]}{K_a * \gamma * [(H+D)^2 - (H+D)*z^2 - D*z^2]} \qquad (3.6)$$

3.1.4   LE Solution with Simplified Method, Superposed Pressure Distribution (2b)

Superposed pressure distribution solution of retaining walls in sand provides exactly the same results with full pressure distribution (2a) for factor of safety due to the formulation. Pressure distribution is presented in figure 3.6.
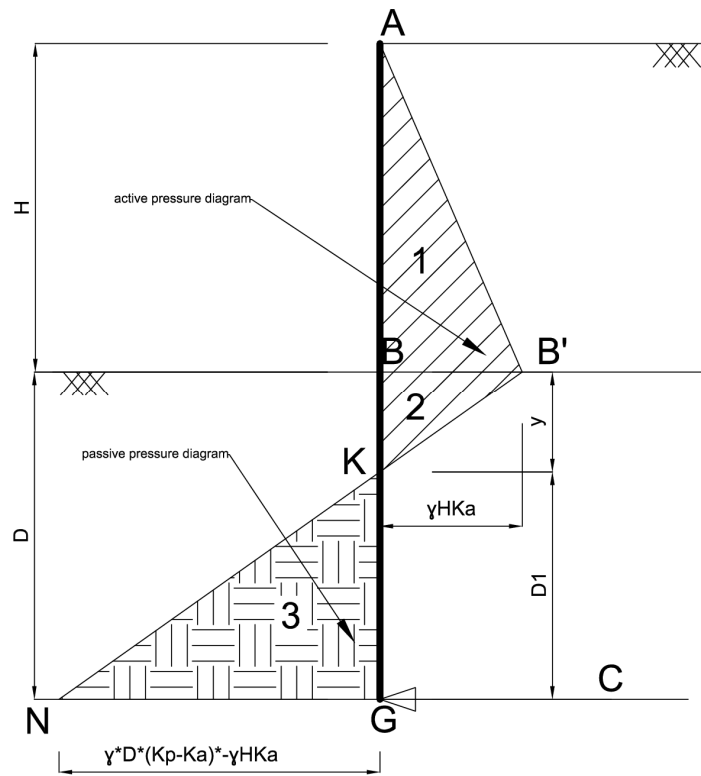
Figure 3. 6; Superposed pressure distribution for limit equilibrium solution with simplified method

Areas 1 & 2 generate the over-turning and area 3 generates the restoring moments. As can be seen from figure 3.6, depth D is divided into D_1 & y in order to distinguish the point where pressure on pile changes the direction. Three equations are required to solve the system with three unknowns; D_1, y & FS value. Since D value is provided at the very beginning of the calculations, first equation is obtained as;

$$D = D_1 + y \tag{3.7}$$

Second equation can be obtained from similarity of triangle KBB' and KGN as;

$$\frac{y}{D_1} = \frac{\gamma_{dry} * H * K_a}{\gamma_{dry} * D * (\frac{K_p}{FS} - K_a) - \gamma dry * H * K_a} \tag{3.8}$$

Third and final equation is obtained from moment equilibrium. Moments of the force areas shown in figure 3.6 is calculated with respect to pile bottom, G, in order to avoid from the

moment generated by the unknown force, C at pile bottom. Table 3.7 presents the forces obtained from areas 1, 2 and 3 with corresponding moment arms.

Table 3. 7; Force equations and corresponding moment arms considering rotation around pile bottom, G

Area	Force Equation	Moment Arm (wrt G)	Direction (wrt G)
1	$\gamma_{dry}.H.K_a.H/2$	$D+H/3$	CCW
2	$\gamma_{dry}.H.K_a.y/2$	$D_1+2y/3$	CCW
3	$\{\gamma_{dry}.D.(K_p/FS-K_a)-\gamma_{dry}.H.Ka\}.D_1/2$	$D_1/3$	CW

3.2   Cantilever Wall Retaining Undrained Clay

7 different solution procedures are presented in this section for cantilever walls retaining undrained clay. Solution procedures are divided into three main categories with their superposed solution procedures.

First category (solutions 1a & 1b) applies traditional limit equilibrium method with superposed pressure distribution. Difference between 1a and 1b is due to the consideration of height of the tension crack, ie, active pressures on retained side of the wall (as in 2a vs 2c and 3a vs 3b).

Second category (solutions 2a, 2b & 2c) considers simplified method with full and superposed pressure distributions on the wall. An additional solution is included in 2b regarding the FS applied to c_u can be seperated as c_u in active and c_u in passive pressure zones.

Approaches in this thesis that involve FS values applied to c_u all over the calculations are very similar to considerations of Eurocode 7 Design Approach 1/2 where partial factors are applied to soil strength parameters (although DA 1/2 provides partial factors for variable unfavourable loads, no loads of this type are involved in this study).

Third category (solutions 3a & 3b) applies the simplified pressure distribution considering the crack height. Full and superposed pressure distributions are presented.

3.2.1 Limit Equilibrium Solution with Traditional Method, Superposed Pressure Distribution with Active Pressures from Full Height (1a)

In this analysis method of cantilever retaining walls retaining clay, pressure distribution presented in figure 3.7 is used. Undrained conditions are valid for the short term conditions. Soil in upper levels can manage to hold itself without the need for a wall due to the cohesion of the soil. The excavation depth, below which soil can carry itself can be calculated from the equation;

$$H_{critical} = \frac{2 * c_u}{\gamma} \tag{3.9}$$

Pressure distributions starting from top level of ground, as suggested by California Trenching & Shoring Manual, are used in analyses. In other words, active pressures start from point A in figure 3.7, not from crack height level, are used in analysis of limit equilibrium conditions.

Formulas used in calculations are presented in tables 3.8, 3.9 & 3.10. A sample analysis result for parameters c_u = 50 kPa and H = 6m is provided. Figure 3.8 is obtained from resultant force and moment equilibrium equations (Equations 3.10 & 3.11).
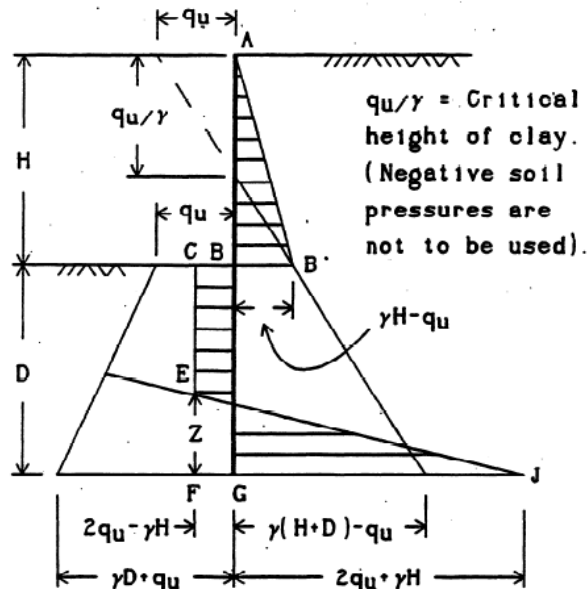
Figure 3. 7; Pressure distribution of cantilever walls retaining clay (California Trenching and Shoring Manual, 1995)

Table 3. 8; Lateral earth pressures

Point	P Formulae
B'	$\gamma.H-2(c_u/FS)$
C, E, F	$4(c_u/FS)-\gamma.H$
J	$4(c_u/FS)+\gamma.H$

Table 3. 9; Force equations

Area ID	Formula	force equilibrium (ΣFx);
ABB'	B'*H/2	
BCFG	C*D	A(ABB')-A(BCFG)+A(JEF) = 0
JEF	(F+J)*z/2	

Table 3. 10; Moment equations

Area	force equilibrium (ΣFx);	Moment Arm (wrt bottom)
ABB'	$(\gamma.H-2(c_u/FS)).H/2$	H/3+D
EFJ	$8c_u/FS.z/2$	z/3
BCFG	$(4(c_u/FS)-\gamma H).D$	D/2

$$\sum F = 0, \rightarrow z = 7.5 - 5.4 * FS \qquad (3.10)$$

$$\sum M = 0, \rightarrow z^2 = 90 - 75.6 * FS \qquad (3.11)$$
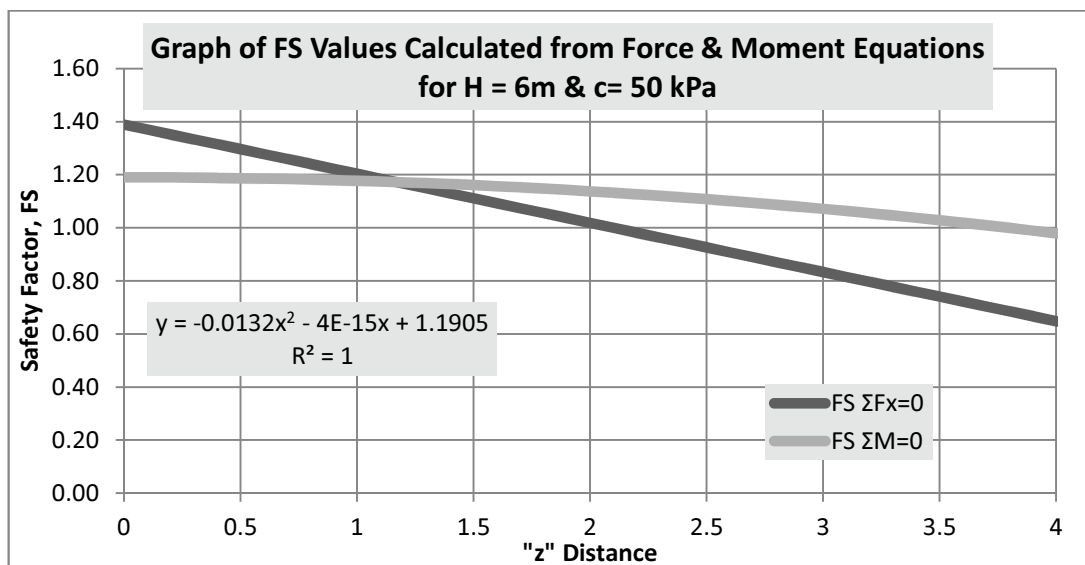
Figure 3. 8; FS vs z graph for moment and force equilibrium

3.2.2 LE Solution with Traditional Method, Superposed Pressure Distribution with Active Pressures from Crack Height (1b)

In this analysis, pressure distribution provided by U.S.S. Steel Sheet Piling Design Manual is used. U.S.S. Steel Piling Manual uses pressure distributions where active lateral pressures are calculated from crack height above which no active pressure occurs (Manual also does not use negative pressures above this level because of the expected tension cracks at top levels). Figure 3.9 presents the pressure distribution used in this analysis, where active pressure zone is the triangular area A'BB' in retained side above dredge level.
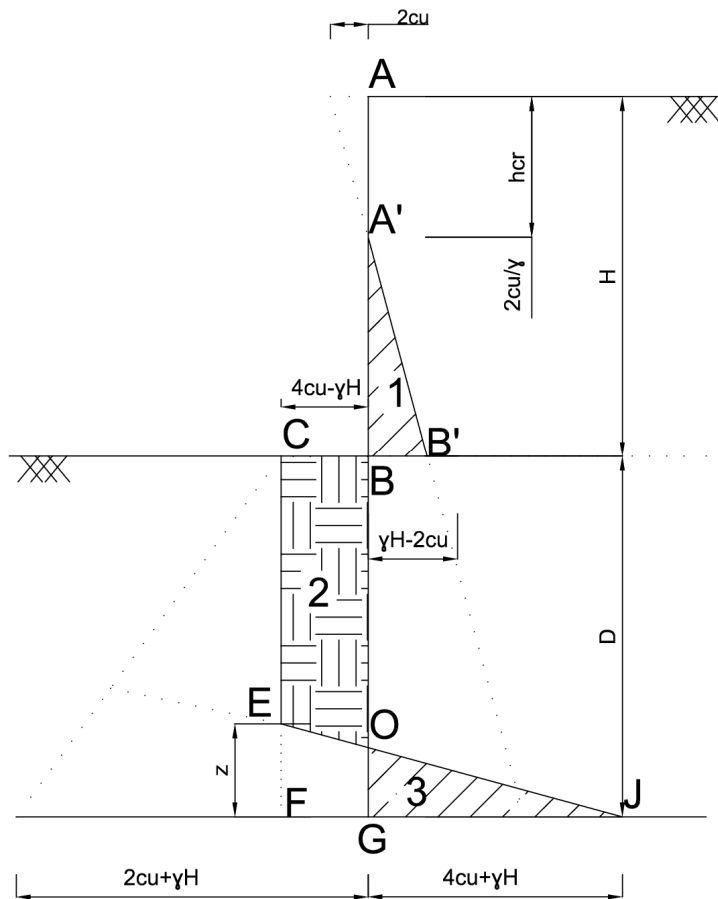
Figure 3. 9; Pressure distribution of retaining walls in clay (U.S.S. Steel Sheet Piling Design Manual, 1984)

This analysis provides higher FS values compared to the solution in 1a where lateral active earth pressures are considered from pile top. This is due to the decrease in the first area. Tables 3.11 & 3.12 present the formulas used in solution for FS and z parameters in this method.

Table 3. 11; Force equations and z equation

Area ID	Formula	force equilibrium (ΣFx);	z formula
1 - A'BB'	$B'*(H-h_{cr})/2$		$z=(4.c_u.FS.\gamma.(2D+H)$
2 - BCFG	$C*D$	$A(A'BB')-A(BCFG)+A(JEF)$	$-FS^2.H.\gamma^2.(2D+H)-4c_u^2)$
3 - JEF	$(F+J)*z/2$		$/(8c_u.FS.\gamma)$

Table 3. 12; Moment equations and z equation

Area ID	force equilibrium (ΣFx);	Moment Arm (wrt bottom)	z formula
A'BB'	$(\gamma.H-2(c_u/FS)).(H-h_{cr})/2$	$(H-h_{cr})/3+D$	$z^2=8c_u^3-FS.\gamma.(12.c_u^2.(D+H)$ $-6c_u.f.\gamma.(2.D^2+2.D.H+H^2)$
EFJ	$8c_u/FS.z/2$	$z/3$	$+FS^2.H.\gamma^2.(3.D^2+3D.H+H^2))$
BCFG	$(4(c_u/FS)-\gamma H).D$	$D/2$	$/(8c_u.FS^2.\gamma^2)$

3.2.3 LE Solution with Simplified Method, Full Pressure Distribution with Active Pressures from Full Height (2a & 2b)

In this analysis method, two different FS values are calculated. In first method (2a), FS is applied to the c_u parameter in both active and passive lateral pressure zones. This is the traditional method for applying safety factor, mentioned in chapter 2.

In second method (2b), FS is applied to the c_u value of the zone which is exposed to passive pressures only (area MNBG in figure 3.10).This resulted in higher FS values compared to the first method. Formulas used for calculating lateral earth pressures, forces and moments are presented below in tables 3.13, 3.14 & 3.15 for both methods.
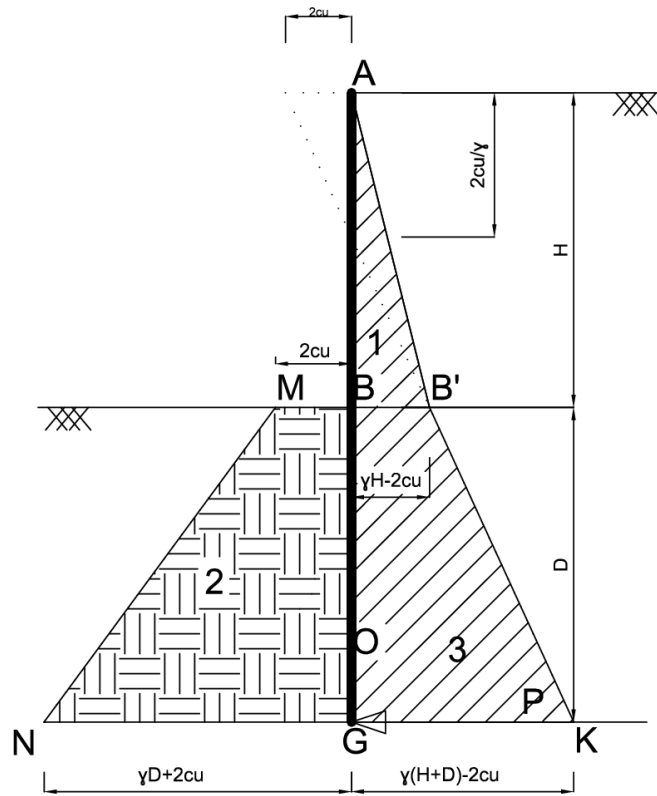
Figure 3. 10; Pressure distribution of cantilever walls retaining clay (California Trenching and Shoring Manual, 1995)

Table 3. 13; Lateral earth pressures

Point	Pressure Formula for FS applied only to Passive (2a)	Pressure Formula for FS applied both Active & Passive (2b)
B'	$\gamma.H-2(c_u)$	$\gamma.H-2(c_u/FS)$
M	$2(c_u/FS)$	$2(c_u/FS)$
N	$2(c_u/FS)+\gamma.D$	$2(c_u/FS)+\gamma.D$
K	$\gamma.(H+D)-2(c_u)$	$\gamma.(H+D)-2(c_u/FS)$

Table 3. 14; Force equations

Area ID	Formula	force equilibrium (ΣFx);
ABB'	B'*H/2	
MNBG	(M+N)/2*D	A(MNBG)-A(ABB')-A(BB'GK)
BB'GK	(B'+K)/2*D	

Table 3. 15; Moment equations

Area	Force Formula for FS applied only to Passive (2a)	Force Formula for FS applied both Active & Passive (2b)	Moment Arm (w.r.t. bottom)
ABB'	$(\gamma.H-2(c_u))*H/2$	$(\gamma.H-2(c_u/FS))*H/2$	H/3+D
MNM'	$(\gamma.D)*D/2$	$(\gamma.D)*D/2$	D/3
MM'GB	$2(c_u/FS)*D$	$2(c_u/FS)*D$	D/2
B'B''K	$(\gamma.D)*D/2$	$(\gamma.D)*D/2$	D/3
BB'B''G	$(\gamma.H-2c_u)*D$	$(\gamma.H-2c_u/FS)*D$	D/2

3.2.4   LE Solution with Simplified Method, Superposed Pressure Distribution with Active Pressures from Full Height (2c)

Pressure distribution used in this solution is the simplified version of the distribution presented in 1a, As can be seen from figure 3.11, lateral pressures below the rotational point G is replaced with a horizontal force P. Results obtained from this method are very close (±0,015) to the results from solution 1a. Formulas used in the calculations are presented below.

Table 3. 16; Lateral pressures

Point	P Formulae
B'	$\gamma.H-2(c_u/FS)$
C, E, F	$4(c_u/FS)-\gamma.H$

Table 3. 17; Force equations with corresponding moment arms

Area ID	Formula	Resultant Force (ΣFx);	force equilibrium (ΣFx);	Moment Arm (wrt bottom)
ABB'	B'*H/2	$(\gamma.H-2(c_u/FS)).H/2$		H/3+D
BCFG	C*D	$(4(c_u/FS)-\gamma H).D$	A(BCFG)-A(ABB')+P	D/2
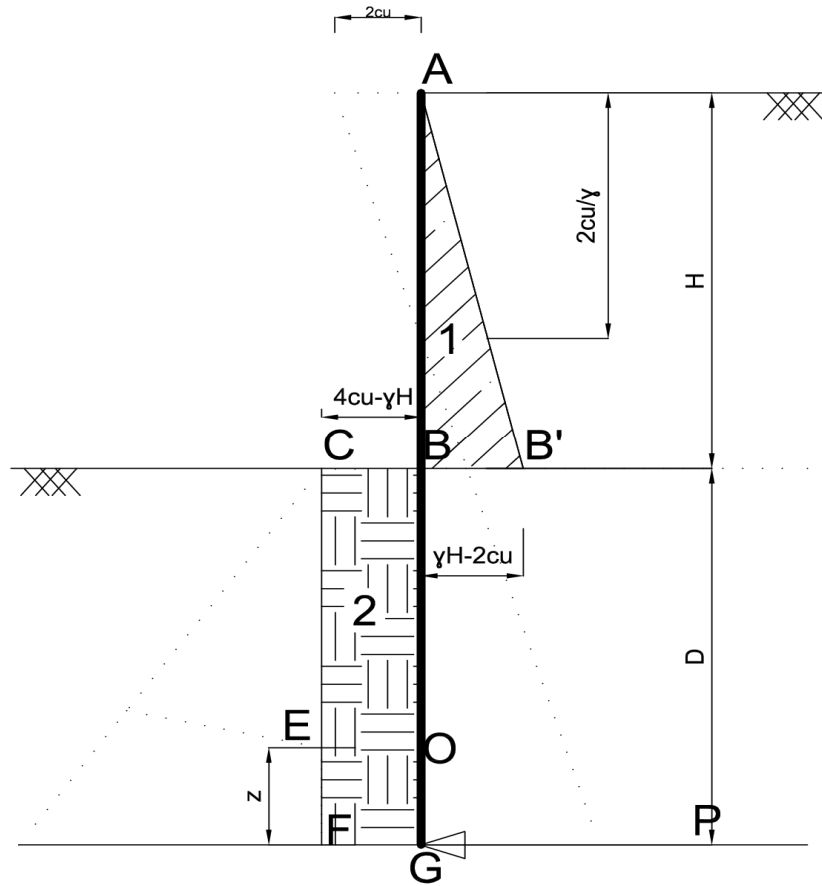
Figure 3. 11; Pressure distribution for cantilever wall retaining clay

3.2.5 LE Solution with Simplified Method, Full Pressure Distribution with Active Pressures from Crack Height (3a)

The difference between analysis methods 2a vs 3a and 2c vs 3b is the height to be considered in calculations of active lateral pressures. In this method, crack height is used in calculations. Pressure distribution used in analysis of 3a is provided in figure 3.12.

Table 3. 18; Lateral earth pressures for areas given in figure 3.12

Point	P Formulae	Area ID	Formula
B'	$\gamma.H-2(c_u/FS)$	AGK	$K*(D+H-2cu/FS/\gamma)/2$
M	$2(c_u/FS)$		
N	$2(c_u/FS)+\gamma.D$	MNBG	$(M+N)/2*D$
K	$\gamma.(H+D)-2(cu/FS)$		
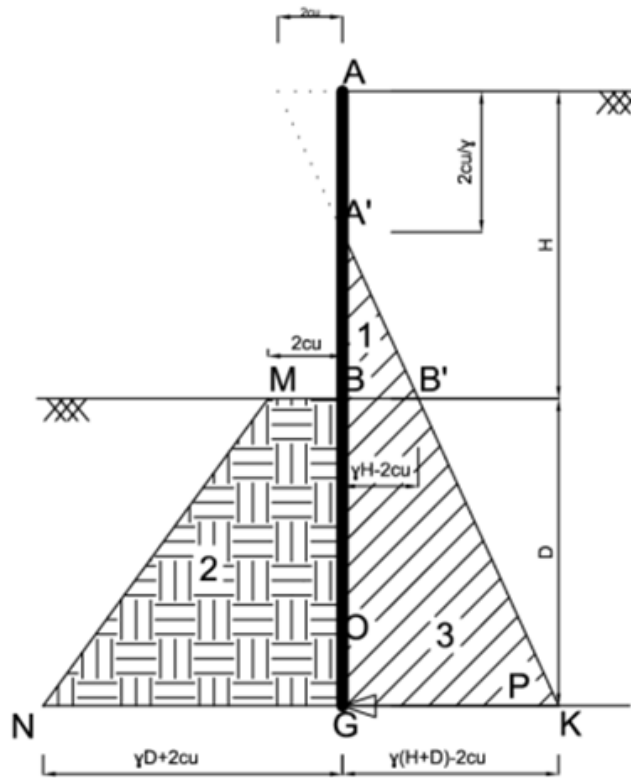
Figure 3. 12; Lateral pressure distribution used in analysis method 3b

Table 3. 19; Force and moment formulas

Area ID	force equilibrium (ΣFx);	force equilibrium (ΣFx);	Moment Arm (wrt bottom)
AGK	$(\gamma.(H+D)-2(c_u/FS))$. $(D+H-2cu/FS/\gamma)/2$		$(D+H-2c_u/FS/\gamma)/3$
MNBG	$(4(c_u/FS)+\gamma D)/2*D$	A(MNBG)-A(ABB')+P	
	Triangular Area		D/3
	Rectangular Area		D/2

3.2.6 LE Solution with Simplified Method, Superposed Distribution with Active Pressures from Crack Height (3b)

Table 3. 20; Force and moment equations used in method 3b

Area ID	Formula	force equilibrium (ΣFx);	force equilibrium (ΣFx);	Moment Arm (wrt bottom)
ABB'	B'*(H-2cu/FS/ɣ)/2	$(\gamma.H-2(cu/FS))*$ $(H-2cu/FS/\gamma)/2$	A(BCFG)-A(ABB')+P	$D+(H-2c_u/FS/\gamma)/3$
BCFG	C*D	$(4(c_u/FS)-\gamma H)*D$		D/2

54
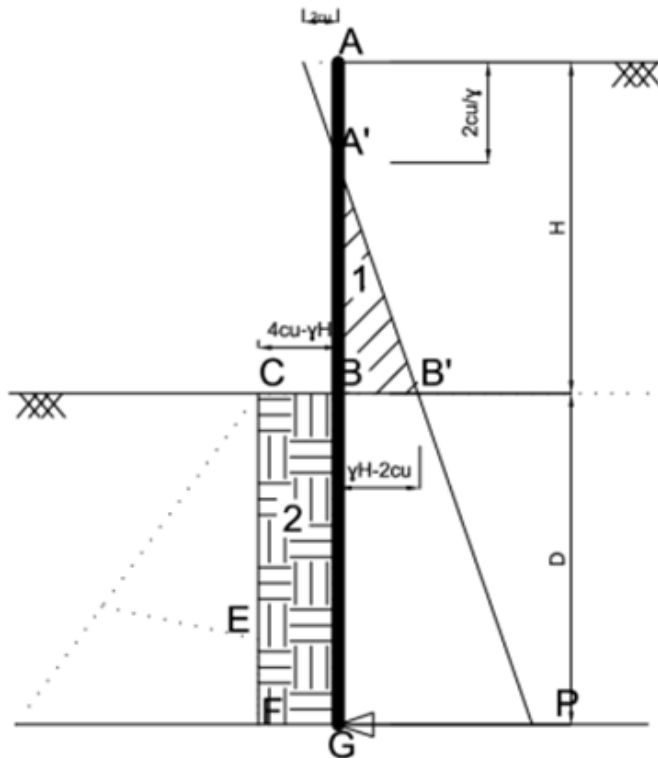
Figure 3. 13; Lateral earth pressure distribution used in analysis method 3b

Since considered lateral pressure zones are exactly the same in 3a and 3b, these two analysis methods provide the same results.

3.3   Strut Supported Wall Retaining Sand

PLAXIS results show that the deformed shapes of the analyzed cases are more in line with the free earth support assumption. Since free earth support method is used in calculations of strut supported walls, pile is free to rotate and translate at toe level. With this consideration, solution procedure is reduced to one equation which is the moment equation with respect to strut level. Calculating moments with respect to level of strut eliminates the moment due to the strut force, hence, the only unknown in the calculations is the factor of safety. In analysis of strut supported walls retaining sand, pressure distribution given in figure 3.14 is used. Strut provides horizontal fixity at depth "d" from ground level. Instead of determining the depth of embedment, "D" in design, in analysis, FS is the unknown with D_1 & y heights as well. To determine these three unknowns; in addition to moment equilibrium, two geometry-based equations given below are solved.

$$\frac{y}{D_1} = \frac{\gamma * H * K_a}{\gamma * (\frac{K_p}{FS} - K_a) * D_1}$$ (3.12)

$$D = y + D_1$$ (3.13)
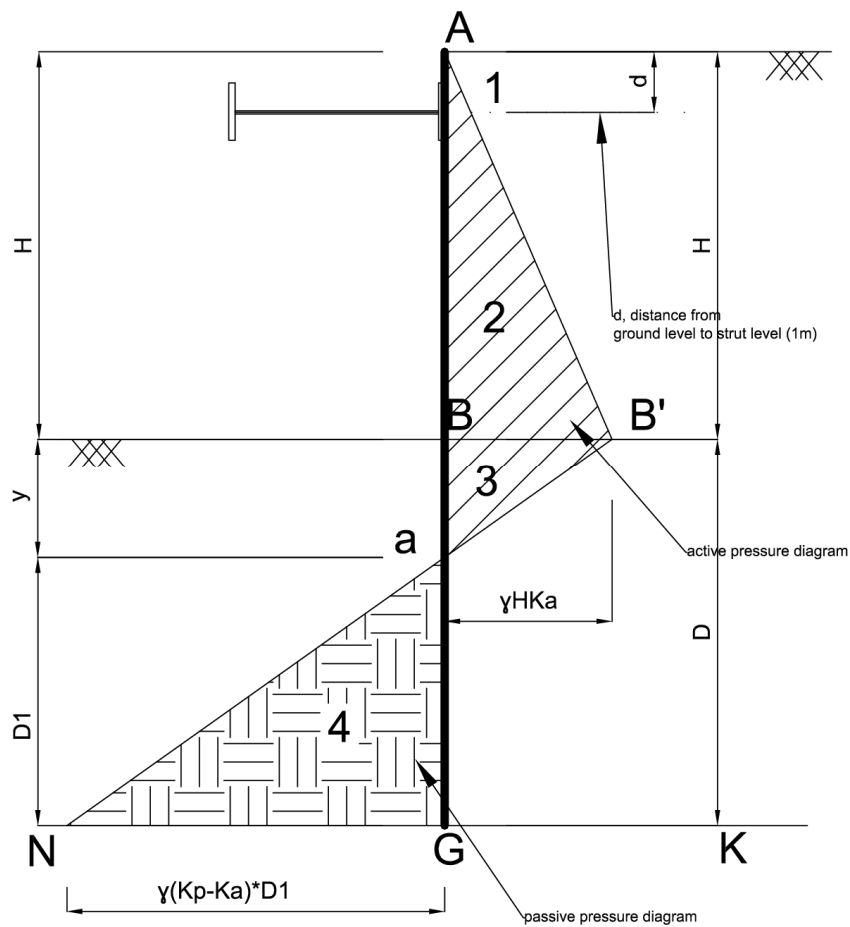
Figure 3. 14; Lateral earth pressure diagram of strut supported wall in sand

Table 3.21 shows the lateral pressures at corresponding points along the wall. Forces are calculated with these pressures with formulas in table 3.22. With these forces, moment calculations are done. Finally, combining the moment equilibrium equation with two equations above, the safety factor is determined. Also, force on the strut for 1 meter of wall can be calculated from ΣF = 0 after determining the unknowns.

Table 3. 21; Lateral earth pressures

Point	Equation
B'	$\gamma_{dry}.H.K_a$
N	$\gamma_{dry}(K_p/FS-K_a).(D_1)$
O	$\gamma_{dry}.K_a.d$

Table 3. 22; Moment equation calculations

Area	Force Equation	Moment Arm (w.r.t. "O")	Direction (wrt "d")	Direction
1	$\gamma_{dry}.d.K_a.d/2$	$d/3$	CCW	Restoring
2a	$\gamma_{dry}.K_a.(d).(H-d)$	$(H-d)/2$	CW	Over Turning
2b	$\gamma_{dry}.K_a(H-d)*(H-d)/2$	$2*(H-d)/3$	CW	Over Turning
3	$\gamma_{dry}.H.(K_a).y/2$	$H-d+(y/3)$	CW	Over Turning
4	$\gamma_{dry}.(K_p/FS-K_a).(D_1)^2/2$	$H-d+y+(2*D_1/3)$	CCW	Restoring

3.4 Strut Supported Wall Retaining Clay

Free earth support pressure diagram used in this method is presented in figure 3.15 and formulas used in calculations are presented in tables 23 & 24.

Table 3. 23; Lateral earth pressures

Point	P Formulae
B'	$\gamma.H-2(c_u/FS)$
M, N	$4(c_u/FS)-\gamma.H$

Table 3. 24; force equations with corresponding moment arms with respect to strut level, O

Area ID	Formula	force equilibrium (ΣFx);	force equilibrium (ΣFx);	Moment Arm (wrt Strut Lvl)
ABB'	B'*H/2	$(\gamma.H-2(cu/FS))*H/2$	A(BCFG)-A(ABB')+P	$2H/3-d$
MNBG	M*D	$(4(c_u/FS)-\gamma H)*D$		$D/2+H-d$
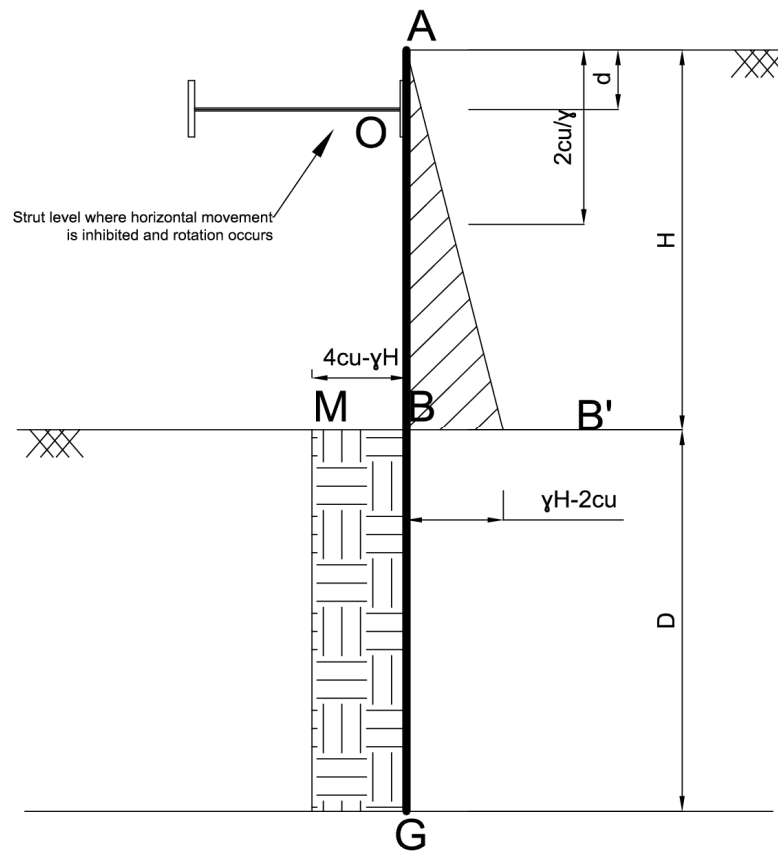
Figure 3. 15; Lateral earth pressure diagram of strut supported wall in clay

3.5   Numerical Modeling Analysis Methods

In numerical modeling, four different methods are used. The first method uses a built-in calculation option of PLAXIS, and the other three are derived from the results of the analyses. Details on how the analyses are carried out is presented in this chapter.

3.5.1   Phi-c Reduction Method Outputs (P1)

The first one of these methods is phi-c reduction analysis of PLAXIS. This section presents the methodology used in obtaining ΣMsf value for the models. ΣMsf is the only value that can be directly reached at the end of analysis, among the others. As discussed in 2.5.2.2.2, phi-c reduction method provides an overall safety factor for the model. Results of these analyses are referred in tables as "PLAXIS Solution -I-".

An important point to be considered in interpreting the results of phi-c reduction is the number of steps to be reached to finish the calculations. In phi-c reduction method, system is loaded (by reducing soil strength) step by step, until it fails. If the inital conditions are

close to the failure conditions, number of steps for the model to fail is not expected to be high and it is expected to fail within the predefined number of maximum steps. But, in some cases, the default number of steps are not high enough for the system to fail. This situation results in a case that, increasing step number leads to increasing ΣMsf values. The curves module should be used to check whether the ΣMsf value converges with increasing number of steps, or not. In order to check the convergence, points in failure zone should be marked for curves output before running analyses. Figure 3.16 below shows an example of curves output.
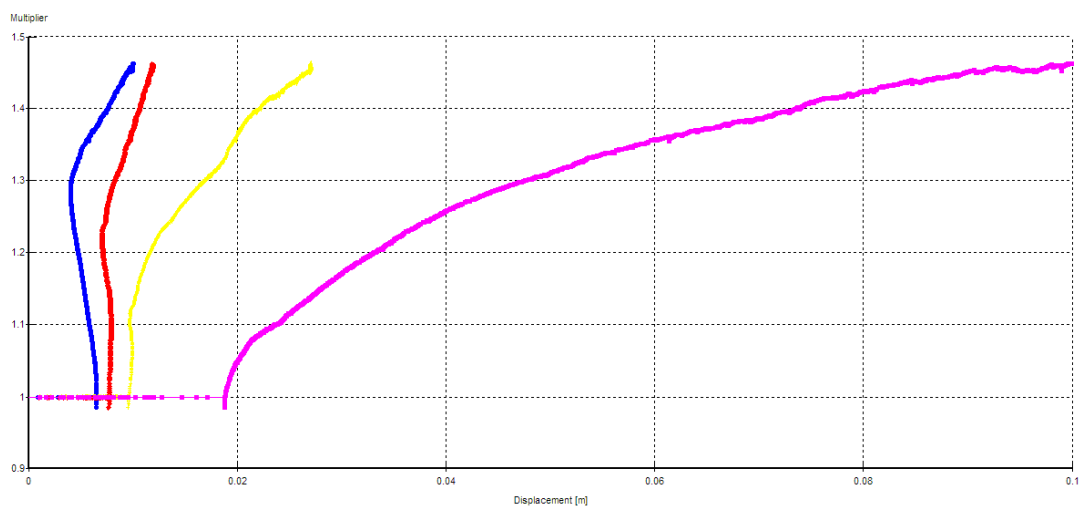
Figure 3. 16; ΣMsf vs displacement curve, values reached at the end of analyses for points picked within the failure zone, x-axis representing displacements and y-axis representing ΣMsf multiplier

For the example curves output given in figure 3.16, three curves on left of the graph presents Msf values obtained at relatively safer zones, compared with the curve on right of the graph, which limits the resultant Msf value to its final value, (1.463 in this case) at the end of 1000th step. If the analysis was run with lower step number, the ΣMsf value provided by output module would have been lower than 1.463.

Figure 3.17 shows two different analyses where curve on the left represents strut supported sand with ϕ = 40˚ and H = 12m, curve on the right represents cantilever sand with ϕ = 40˚ and H = 8m. It can be seen from the figure that strut supported model (curve on left) reaches its limiting ΣMsf value at early steps and deviates very little from the first reached value. On the other hand, for cantilever model, it takes more than 1000 steps

(actually, for PLAXIS v8.2, ultimate number of additional steps is 1000) for the ΣMsf value to be used in calculations to reach its limiting value.
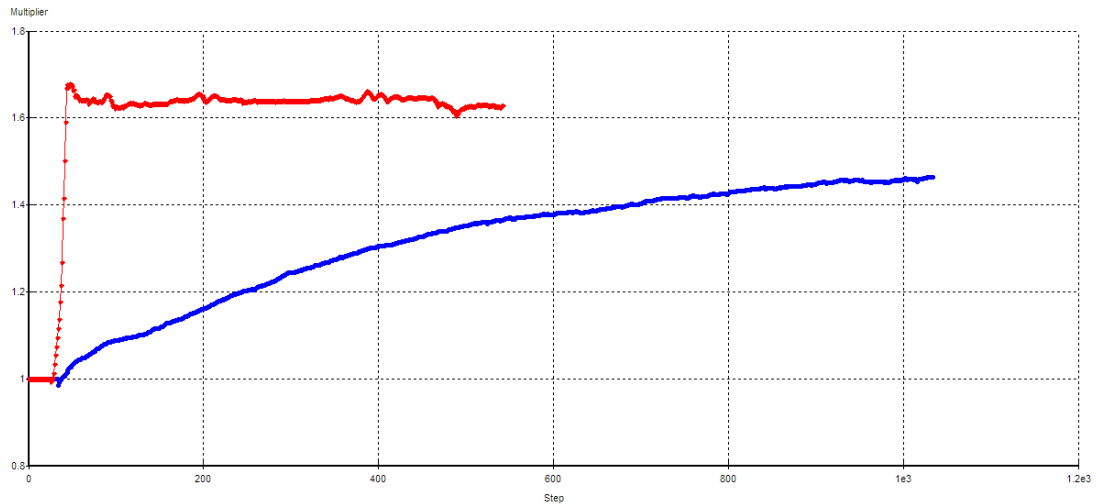
Figure 3. 17; ΣMsf vs Number of Steps Curve for a cantilever and a strut supported model, x-axis representing step number and y-axis representing ΣMsf multiplier

Another point to be considered in analysis results is that, while working with undrained clay models, after some step where the ΣMsf converges to a value, it drops excessively. Since the dropped value is the final value of ΣMsf, reached value in calculations module displays the dropped – incorrect ΣMsf. Figure 3.18 shows the situation mentioned.
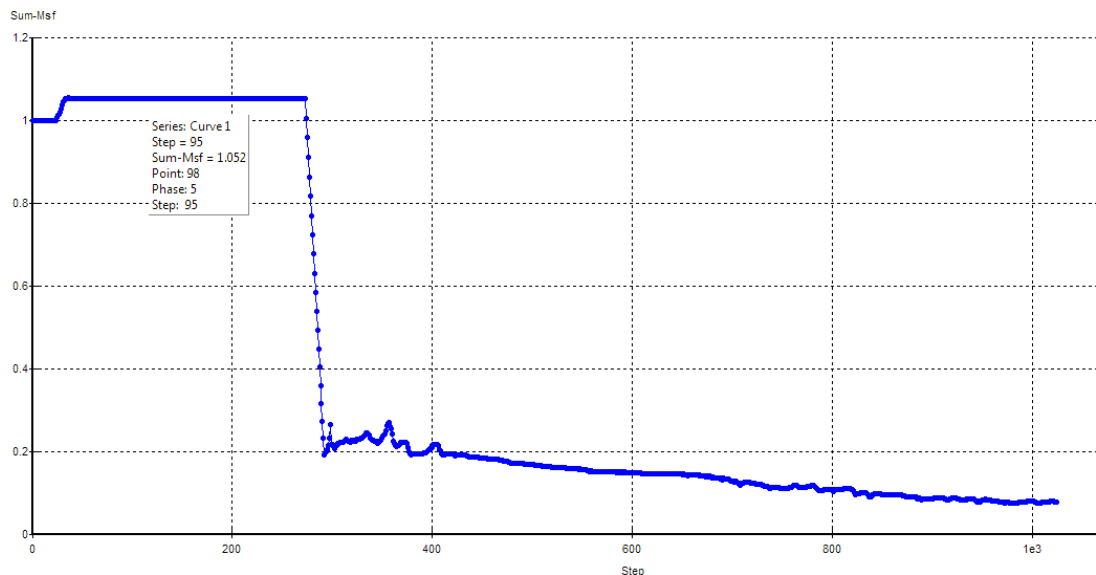
Figure 3. 18; ΣMsf vs Number of Step Chart for strut supported clay, c = 75 kPa & H = 12m, x-axis representing step number and y-axis representing ΣMsf multiplier

As can be seen from the figure 3.18, the ΣMsf value is 1.052 up to step 271, after then, it reduces down to 0.09 and analysis ends. The final value for the analysis is displayed as 0.09 in reached values tab in calculations module, however, obviously it is not. The reason for this situation is the excessive displacements of the wall, which is due to reduced soil parameters.

For the reasons explained above, phi-c reduction analyses in this research were carried out upto the maximum number of steps, in order to prevent any misleading ΣMsf values. Curves module is used in each analysis to determine the ΣMsf value accurately.

3.5.2 Solutions Obtained from the Ratio of Ultimate Passive Forces to Working State Passive Forces (P2)

Lateral earth pressures acting on the wall are different in limit equilibrium analyses and PLAXIS outputs. Limit equilibrium analyses consider the ultimate case with fully active and passive lateral pressures. On the other hand, PLAXIS calculates the stresses at the working state.

PLAXIS analyzes working state and its outputs provide working state lateral earth pressure components along the wall for each node point. Lateral forces acting on wall can be calculated from the outputs.

The passive pressures calculated by PLAXIS are the stress applied to the soil by the wall, and the passive pressures given by Rankine distribution are the available resistance. Ratio of resultants these stresses (i.e. total passive forces) presents the FS value to be obtained from this method of analysis.

$$ FS = \frac{F_{passive, \, limit \, equilibrium \, analysis}}{F_{passive, \, plaxis \, outputs}} $$

(3.14)

For limit equilibrium analysis, this is achieved by calculating the forces using FS = 1 in calculations. γ is the dry unit weight of soil, D is the embedment depth of wall, x is the distance from pile toe. Equations 3.15 and 3.16 express available passive resistance for sand and clay, respectively.

$$F_{passive,\,limit\ equilibrium\ analysis} = \gamma_{dry}*(D\text{-}x)*K_p*\frac{(D\text{-}x)}{2} \qquad (3.15)$$

$$F_{passive,\,plaxis\ outputs} = \sum \frac{(a_i + b_i)}{2}*\partial_i \qquad (3.16)$$

For PLAXIS outputs, forces are calculated from lateral pressure data of each node component along the wall, as shown below in figure 3.19. Triangular mesh elements by which PLAXIS is establishing matrices of parameters and handling calculations can be seen in the figure. Each element is formed from 15 nodes (red crosses). PLAXIS calculates lateral pressures to be used in calculations, as well as displacements and other unknowns for these elements.

a

b
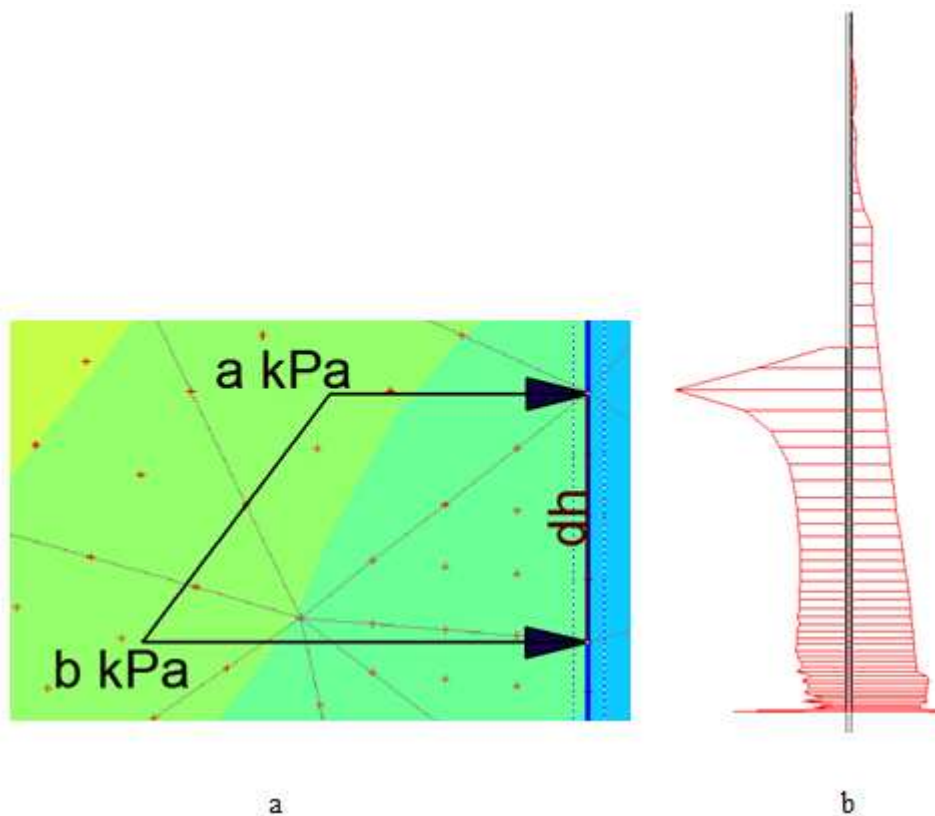
Figure 3. 19; a. Lateral earth pressures acting on pile forming trapezoidal areas for calculation of lateral forces (showing single trapezoidal area), b. Sample of general view of lateral pressure distribution on wall (ϕ = 40˚ and H = 5.5m)

As can be seen from the figure, lateral forces can be calculated for various depths of wall. Formulative expression of the numerical integration is presented below.

In order to visualize the difference between the forces calculated from limit equilibrium methods and PLAXIS outputs, force vs depth diagram is presented below, in figure 3.20. It can be easily seen that, active forces generated in retained side of the wall are very close, on the other hand, passive forces calculated from limit equilibrium methods are greater than PLAXIS calculations. This shows that, active lateral pressures are almost fully generated, but passive lateral forces are not, yet, with the present displacements.
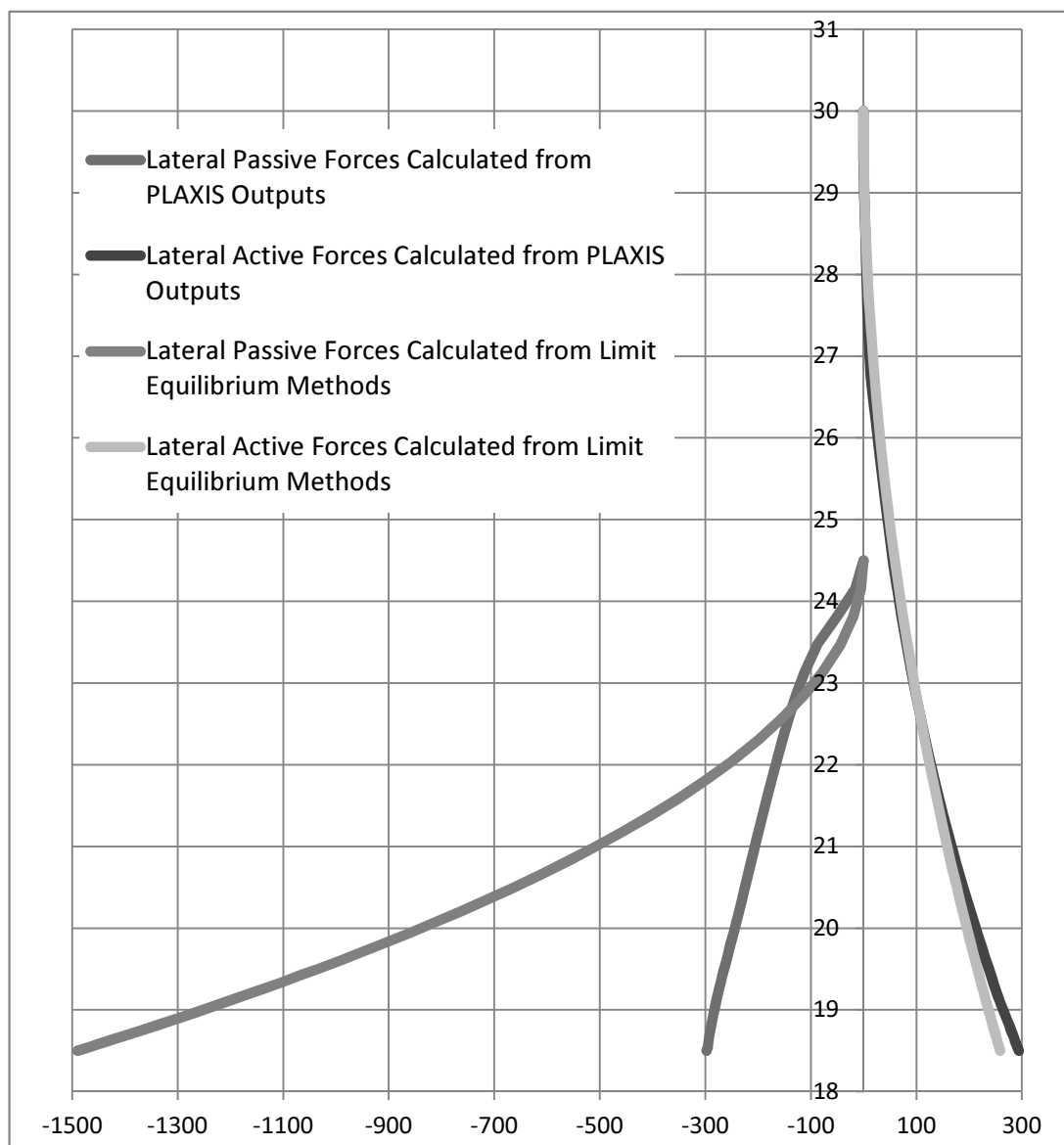
Figure 3. 20; Force comparison diagram for limit equilibrium & PLAXIS results

3.5.3 Solutions Obtained from Calculation of Shearing Forces Along the Shearing Planes (P3)

In this analysis method, shearing planes on which soil fails are concerned. Stresses along these planes are calculated and the safety factor of the model is derived from formula 3.17;

$$FS = \frac{\int_0^D (c + \sigma \tan \varphi)\, dL}{\int_0^D \tau \cdot dL} = \frac{c \cdot \int_0^D dL + \tan \varphi \cdot \int_0^D \sigma \cdot dL}{\int_0^D \tau \cdot dL} \tag{3.17}$$

Where, c_u is the undrained shear strength, ϕ is the internal friction angle of soil, dL is the length between two nodes where stresses are provided, σ and τ are the normal and shear stresses, respectively. Similar to figure 3.19, trapezoidal stress distributions are created between consecutive nodes and forces are calculated for each element along the shearing planes, by numerical integration.

Shearing planes are determined by PLAXIS displacement outputs of phi-c reduction analysis method, which provides visualisation of these failure planes. A sample of these shearing planes is shown in figure 3.21.
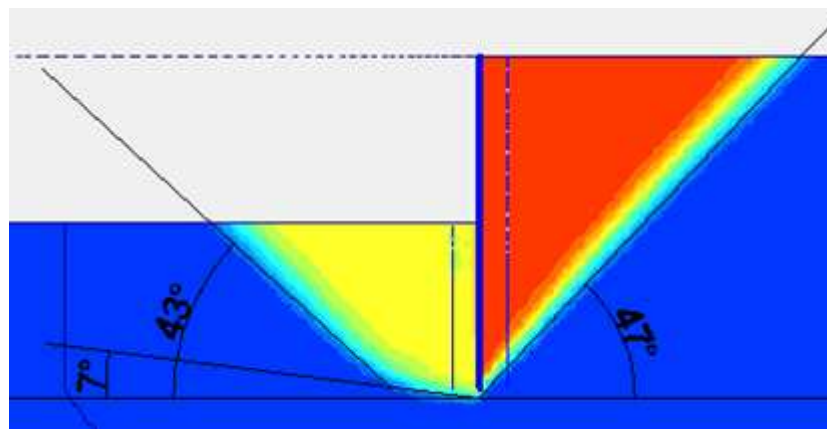
Figure 3. 21; Total displacements of an undrained clay model failed after phi - c reduction

After determining the planes, the coordinates of these planes are defined in PLAXIS and stresses along them are derived. Figure 3.22 presents the potential shear failure planes, drawn at the end of staged construction phase (working state).
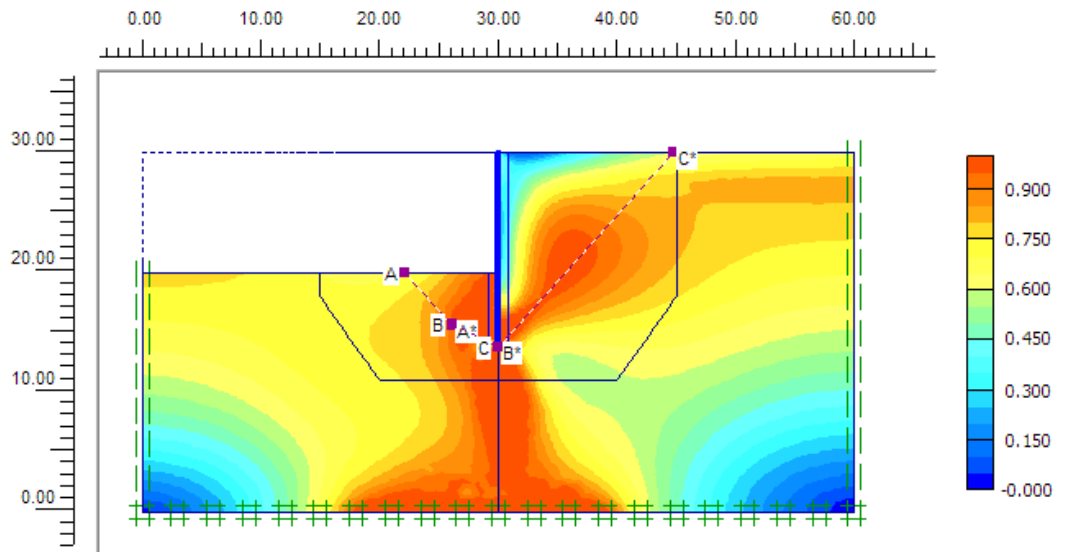
Figure 3. 22; Shearing planes applied at the end of staged construction (NOT in phi - c reduction phase)

In determining shearing planes of cohesionless models, the failure plane is not clear in excavated side of wall, even after phi-c reduction analysis. Therefore, shearing planes are selected as estimated by Rankine Theory (i.e. $45 + \phi/2$ on active and $45 - \phi/2$ on passive side).

3.5.4 Solutions Obtained from Ratio of Strength Reduced in Excavated Side of the Model (P4)

Phi-c reduction method reduces the soil parameters step by step in the entire model, and determines the lowest strength parameter with which the section can withstand lateral earth pressures. However, the conventional hand solutions generally apply an FS only to the passive side (see section 2.3.2). With the aim of catching a better correlation, instead of reducing the parameters in all model, in this methodology, reducing the soil parameters of only the excavated side of the model is investigated. The difference between the two approaches and how the results are derived is explained below.

The critical case to be obtained at the end of the analysis is achieved by decreasing ΣMsf value as low as possible, close to 1. In order to achieve this condition, for cohesionless models ϕ, and for undrained cohesive models, c_u parameter of soil in excavated side is reduced gradually.

The logic behind keeping the ΣMsf value equal to 1 is that, by this way, phi- c reduction method can not reduce the soil parameter of the retained side (which is expected to be kept constant for this methodology to success), resulting in, the only difference that is driving the system to failure is reducing excavated side's parameter manually.

The lowest parameter that provides the lowest ΣMsf value is used for obtaining an FS from the ratio of unchanged parameters and dropped parameters, as equations 3.18 and 3.19 below presents.

$$FS_{cohesionless} = \frac{\tan \phi_{initial}}{\tan \phi_{dropped}}$$

(3.18)

$$FS_{cohesive} = \frac{c_{u,\ initial}}{c_{u,\ dropped}}$$

(3.19)

A sample analysis procedure is presented in table 3.25. As can be seen from the table, the lowest phi parameter in excavated that satisfies ΣMsf = 1 is 18 degrees. The FS value to be calculated following the metholodgy described above is given in equation 3.20.

Table 3. 25; ΣMsf values of sand model, initial ϕ = 30˚ and H = 6m

excavated ϕ	retained ϕ	ΣMsf	Disp. (mm)
30	30	1.320	40.19
16	30	0.973	NA
18	30	1.017	88.78

$$FS = \frac{\tan 30}{\tan 18} = 1,78$$

(3.20)

It should be noted that this method takes a lot more time than any of the other manual or numerical procedures described in the preceding sections. Therefore it is the most impractical way of estimating the FS.

3.5.5   Parameters Used in PLAXIS

Cohesionless and cohesive soils are divided into three main analysis group. For cohesionless soils, ϕ = 30, 35 & 40°, and for cohesive soils c = 50, 75 & 100 kPa are chosen as main groups. Additional analyses are done for parameters in between these major in order to increase number of analyses in an interval. Parameters of these groups are assigned as;

Table 3. 26; Soil properties

Material Model			Mohr Coulomb	
Parameter			Sand	Clay
Type of Material Behaviour			Drained	Undrained
Soil Unit Weight Above Phreatic Level	γ_{unsat}	kN/m^3	18	18
Soil Unit Weight Below Phreatic Level	γ_{sat}	kN/m^3	20	20
Permeability in Horizontal Direction	k_x	m/day	1	0.001
Permeability in Vertical Direction	k_y	m/day	1	0.001
Poisson's Ratio	ν	-	0.3	0.35
Young's Modulus	E	kN/m^2	50000	50000
Cohesion	c	kN/m^2	1	50-75-100
Friction Angle	ϕ	°	30-35-40	40
Dilatancy Angle	ψ	°	0	0
E_{incr}	E	kN/m^2	0	0
c_{incr}	c	kN/m^2	0	0
y_{ref}		m/day	0	0
R_{inter}		-	0.67	0.67

Additional material info is required for modeling with hardening soil. Parameters used in addition are listed in table 3.27.

Table 3. 27; Additional soil properties

E_{50}^{ref}	E_{oed}^{ref}	E_{ur}^{ref}	ν_{ur}	P_{ref}	Power	R_f
kN/m^2	kN/m^2	kN/m^2	-	kN/m^2	-	-
50000	50000	150000	0.2	100	0.5	0.9

Piles with diameter of 1m and spacing with center to center distance of 1.20 meters, is used in calculations. Parameters calculated are listed in table 3.28.

Table 3. 28; Pile properties

EA	EI	w	ν	M_p	N_p
kN/m	kN*m^2/m	kN/m^2	-	kN*m/m	kN/m
19600000	1230000	19.64	0.2	1.00E+15	1.00E+15

Equivalent length (half of the excavation width) is taken as 10 meters and struts are planned to be placed in each 5 meters. Parameters obtained for struts are given in table 3.29.

Table 3. 29; Strut properties

EA	$F_{max,comp}$	$F_{max,tens}$	L_e	L_s
kN/m	kN/m	kN/m	m	m
4000000	2.00E+14	2.00E+14	10	5

CHAPTER 4

RESULTS OF ANALYSIS

In this chapter, results obtained from limit equilibrium analyses, PLAXIS results and derivations are presented. Results are grouped in four main categories as; cantilever sand, cantilever clay, strut supported sand and strut supported clay. In each branch, data is plotted with respect to retained height and soil strength parameter. Models considering varying modulus of elasticity and soil model (Mohr Coulomb or Hardening Soil) are plotted as well, individually, and presented in corresponding category.

4.1 Results of Cantilever Walls Retaining in Undrained Sand

Results obtained from four limit equilibrium methods and four PLAXIS methods are presented in table 4.2. For limit equilibrium methods 1a and 1b, distance x from pile tip to rotational point, O is provided below the corresponding FS value.

It can be observed that, this distance is very close for varying retained heights with constant ϕ values. Also, for constant heights, distance is constant as well for varying ϕ values. It can be said that, in limit equilibrium method solutions for cantilever sand models, the distance from pile tip to the rotational point is constant and independent of ϕ value, also, it slightly changes with the retaining height, H. Embedment depth, D, is the determinative parameter for this distance. Table 4.1 shows the change of x distance with changing embedment depths.

Table 4. 1; D vs x comparison

Method	ϕ (˚)	D (m)	H (m)	x (m)	FS
1a	30	6	6	0.64	1.03
		7	6	0.75	1.29
		6	7	0.63	0.81
		7	7	0.74	1.09

Table 4. 2; Cantilever sand analyses results

Safety Factors Obtained All Over the Calculations (Cantilever Sand)	Cantilever Model varying H constant ø=30°			Cantilever Model varying H constant ø=35°					Cantilever Model varying H constant ø=40°							Cantilever Model varying E constant ø=35° & H=8m			Hardening Soil Model		
	ø=30 H=5m	ø=30 H=6m	ø=30 H=7m	ø=35 H=5m	ø=35 H=6m	ø=35 H=7m	ø=35 H=8m	ø=37.5 H=8m	ø=40 H=5m	ø=40 H=5,5m	ø=40 H=6m	ø=40 H=7m	ø=40 H=8m	ø=40 H=9m	ø=40 H=10m	ø=35 H=5m E=30Mpa	ø=35 H=5m E=40Mpa	ø=35 H=5m E=60Mpa	ø=30 H=5m	ø=30 H=6m	ø=30 H=7m
ø°	30	30	30	35	35	35	35	37.5	40	40	40	40	40	40	40	35	35	35	30	30	30
H (m)	5	6	7	5	6	7	8	8	5	5.5	6	7	8	9	10	5	5	5	5	6	7
D (m)	6	6	6	6	6	6	6	6	6	6	6	6	6	6	6	6	6	6	6	6	6
E (Mpa)	50	50	50	50	50	50	50	50	50	50	50	50	50	50	50	30	40	60	50	50	50
1a. Limit Equilibrium Solution with Traditional Method (Full Pressure Distribution)	1.35	1.03	0.81	2.03	1.56	1.22	0.97	1.21	3.16	2.76	2.42	1.89	1.51	1.23	1.01	2.03	2.03	2.03	1.35	1.03	0.81
x (m)	0.64	0.64	0.62	0.64	0.64	0.62	0.61	0.61	0.64	0.64	0.64	0.62	0.61	0.60	0.58	0.64	0.64	0.64	0.64	0.64	0.62
2a. Limit Equilibrium Solution with Simplified Method (Full Pressure Distribution)	1.13	0.85	0.65	1.70	1.28	0.99	0.78	0.96	2.64	2.28	1.99	1.53	1.20	0.96	0.78	1.70	1.70	1.70	1.13	0.85	0.65
1b. Limit Equilibrium Solution with Traditional Method (Superposed Pressure Distribution)	1.30	0.99	0.78	1.97	1.50	1.18	0.94	1.16	3.06	2.66	2.34	1.83	1.46	1.18	0.97	1.97	1.97	1.97	1.30	0.99	0.78
x (m)	0.96	0.95	0.95	0.96	0.96	0.95	0.94	0.94	0.96	1.05	0.96	0.96	0.94	0.93	0.91	0.96	0.96	0.96	0.96	0.95	0.95
2b. Limit Equilibrium Solution with Simplified Method (Superposed Pressure Distribution)	1.12	0.85	0.65	1.70	1.28	0.99	0.77	0.96	2.64	2.28	1.99	1.53	1.20	0.96	0.78	1.70	1.70	1.70	1.13	0.85	0.65
Plaxis Solution -I- ΣMsf Value Obtained from ø-c Reduction Method	1.56	1.32	1.18	1.87	1.58	1.39	1.26	1.36	2.23	2.00	1.87	1.63	1.46	1.32	1.20	1.88	1.87	1.87	1.52	1.34	1.18
Disp. (mm)	11.46	29.85	86.13	7.61	17.46	44.11	103.30	78.28	6.47	8.75	14.30	34.72	67.55	100.00	104.00	58.24	43.66	29.13	11.95	23.75	47.76
Plaxis Solution -II- Ratio of Ultimate Passive Forces to Working State Passive Forces	2.34	1.99	1.60	3.48	3.02	2.52	1.91	2.45	5.55	5.01	4.50	3.60	2.93	2.39	2.04	3.48	3.48	3.47	1.89	1.61	1.40
Plaxis Solution -III- Shear Calculations	2.49	2.31	1.80	2.42	2.25	2.20	2.56	2.83	2.38	2.26	2.30	3.09	2.98	2.49	2.33	2.43	2.20	2.19	2.63	2.50	2.16
Plaxis Solution -IV- Ratio of ø Reduced in Excavated Side	2.72	1.78	1.39	4.98	2.61	2.03	1.50	1.81	7.98	5.30	4.76	2.44	1.89	1.45	1.40				2.32	1.78	1.36

70

FS values obtained for traditional methods from superposed pressure distributions (1a and 1b) are very close to full pressure distributions. It can be concluded that both methods can be used in analysis, where ±0.05 difference in FS exists between the results. FS values obtained for simplified methods from superposed and full distributions provide same results. Because of this, in regression analysis of results, data obtained from solution 2b is not used.
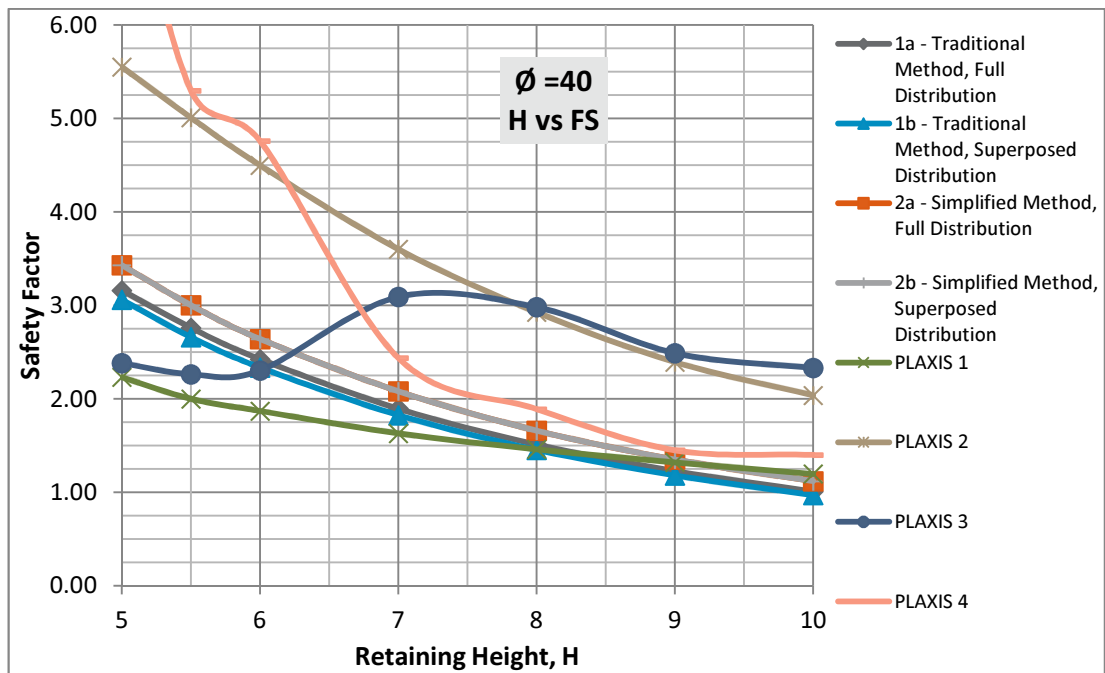

Figure 4. 1; Retaining height vs factor of safety graph for ϕ = 40 (see Appendix A for ϕ = 30 and ϕ = 35 graphs)

FS values obtained from simplified methods are relatively lower than traditional method's results, which is reasonable, since, in simplified method, it is considered that the whole embedment depth is in passive zone below dredge level (explained in detail in section 3.1). An example may given as follows; D is provided as 5m in simplified methods. On the other hand, if cantilever sand model with ϕ = 30 is considered, for traditional methods, depth of passive resistance is calculated as 6m (embedment depth) – 0.64m (distance from pile tip to rotational point) = 5.36m, which is greater than 5m and hence provides larger passive resistance. As a result, higher FS is obtained.

Phi-c reduction method results (PLAXIS Solution 1) are provided in table 4.2 with corresponding working state results' maximum horizontal pile displacements of each model. For small heights, results obtained from PLAXIS 1 are lower compared to limit equilibrium methods. With increasing retained height, limit equilibrium method's FS results drop faster than PLAXIS 1 results. This is an expected situation since limit equilibrium methods use full passive capacity in D depth for all heights, so, no additional passive – restoring force can be obtained from passive zone to compensate increasing lateral forces due to increase of retaining height. On the other hand, in PLAXIS 1, passive pressures are generated gradually with increasing retained heights, which provides PLAXIS 1 FS results to be higher than limit equilibrium results for increasing heights, also resulting in increasing displacements (see figure 4.1).
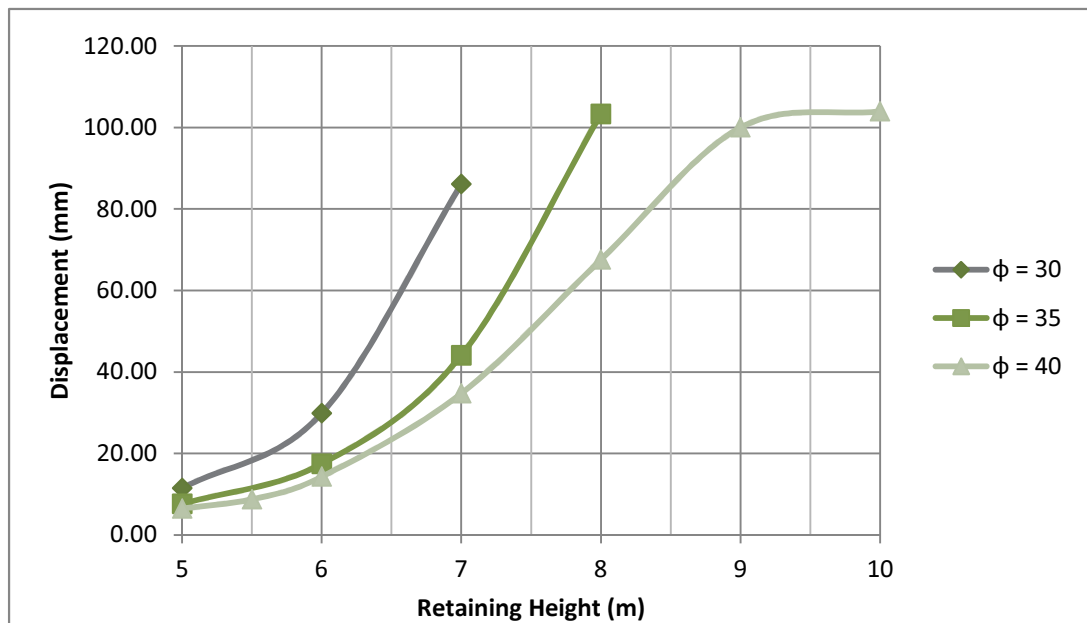

Figure 4. 2; Retaining height, H vs displacement graph for ϕ = 30, 35 & 40

As heights increase, for constant embedment depth, wall displacements are increased as well, as expected. Figure 4.2 shows the horizontal displacements of models with increasing retaining heights, for each ϕ value.

In staged construction analysis step of full depth excavation, for higher retaining heights, the relatively high displacements cause wedges to form in retained side of wall (see figure 4.3). This situation leads PLAXIS calculation module to failure. In order to avoid this situation, instead of "standard settings" in "iterative procedure" menu, manual controls with higher "tolerated errors" are used. FS fields filled with grey in table 4.2 represent this

type of analyses. Figure 4.3 shows an example of formation of wedges on retained side of walls. Wedges are surrounded by Mohr-Coulomb points. Red squares represent Mohr-Coulomb points (plastic points) where $\tau = \sigma * \tan\phi + c$.
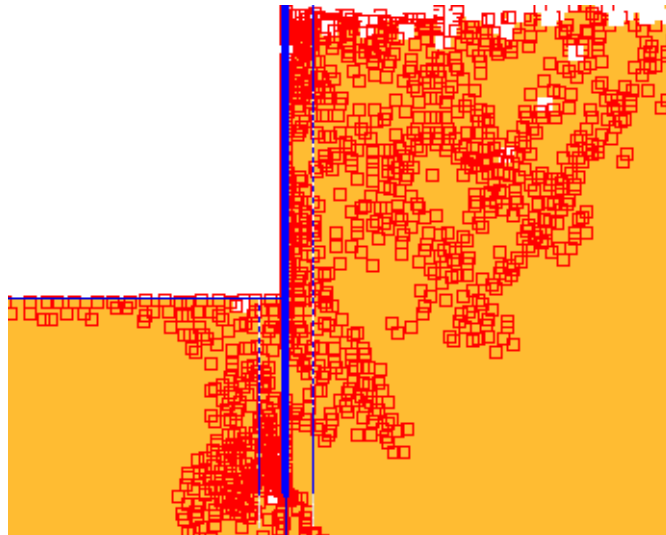

Figure 4. 3; Wedge formation at upper elevations on retained side of cantilever wall in sand, ϕ = 40 & H = 9m

PLAXIS 2 results provide higher FS values compared to limit equilibrium and PLAXIS 1 results. Other than that, results obtained match well with the rest of the data set, except that results of PLAXIS 2 are slightly higher compared to other solutions.

PLAXIS 3 analyses on the other hand, provide unreliable results. For heights of 6 & 7m, although the retaining height increases, FS increases as well, which is an unrealistic situation. The reason for this is that the true failure planes do not match with the 45 ± ϕ /2 Rankine failure planes. Very little slope differences or non-linearities in shear plane formations result in great difference between real and calculated FS values. This may be the reason of unexpected results of PLAXIS 3. Also, the difference of results between PLAXIS 3 and other methods can be seen in figure 4.4. Since the results are not reliable, they are not used in regression analyses of cantilever sand models.

PLAXIS 4 analyses provided very high results for safer conditions where retaining heights are relatively low. On the other hand, with increasing H, results converge to limit equilibrium results, as can be seen in figure 4.1. Also, for increasing ϕ values (safer conditions), PLAXIS 4 results increase more rapid than other methods (see figure 4.4).

Solutions from 1a, 1b, 2a, PLAXIS 1, PLAXIS 2 and PLAXIS 4 are used in further calculations. Additional analysis results are also presented in table 4.2 for varying modulus of elasticity and hardening soil model. Graphs regarding comparison of these models are presented in figures 4.5 & 4.6, respectively. Since the analysis is related to PLAXIS results, outputs are provided for FS values of PLAXIS results only.
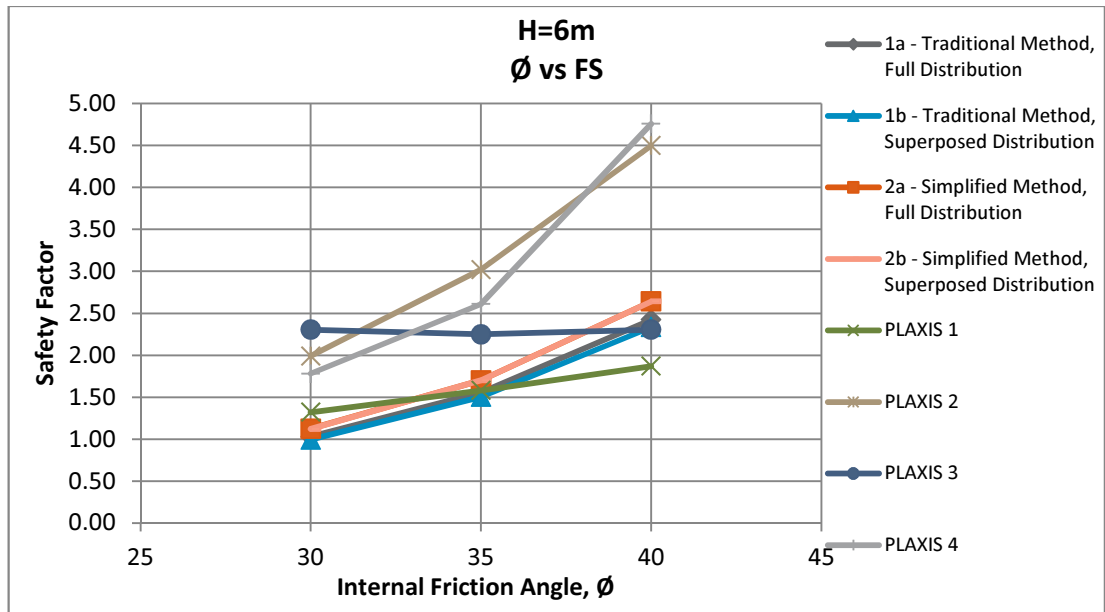

Figure 4. 4; Internal friction angle, ϕ vs safety factor for H = 6m

Results obtained using hardening soil model provided very close (almost the same) results with Mohr Coulomb model considering ΣMsf values in PLAXIS 1 results. This situation can be explained by emphasizing that phi-c reduction method uses the initial parameters for stress and stiffness matrices, obtained at the beginning of the calculations, that are obeying Mohr Coulomb soil model. PLAXIS manual describes this situation in detail, as; "When using phi-c reduction in combination with advanced soil models, these models will actually behave as a standard Mohr-Coulomb model, since stress-dependent stiffness behaviour and hardening effects are excluded". Also PLAXIS 4 results are the same for the models.

PLAXIS 2 results of hardening soil model provide lower FS values, which indicates that passive forces generated in hardening soil models are greater than those in Mohr Coulomb model, so that the LE / PLAXIS 2 ratios are lower, where LE is constant.

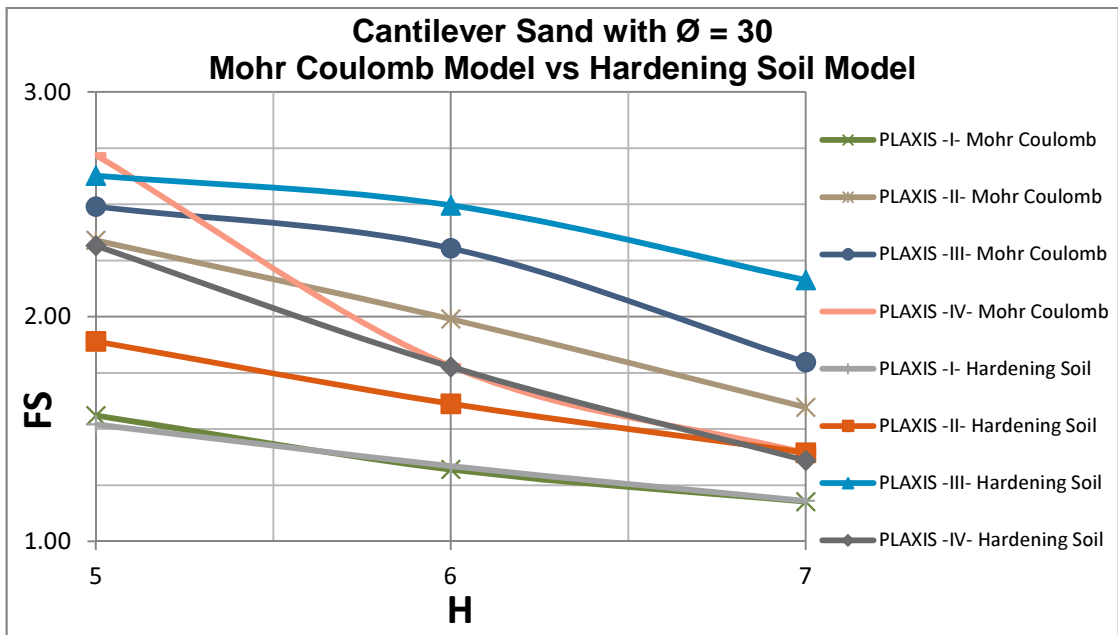PLAXIS 3 results for hardening soil model are higher than Mohr Coulomb model results.

Figure 4. 5; Cantilever sand models, Mohr Coulomb vs Hardening Soil Model comparison chart

Results obtained for varying modulus of elasticity provided in figure 4.6 show that this parameter does not effect the safety factors obtained and calculated (fluctuations in results of PLAXIS 3 analysis are due to uncertainty in the determination of shearing planes). On the other hand, displacements obtained strongly depends on E and can be seen in figure 4.6.
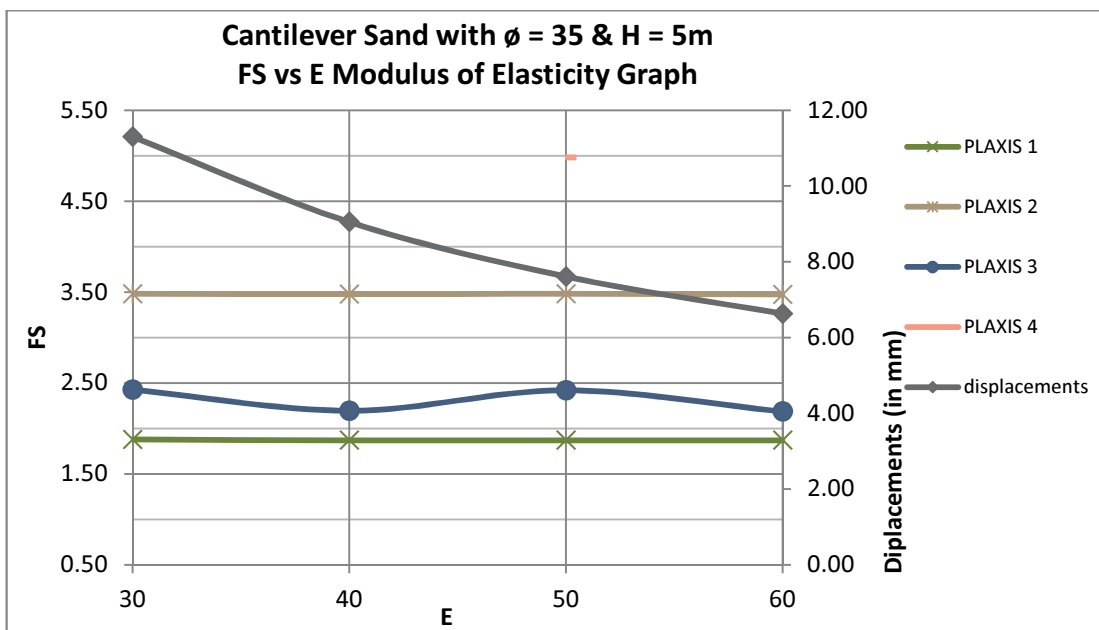

Figure 4. 6; Cantilever sand models, modulus of elasticity vs FS and displacement graph

4.2   Results of Cantilever Walls Retaining in Undrained Clay

Analysis results of cantilever clay models are presented in table 4.3. Grey fields are corresponding to PLAXIS 1 results obtained with manual settings, as in sand models. x and z distances for analyses 1a & 1b are presented below the corresponding FS values.

Lowest safety factor values for cantilever retaining walls in undrained clay, are obtained from solutions 1a. x distances for analysis methods 1a & 1b are presented as well. Different from sand models, in clay models, x distance increases with increasing retained heights.

Safety factors obtained from 1b analyses (where disturbing forces are calculated from crack depth) are higher compared to solutions of 1a. This is an expected situation for all models, since in 1b analysis, total disturbing forces are less than 1a analysis due to reducing active pressure height, whereas resisting forces are the same.

Results obtained from 2a are the same with results of 2c and these two are very close to the results obtained from 1a (2a is the simplified method of 1a and the difference is ±0.05 in FS). This can be explained as 2c pressure diagram is obtained by exactly summing up (without any changes) formulas for lateral pressures at corresponding points.

The reason why the values obtained from 1a is very close (±0.05 in FS) to results of 2a & 2c can be explained with the low value of z depth.

Methodology developed in analysis 2b (FS applied to c_u in passive zone only) provided very high FS values for low retained heights, and very low FS values for increasing H values. The change of 2b results with H is plotted in figure 4.7 (1b results are plotted as well for comparing) for c = 75kPa. The reason why FS values are very high for relatively low retained heights can be explanied as; below dredge level, resultant lateral pressure is $4c_u - \gamma H$ and constant with depth. This results in high FS values for low retained heights where lateral pressures to fail the system is small compared to larger retained heights.

Results obtained from 3a and 3b (which are using the soil below crack depth instead of full height for lateral pressures on the retained side) provided very close results with 1b, which also uses crack height with traditional approach. Again, FS are very close due to small z heights.

Table 4. 3; Safety factors obtained for cantilever clay models

Safety Factors Obtained All Over the Calculations — Cantilever Clay

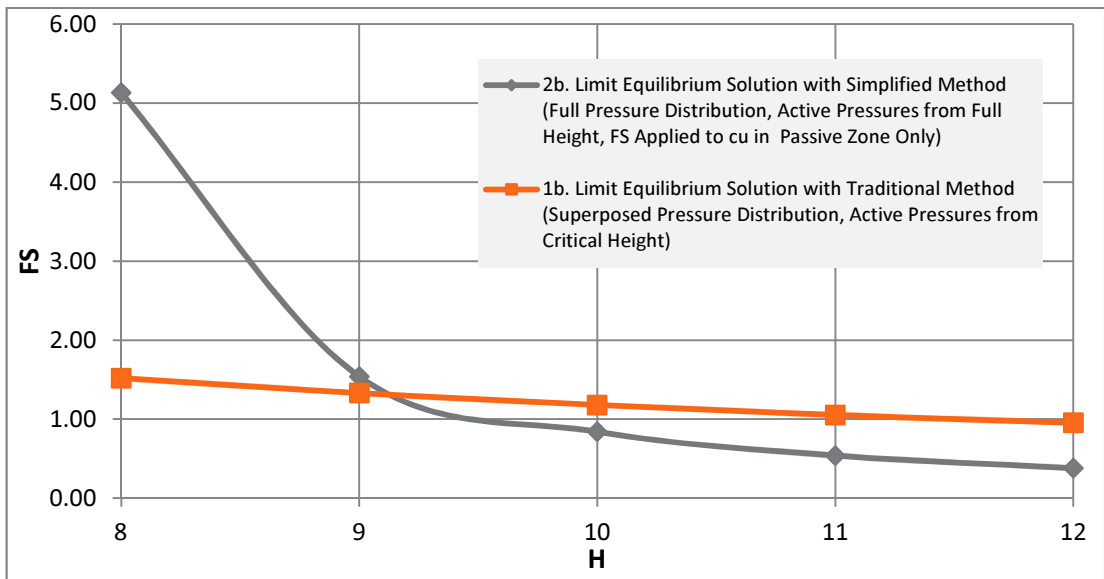| Plaxis Model ID	Cantilever Model varying H constant c =50kPa					Cantilever Model varying H constant c =75kPa							Cantilever Model varying H constant c =100kPa								Cantilever Model varying E constant c =50kPa & H=6m			Hardening Soil Model		
	c=50 H=6m	c=50 H=7m	c=50 H=8m	c=50 H=9m	c=50 H=10m	c=75 H=6m	c=75 H=7m	c=75 H=8m	c=75 H=9m	c=75 H=10m	c=75 H=11m	c=75 H=12m	c=100 H=6m	c=100 H=7m	c=100 H=8m	c=100 H=9m	c=100 H=10m	c=100 H=11m	c=100 H=12m	c=150 H=6m	c=50 H=6m E=30	c=50 H=6m E=40	c=50 H=6m E=60	c=75 H=6m	c=75 H=7m	c=75 H=8m
c (kPa) [x]	50	50	50	50	50	75	75	75	75	75	75	75	100	100	100	100	100	100	100	150	50	50	50	50	50	50
H (m)	6	7	8	9	10	6	7	8	9	10	11	12	6	7	8	9	10	11	12	6	6	6	6	6	7	8
D (m)	6					6							6							6	6	6	6	6		
E (Mpa) [z]	50					50							50							50	30	40	60	50		
1a - Traditional Method, Superposed Distribution, Full Height	1,17	0,97	0,82	0,71	0,63	1,76	1,45	1,23	1,07	0,94	0,84	0,75	2,35	1,94	1,65	1,42	1,25	1,11	1,00	3,52	1,17	1,17	1,17	1,76	1,45	1,23
1b - Traditional Method, Superposed Distribution, Crack Height	1,00	1,09	1,18	1,25	1,32	1,00	1,09	1,18	1,25	1,32	1,37	1,42	1,00	1,09	1,18	1,25	1,31	1,37	1,42	1,00	1,17	1,17	1,17	1,00	1,09	1,18
2a - Simplified Method, Full Distribution, Full Height	1,40	1,18	1,01	0,88	0,78	2,10	1,76	1,52	1,33	1,18	1,05	0,95	2,80	2,35	2,02	1,77	1,57	1,41	1,27	4,19	1,40	1,40	1,40	2,10	1,76	1,52
2a (only passive ratio)	0,56	0,62	0,68	0,74	0,79	0,56	0,62	0,68	0,74	0,79	0,84	0,88	0,56	0,62	0,68	0,74	0,79	0,84	0,88	0,56	0,56	0,56	0,56	0,56	0,62	0,68
2b - Simplified Method, Full Distribution, Full Height (only passive)	1,87	0,82	0,48	0,32	0,23	50,00	50,00	4,34	1,29	0,69	0,45	0,31	50,00	50,00	50,00	50,00	50,00	2,08	0,94	50,00	1,87	1,87	1,87	50,00	50,00	4,34
2c - Simplified Method, Superposed Distribution, Full Height	1,14	0,95	0,81	0,70	0,62	1,72	1,42	1,21	1,05	0,92	0,82	0,74	2,29	1,90	1,61	1,40	1,23	1,10	0,99	3,43	1,14	1,14	1,14	1,72	1,42	1,21
3a - Simplified Method, Full Distribution, Crack Height	1,37	1,15	0,99	0,87	0,77	2,06	1,73	1,49	1,30	1,15	1,03	0,94	2,75	2,31	1,98	1,73	1,54	1,38	1,25	4,12	1,37	1,37	1,37	2,06	1,73	1,49
3b - Simplified Method, Superposed Distribution, Crack Height	1,37	1,15	0,99	0,87	0,77	2,06	1,73	1,49	1,30	1,15	1,03	0,94	2,75	2,31	1,98	1,73	1,54	1,38	1,25	4,12	1,37	1,37	1,37	2,06	1,73	1,49
Plaxis Solution -I- ΣMsf Value Obtained from ø-c Reduction Method	1,79	1,56	1,38	1,24	1,12	2,68	2,34	2,07	1,86	1,68	1,54	1,41	3,57	3,12	2,76	2,48	2,24	2,05	1,88	5,34	1,79	1,79	1,79	2,65	2,32	2,06
Plaxis Solution -I- (Disp.)	18,16	22,59	27,56	32,79	39,00	16,78	19,85	23,76	27,83	32,23	36,61	41,24	16,73	19,25	22,30	25,87	29,83	33,88	37,99	16,72	30,16	22,66	15,17	9,25	11,55	14,84
Plaxis Solution -II- Ratio of Ultimate Passive Forces to Working State Passive Forces	0,87	0,77	0,70	0,63	0,59	1,18	1,06	0,93	0,84	0,77	0,71	0,66	1,46	1,36	1,22	1,09	0,98	0,89	0,82	2,25	0,85	0,85	0,85	1,21	1,07	1,02
Plaxis Solution -III- Shear Calculations	2,78	1,84	1,56	1,35	1,19	4,30	3,05	2,83	2,29	2,04	1,70	1,56	5,20	4,60	4,35	3,60	2,87	2,55	2,24	9,02	2,56	2,49	2,58	3,85	3,20	2,52
Plaxis Solution -IV- Ratio of ø Reduced in Excavated Side	12,50	5,56	2,63	1,85	1,39	50,00	50,00	50,00	50,00	50,00	50,00	6,82	3,95													

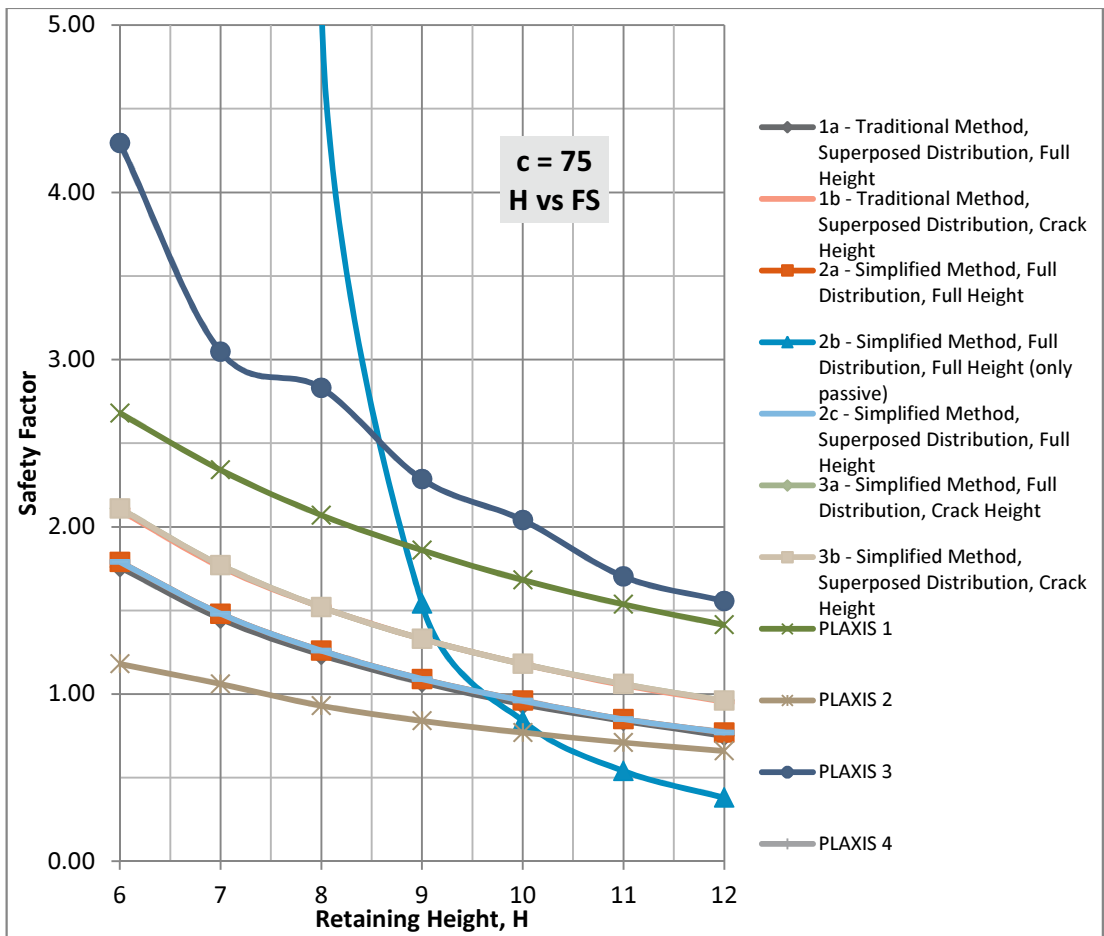Figure 4. 7; FS vs H graph for analysis results 1b & 2b

Figure 4. 8; FS vs H graph for cantilever clay analysis results (see Appendix A for graphs of c_u = 50 kPa & c_u = 100 kPa, also, data plotted for varying c_u values for constant H)

78

Limit equilibrium results obtained from 4 methods; 1a, 1b, 2a and 3a will be used in regression analyses.

PLAXIS 1 method provided higher results compared to limit equilibrium methods throughout the cantilever clay cases, different than sand models where PLAXIS 1 results are below LE results for safer models. Results are in accordance with the rest of data where, no irregularities are present within the FS result set. Also, ultimate lateral displacements of wall is provided below PLAXIS 1 results. Displacement data is as expected; increasing retained heights causes increase in displacements.

Results obtained from PLAXIS 2 analyses provide the lowest FS values, compared to other methods. This situation is because, instead of the assumption of rotating wall in limit equilibrium methods, wall translates horizontally to the excavated zone as well. Soil in excavated area below dredge level, which is under compression, provides higher passive forces compared to limit equilibrium methods. Since PLAXIS 2 uses the ratio of passive forces obtained from limit equilibrium methods and PLAXIS analysis results, FS values obtained are relatively low compared to other methods.

PLAXIS 3 results provide higher FS values within the considered data set (see figure 4.8). Shearing planes are visible through PLAXIS phi-c reduction outputs, and it is easy to obtain the stresses using these planes with working stress analysis outputs. Some fluctuation in data at heights 7 & 8m was observed. Although the shearing planes are easy to locate, the lines to be used in deriving the most critical stresses are placed manually in software, which may lead to small deviations from the main trend of results. PLAXIS 3 results are in well accordance with PLAXIS 1 results especially when models with FS close to 1 are considered.

PLAXIS 4 results provide the highest FS values of the data set. Method involves the ratio of undrained strength in retained side and undrained strength reduced in excavated side where model is at the edge of collapse. This consideration leads to very high FS values for lower retaining heights where crack height is close to dredge level and little lateral pressure trying to fail the system is generated. So, the c_u value of excavated side can be lowered more, compared to a model with greater retained height. In order to explain more clearly, a sample is provided in table 4.4.

Table 4. 4; PLAXIS 4 method example

H (m)	c_u retained side	c_u excavated side	ΣMsf
6	50	50	1.79
		4	1.01

As can be seen, c_u can be dropped to 4 kPa in order to reach ΣMsf = 1. Excessively dropped c_u value results in $FS = 50/4 = 12.5$ which is very high compared to ΣMsf value which is 1.79 for the model. The reason how c_u value can be dropped this much, can be explained as H_{crack} removes most of the active pressure (where $H_{crack} = \dfrac{2*c_u}{\gamma}$). Although the results become closer with increasing retaining heights, still very high to be used, therefore this method is discarded for further calculations. For models of cantilever walls retaining in undrained clay, results obtained from methods 1a, 1b, 2a, 3a, PLAXIS 1, PLAXIS 2 and PLAXIS 3 are used in regression analyses.
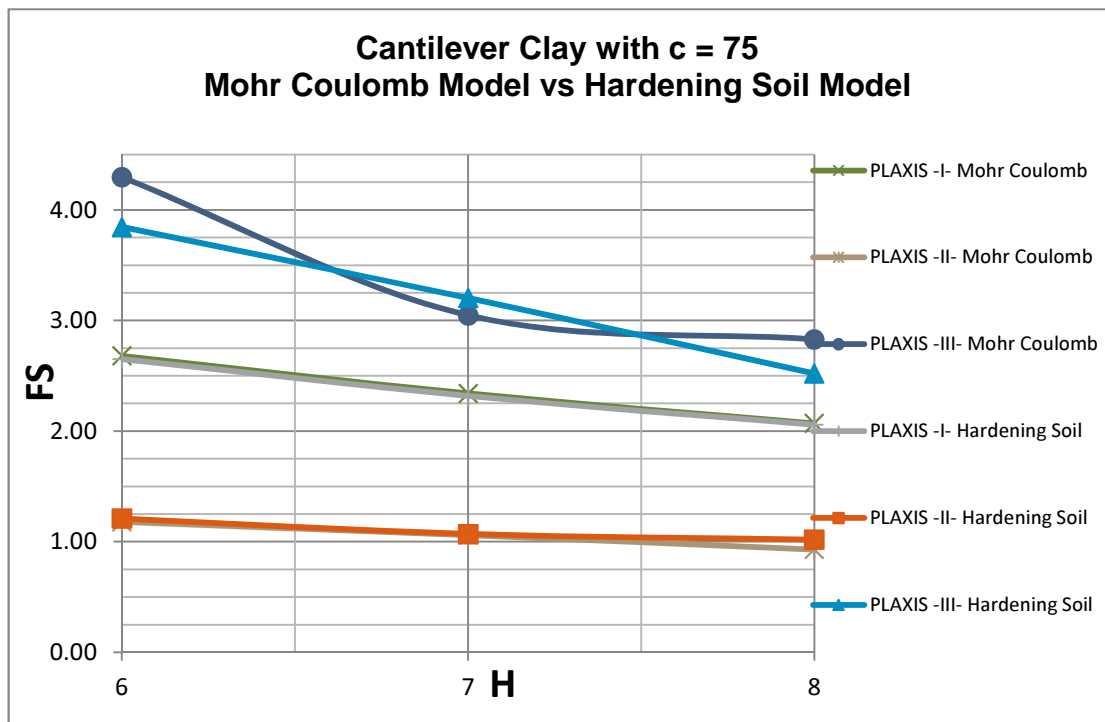
Figure 4. 9; FS vs H graph for cantilever clay analysis results with hardening soil model

Results obtained for hardening soil models provide very close results compared to Mohr Coulomb model. PLAXIS 1 & PLAXIS 2 outputs have ±0.03 & ±0.09 difference, respectively,

as can be seen from figure 4.9. PLAXIS 3 results obtained from hardening soil model provide linear outputs compared to Mohr Coulomb model. Also, displacements are relatively low.

To be compared with sand cases, PLAXIS 1 & 2 outputs are similar, on the other hand, PLAXIS 3 results are dropped in clays, compared to sand models.

Varying modulus of elasticity analyses provided the same FS values, similar to cantilever sand models. Also, as in sand models, displacements are strongly dependent on E. Outputs of modulus of elasticity analyses are plotted in figure 4.10.
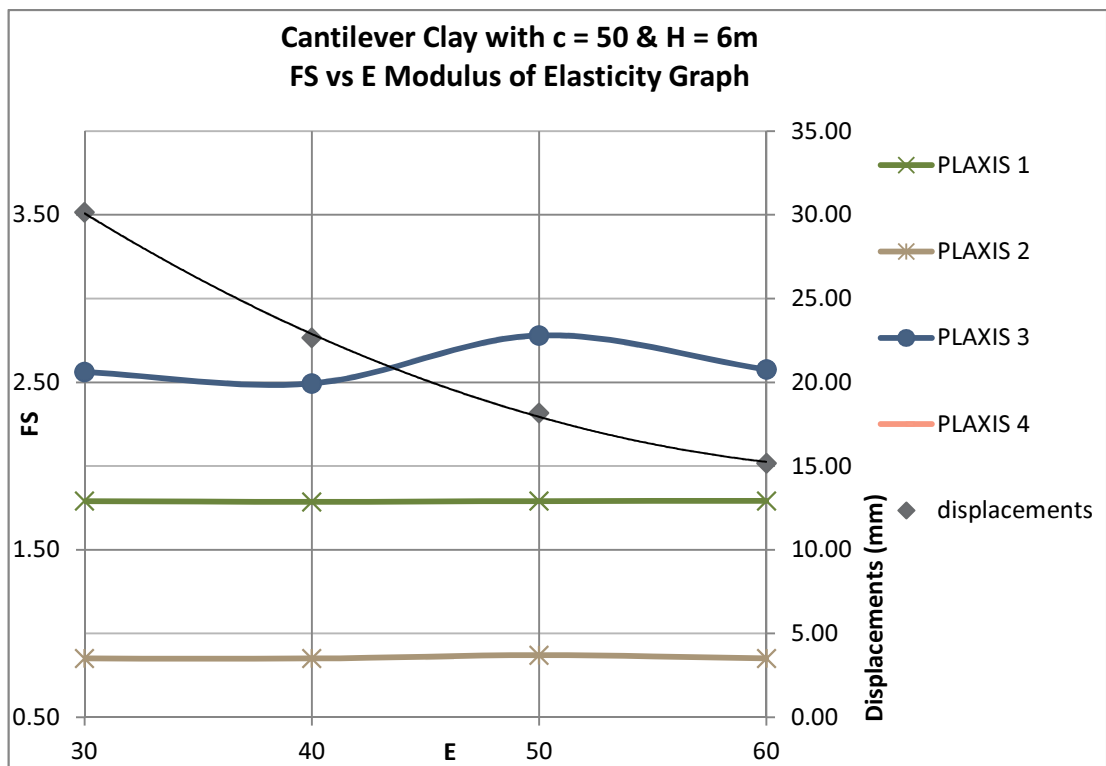
Figure 4. 10; FS vs E & pile displacements vs E graphs for cantilever clay analysis results with varying modulus of elasticity

4.3   Results of Strut Supported Walls Retaining in Sand

Results obtained for strut supported sand and clay models are presented in table 4.5 and results are plotted for H vs FS value in figures 4.11 &12.

Results obtained from limit equilibrium solutions with free earth support method for strut supported sand models provide decreasing FS values with increasing retained height. PLAXIS 1 outputs provide similar FS values with limit equilibrium FS values. For less critical

cases, PLAXIS 1 provide lower FS values, hence, FS line representing PLAXIS 1 outputs is below the limit equilibrium line (similar to cantilever sand results). For more critical cases where retained height is larger or internal friction angle is lower, PLAXIS 1 results' line is above the limit equilibrium's line.

PLAXIS 2 analyses provide very close results with limit equilibrium's, compared to PLAXIS 1. It can be said that, methodology developed in PLAXIS 2 seems to work very well for strut supported sands.
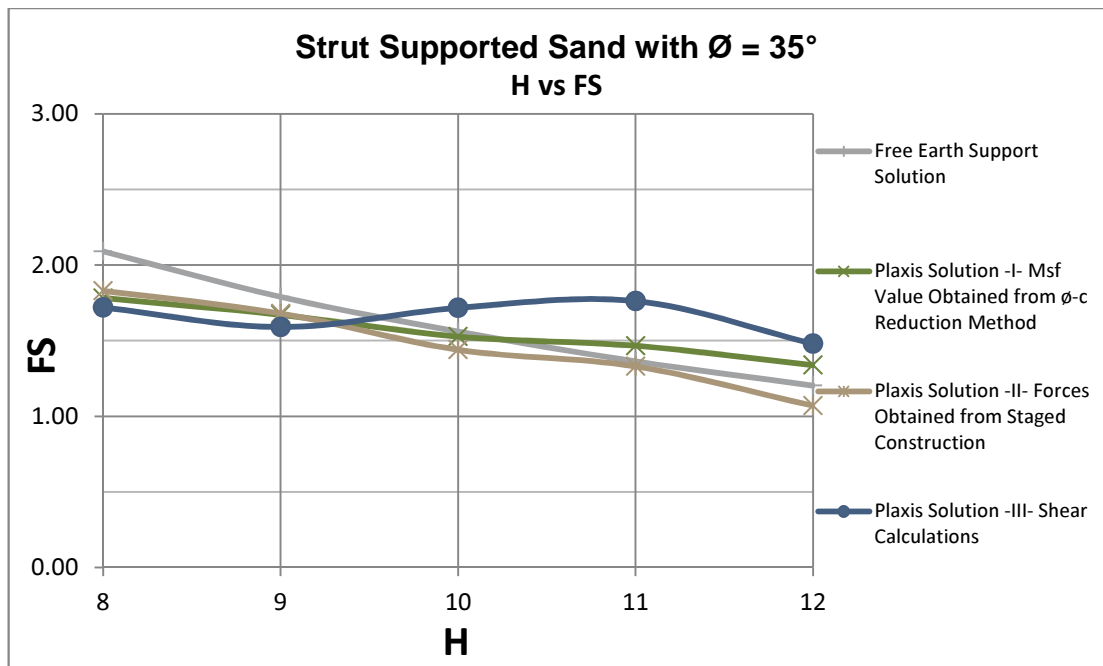
Figure 4. 11; Strut supported sand, H vs FS graph for ϕ = 35

PLAXIS 3 method, on the other hand, provided fluctuating results. Again, the reason is due to determination of shearing planes. Plot of H vs FS for ϕ = 35˚ is in figure 4.11 and ϕ = 30 & 40 are in appendix A with ϕ vs FS plots for each height. Hardening soil vs Mohr Coulomb models' graphs for PLAXIS results are provided in Appendix A as well.

Considering figure 4.11, it can be seen that results obtained from methods mentioned above are very close and forming similar lines, providing close results with small differences with each other, except for PLAXIS 3.

Table 4. 5; Results obtained for strut supported sand and clay models

Safety Factors Obtained All Over the Calculations — Strut Supported Sand

Constant Embedment Depth, D=4m (varying H) and Hardening Soil Model

Plaxis Model ID	ø°	H (m)	D (m)	E (Mpa)	Free Earth Support Solution	Plaxis Solution -I- Msf Value Obtained from ø-c Reduction Method	Disp.(mm)	Plaxis Solution -II- Forces Obtained from Staged Construction	Plaxis Solution -III- Shear Calculations
	30	8	4	50	1.38	1.46	0.56	1.19	1.57
	30	9			1.19	1.39	0.53	1.06	1.38
	30	10	4	50	1.03	1.27	0.67	1.00	1.44
	30	11			0.90	1.23	0.77	0.98	1.56
	30	12			0.80	1.20	1.00	0.85	1.30
	35	8			2.09	1.78	0.39	1.83	1.72
	35	9			1.79	1.67	0.46	1.68	1.59
	35	10	4	50	1.56	1.53	0.55	1.44	1.72
	35	11			1.36	1.47	0.60	1.33	1.76
	35	12			1.20	1.34	0.79	1.07	1.48
	40	8			3.25	2.12	0.27	2.89	1.85
	40	9			2.79	1.99	0.39	2.46	1.80
	40	10	4	50	2.42	1.80	0.46	2.14	1.79
	40	11			2.12	1.76	0.55	1.74	1.84
	40	12			1.87	1.63	0.64	1.58	1.70
Hardening Soil Model	ø = 35	H = 8m			2.09	1.77	0.25	1.43	1.97
Hardening Soil Model	ø = 35	H = 10m			1.56	1.53	0.35	1.14	1.81
Hardening Soil Model	ø = 35	H = 12m			1.20	1.37	0.48	0.94	1.57

Safety Factors Obtained All Over the Calculations — Strut Supported Clay

Constant Embedment Depth, D=4m (varying H) and Hardening Soil Model

Plaxis Model ID	c (kPa)	H (m)	D (m)	E (Mpa)	Free Earth Support Solution	Plaxis Solution -I- Msf Value Obtained from ø-c Reduction Method	Disp.(mm)	Plaxis Solution -II- Forces Obtained from Staged Construction	Plaxis Solution -III- Shear Calculations
	50	8	4	50	1.05	1.56	3.17	0.68	1.88
	50	9			0.91	1.39	3.30	0.61	1.62
	50	10	4	50	0.80	1.25	3.39	0.56	1.42
	50	11			0.72	1.15	3.48	0.51	1.32
	50	12			0.65	1.05	3.69	0.49	1.14
	75	8			1.57	2.34	3.10	0.95	3.42
	75	9			1.37	2.09	3.21	0.84	2.84
	75	10	4	50	1.21	1.87	3.28	0.76	2.40
	75	11			1.08	1.73	3.35	0.66	2.17
	75	12			0.97	1.57	3.48	0.63	1.97
	100	8			2.09	3.13	3.09	1.23	5.41
	100	9			1.82	2.79	3.18	1.10	4.63
	100	10	4	50	1.61	2.51	3.23	0.98	3.90
	100	11			1.44	2.31	3.29	0.84	3.94
	100	12			1.29	2.09	3.37	0.80	2.56
Hardening Soil Model	c=75kPa	H=8m			1.57	2.35	1.54	0.96	3.51
Hardening Soil Model	c=75kPa	H = 10m			1.21	1.88	1.65	0.78	2.36
Hardening Soil Model	c=75kPa	H = 12m			0.97	1.57	1.87	0.65	2.14

4.4 Results of Strut Supported Walls Retaining in Undrained Clay

Results obtained for strut supported clay models provided graphs that are easier to interpret, as can be seen in figure 4.12. Results show similarity in general trend, but the difference between the resultant FS' are very high, compared to strut supported sand results. Limit equilibrium FS results are very close to 1. PLAXIS 1 FS are higher than LE and providing the second highest result data set.

PLAXIS 2 outputs provided very low results. Resultant line of PLAXIS 2 is almost parallel to those of LE's but it is below the limit equilibrium method's line of FS vs H, as can be seen in figure 4.12. The results of PLAXIS 2 are even below FS = 1 line where LE results are higher.

PLAXIS 3 results are providing the highest FS factors for models. Unlike the results of sand cases, PLAXIS 3 results are reasonable and following the general trend of other solutions.
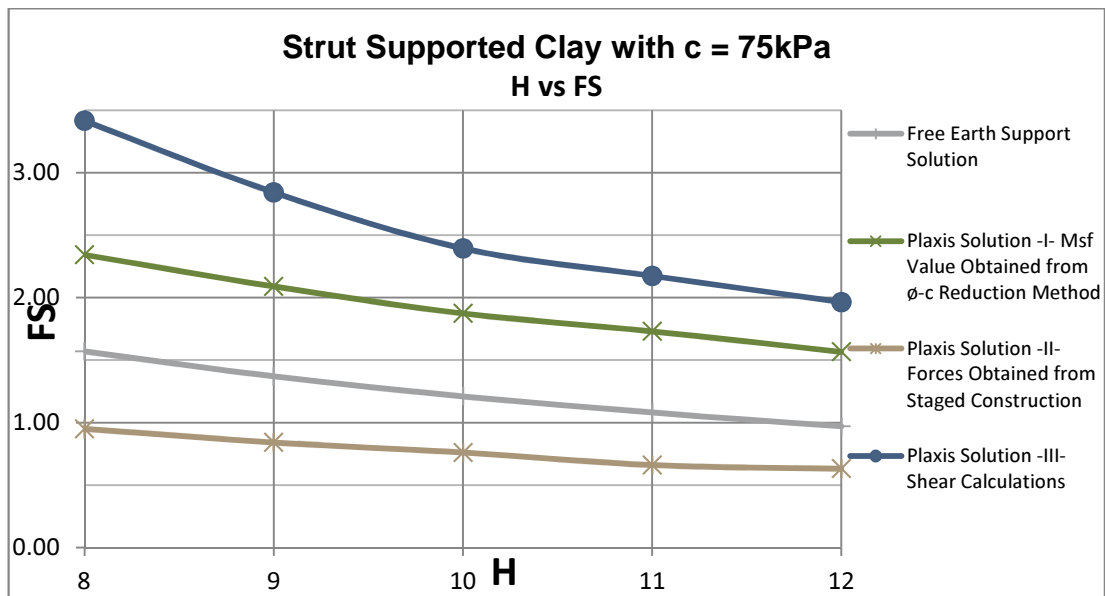
Figure 4. 12; Strut supported clay, FS vs H graph for c=75kPa

Hardening soil model analysis results are very close to results of Mohr Coulomb model. These results are presented in figure 4.13. On the other hand, strut displacements obtained from these models differ from each other. Hardening soil models provide lower strut displacements for the same models in Mohr Coulomb soil (see figure 4.14).
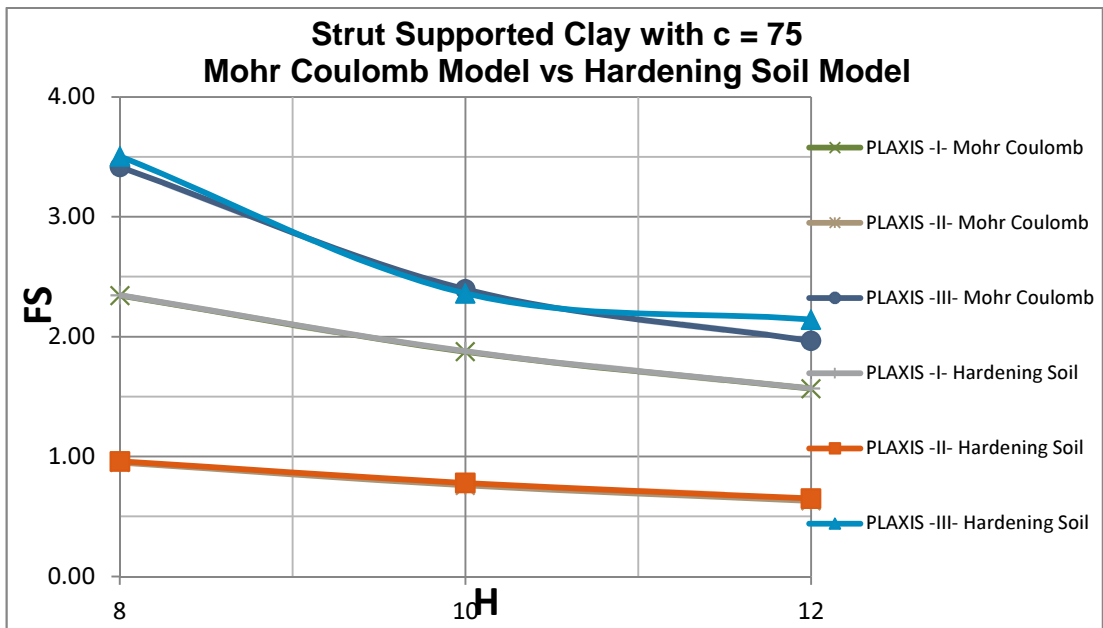
Figure 4. 13; Strut supported clay, FS vs H graph for c=75kPa
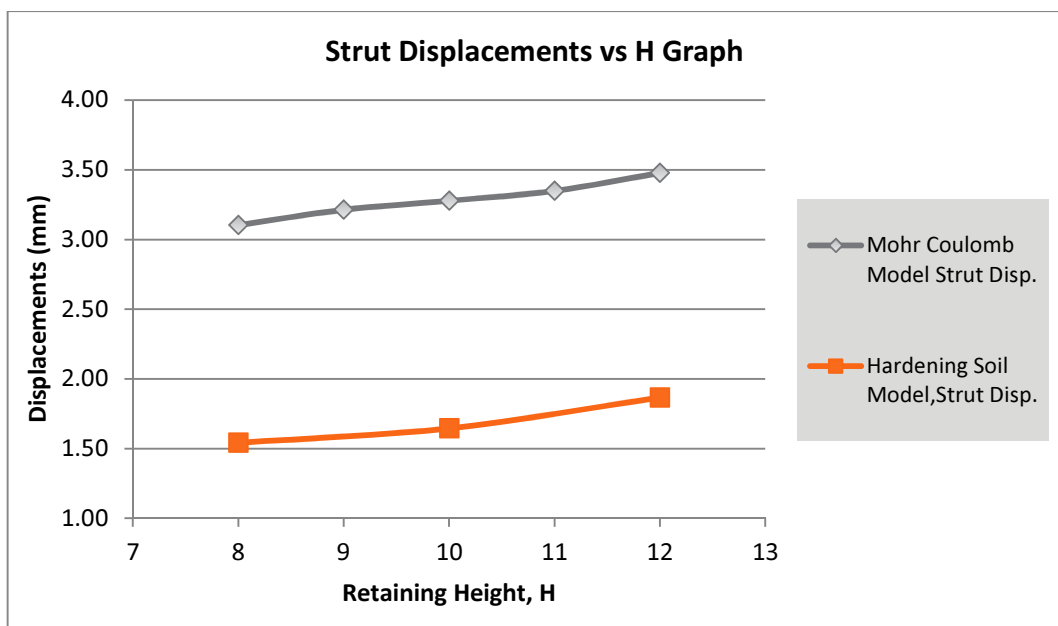
Figure 4. 14; Strut supported clay, strut displacements vs H graph for Mohr Coulomb and hardening soil models

CHAPTER 5

REGRESSION ANALYSIS

In this chapter, results described in the previous chapter are subjected to regression analysis in order to form relations between different analysis procedures. As described at the end of each analysis procedure in chapter 4, FS values from only the solution methods that give realistic results are used in this chapter. Section 5.1 explains briefly the methods used and developed, and 5.2 provides results of analyses with methods used in regression analyses.

5.1   Methodology

In order to obtain relations, 3 different major methods are used in regression analyses, which is done through least squares curve fitting technique. The data is initially analyzed as if it were independent of soil strength. If it shows dependency on soil strength (tan ϕ or c_u), this relation is also modeled by least squares fitting of a surface over three dimensional (FS-FS-strength) space. In these function fitting analyses, coefficient of determination, R^2, is found to be very close to 1.

5.1.1   Linear fit

First of these methods, linear regression, involves direct relation of two different analysis results. An example for this type of results is provided in figure 5.1 for methods 1a & 1b of cantilever retaining sand.

As can be seen from figure 5.1, FS obtained from 1a method can be related to 1b as;

$$FS_{1b} = 0,9678 * FS_{1a} - 0,0045 \tag{5.1}$$
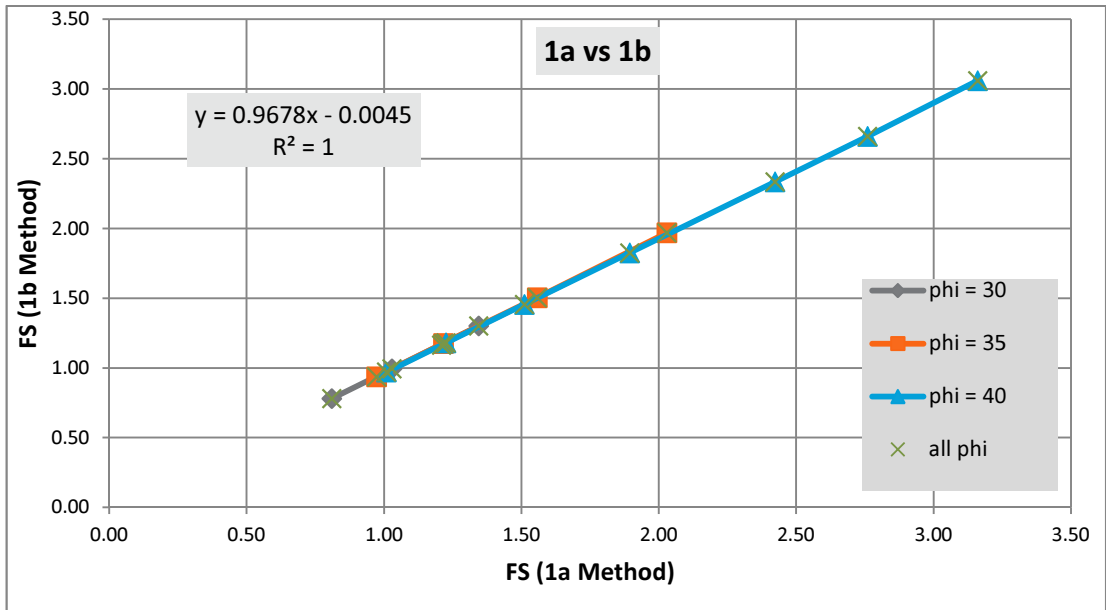
Figure 5. 1; Cantilever sand, linear regression of methods 1a & 1b

5.1.2 Planar Fit

Most limit equilibrium methods can be related within themselves, using linear regression. In cases where the entire data does not fit to a line, but the data belonging to each soil strength fit onto parallel lines, a plane is used to relate the results. An example data set where plane fit is used, is presented in figure 5.2 where FS values of methods PLX1 and 3a are plotted for cantilever clay model. As can be seen from the graph, outputs for different undrained shear strengths are not exactly on the same line, but they are parallel to each other. In order to relate these outputs, both FS values and c_u parameters are used.

Matrix equation 5.2 presents the formulation used for obtaining the relation where x & y are coordinates of the data points (i.e. safety factors) for corresponding methods, and c_u is the undrained shear strength of clay.

$$
\begin{bmatrix}
\Sigma x^2 & \Sigma x * c_u & \Sigma x \\
\Sigma x * c_u & \Sigma c_u^2 & \Sigma c_u \\
\Sigma x & \Sigma c_u & n
\end{bmatrix}
*
\begin{bmatrix}
A \\
B \\
C
\end{bmatrix}
=
\begin{bmatrix}
\Sigma x * y \\
\Sigma y * c_u \\
\Sigma y
\end{bmatrix}
\tag{5.2}
$$
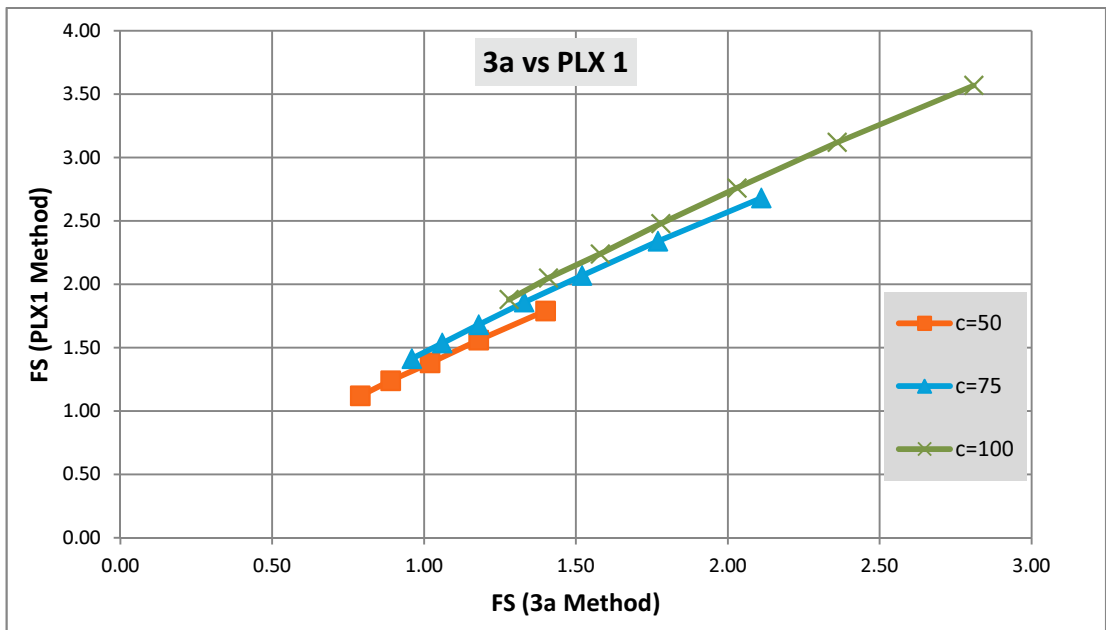
Figure 5. 2; Cantilever clay, results for methods 3a and PLX 1, in the form of parallel lines, suitable for planar fit
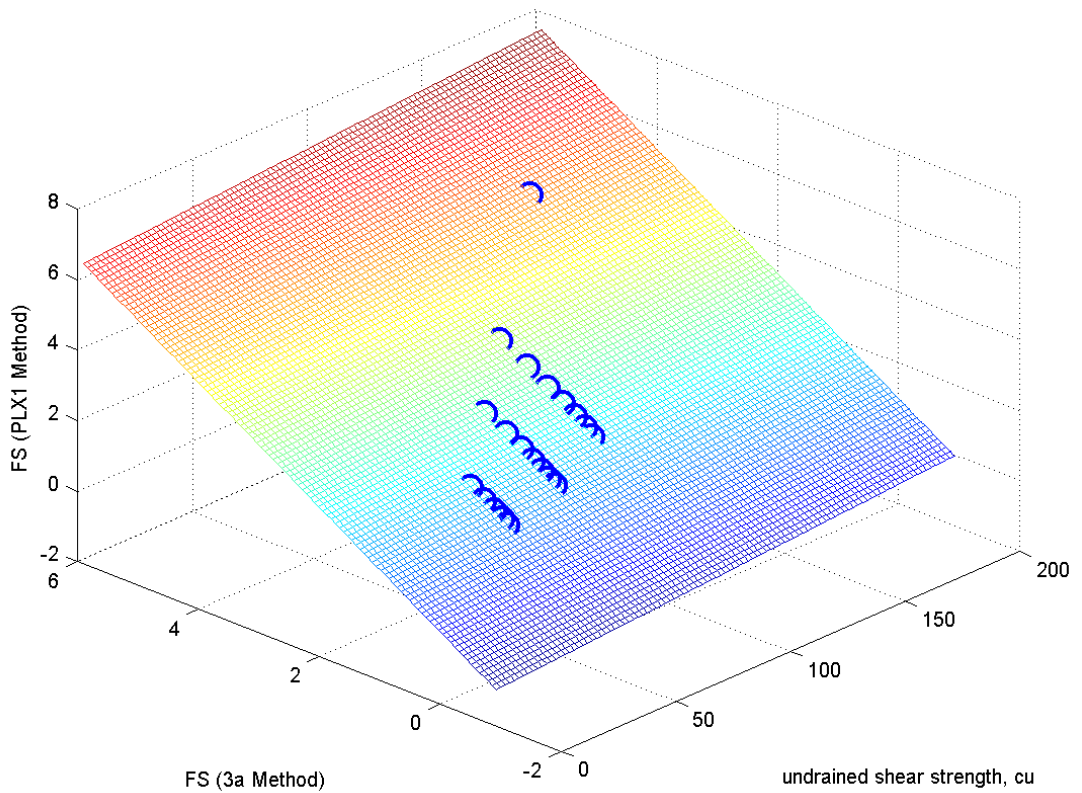
Figure 5. 3; Plane fit for data set 3a and PLX1

Results can be formed from the relation $y = A*x + B*c_u + C$ and the output plane for the example provided above is given in figure 5.3. Also the resulting correlation between FS (PLX1 Method) and FS (3a Method) of cantilever clay model is given in equation 5.3.

$$FS_{PLX1} = 1,0946 * FS_{3a} + 0,0048 * c_u + 0,0238 \qquad (5.3)$$

When used for sand, tan ϕ replaces c_u in both the matrix equation and resulting correlation.

5.1.3 Twisted Plane Fit

Plane fit suits well with linear and parallel data. But in some cases, the output data is not even parallel to each other, as shown in figure 5.4. This situation is observed in PLAXIS 1 cases of sand models mostly, and handled by using a "twisted plane" fit.
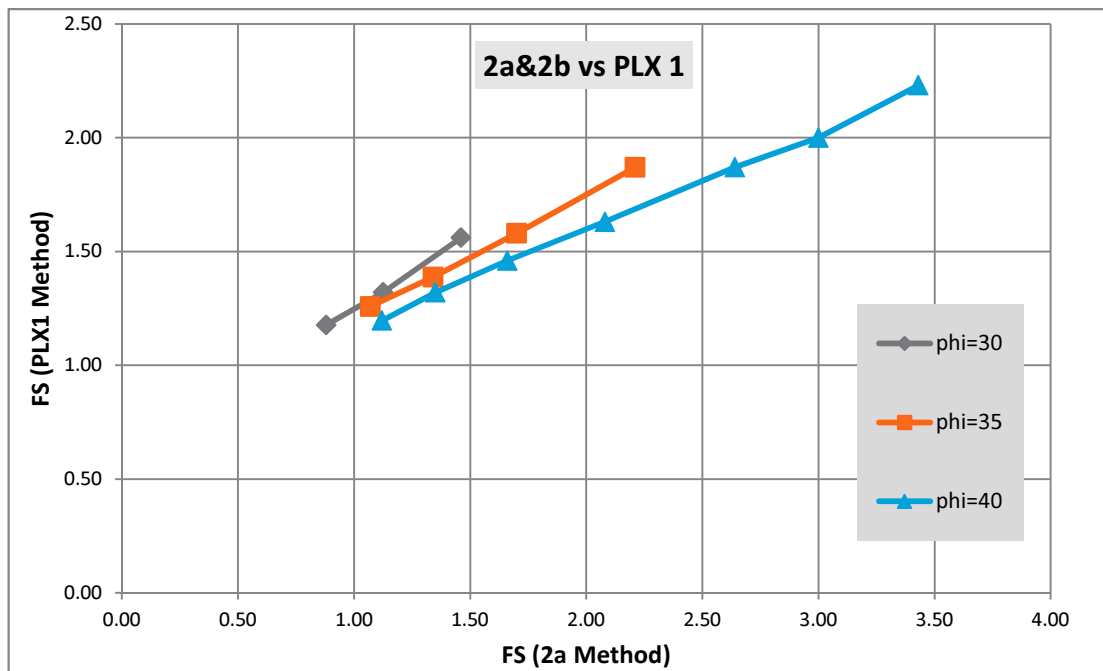
Figure 5. 4; Cantilever sand, results graph for methods 2a and PLX 1, in the form of lines, suitable for twisted plane fit

Formulation used in plane fit is modified to take into account the non parallelity of data outputs. Equation 5.4 presents the solution matrix, where the resultant equation is presented in equation 5.5, also the twisted plane is shown in figure 5.5 for relating cantilever sand model PLX1 and 2a methods.

$$\begin{bmatrix} \Sigma\tan^2\phi * x^2 & \Sigma\tan\phi * x^2 & \Sigma\tan^2\phi * x & \Sigma\tan\phi * x \\ \Sigma\tan\phi * x^2 & \Sigma x^2 & \Sigma\tan\phi * x & \Sigma x \\ \Sigma\tan^2\phi * x & \Sigma\tan\phi * x & \Sigma\tan^2\phi & \Sigma\tan\phi \\ \Sigma\tan\phi * x & \Sigma x & \Sigma\tan\phi & n \end{bmatrix} * \begin{bmatrix} A \\ B \\ C \\ D \end{bmatrix} = \begin{bmatrix} \Sigma\tan\phi * x * y \\ \Sigma x * y \\ \Sigma\tan\phi * y \\ \Sigma y \end{bmatrix} \quad (5.4)$$

$$y = [A*\tan\phi + B]*x + [C*\tan\phi + D] \quad (5.5)$$
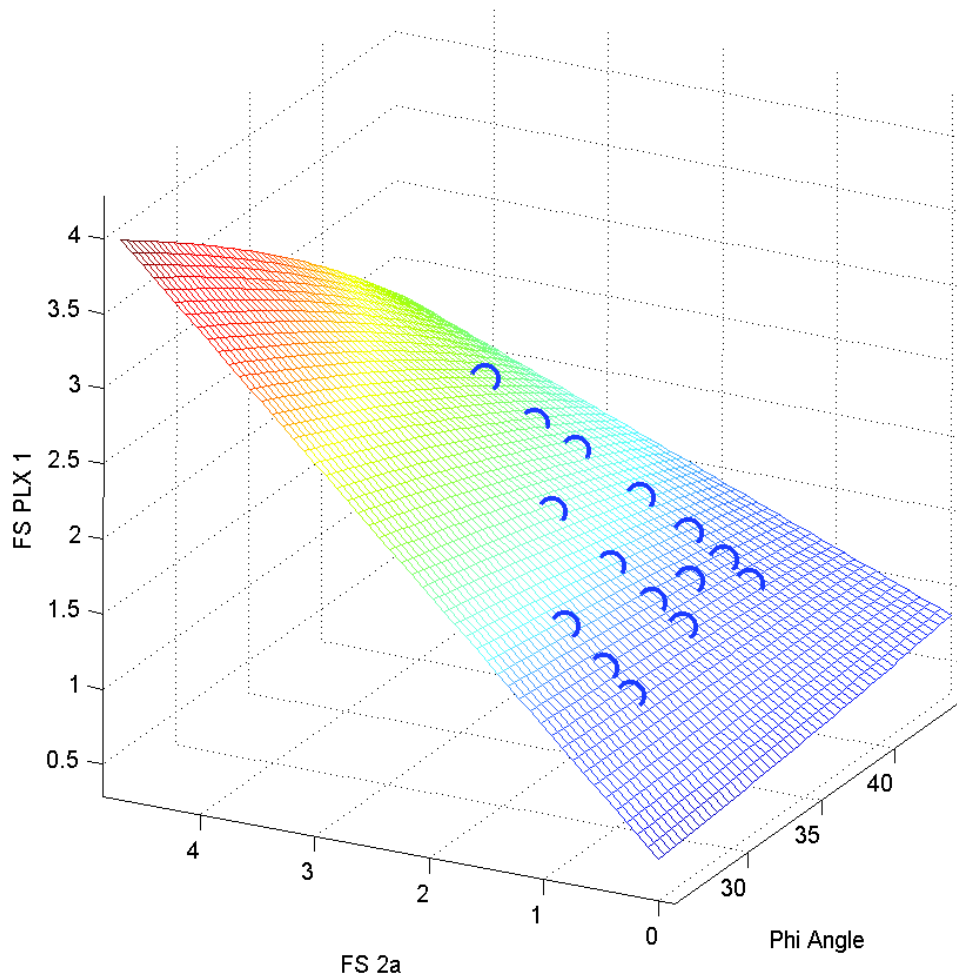
Figure 5. 5; Twisted plane fit for data set 2a and PLX1

5.1.4 Logarithmic Twisted Plane Fit
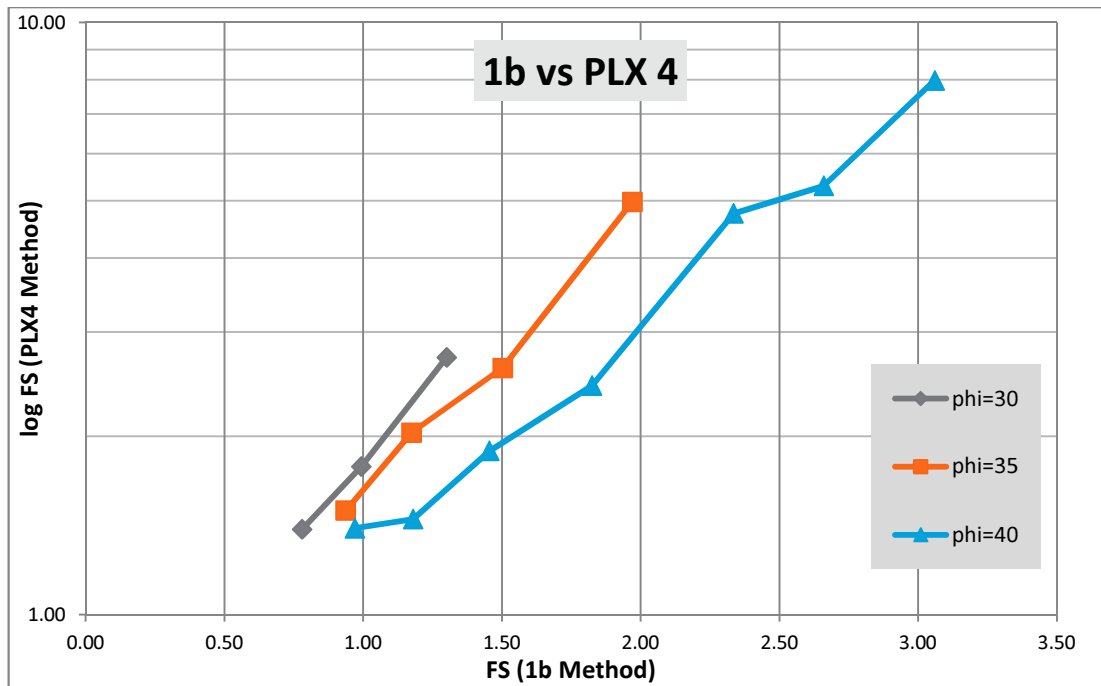
Figure 5. 6; Cantilever sand, logarithmic twisted plane results graph for methods 1b and PLX4
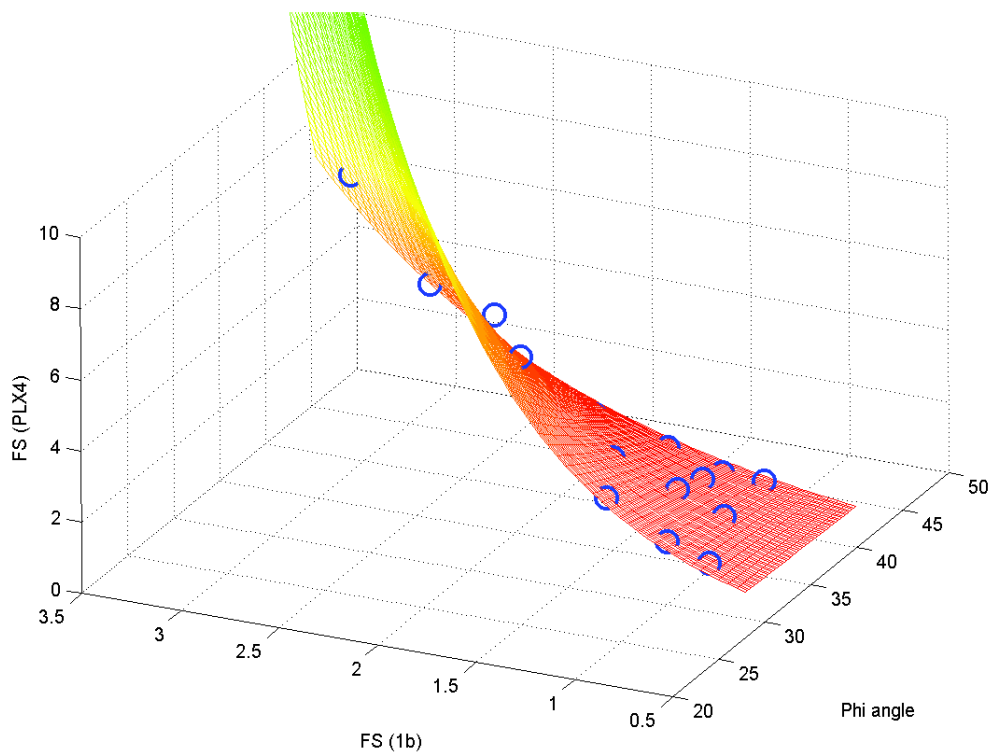
Figure 5. 7; Log - twisted plane fit for data set 1b and (PLX4)

In addition to three major cases mentioned above, logarithmic fits are used in some cases. Procedure is the same with twisted plane, but one of the coordinates' scale is replaced with logarithmic scale. An example of this case's data is provided in figure 5.6 and logarithmic twisted plane is shown in figure 5.7.

5.1.5 Power Fit & Modified Power Fit

In comparison of FS values of strut supported walls in clay, it has been observed that, plots involving PLAXIS 3 analysis' FS values are better correlated with other methods' FS values using power fit. Considering three pairings involving PLAXIS 3 FS values for strut supported walls in clay, following results are obtained.

For only one pair of data sets (PLX 1 vs. PLAXIS 3), power fit ($y=ax^b$) happened to be the best, as it yielded the highest R^2.

$$FS_{PLX3} = 1,0204 * FS_{PLX1}^{1,4411}$$

(5.6)

For remaining two pairs of data sets (LE vs. PLAXIS 3 & PLAXIS 2 vs. PLAXIS 3), modified power fit, involving strength parameter, fits better (PLX 2 vs. PLX 3 equation can be seen in table 5.3).

$$FS_{PLX3} = 1,2683 * FS_{LE}^{1,6576} + 0,0104 * c_u$$

(5.7)

5.1.6 Parabolic Fit

Another fit method to be applied for analysis is the parabolic fit. This method is applied to FS results of PLAXIS 2 in cantilever sand results (except for PLAXIS 1, data couple of these two is observed to fit better to plane fit). Regression lines involving PLAXIS 2 produced outputs similar to those shown in figure 5.8.
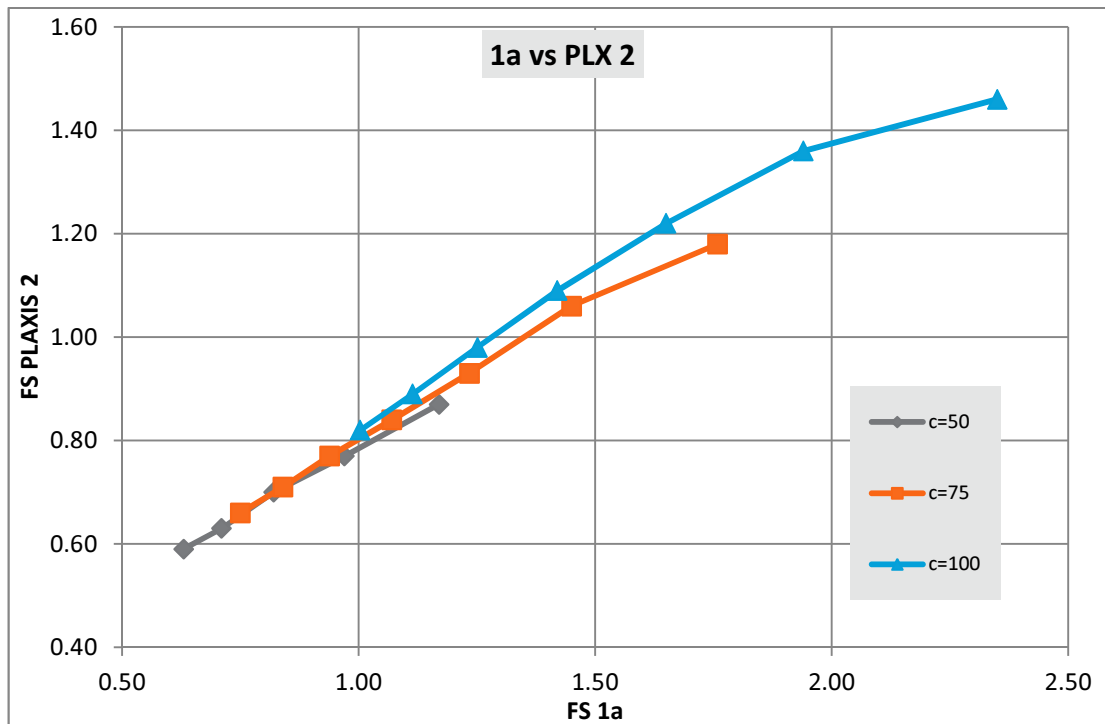
Figure 5. 8; Cantilever clay, LE 1a vs PLAXIS 2 results

As can be seen, for low FS values, data seems to be fitting to a plane, but for higher FS values, data sets start to bend. In order to obtain a better correlation, these two data sets are fitted manually using parabolic fit. This was not performed as a real least squares fit regression, because of increased complexity of math of the problem. Instead, it was done in MS Excel by manipulating the coefficients in the general expression until the R^2 reached a high value. Formulation of LE 1a and PLAXIS 2 with parabolic fit is provided in equation 5.7.

$$FS_{PLX2} = \frac{[-0,1129*(FS_{1a})^2+0,7261*(FS_{1a})+0,3992-0,0044*c_u]}{(1,3-0,006*c_u)} \quad (5.8)$$

5.2 Analysis Results

Table 5. 1; Models of cantilever walls retaining sand, regression analysis results with resulting correlations in the lower triangular matrix, and R^2 parameters & function types in the upper triangle

	1a	2a & 2b	1b	PLAXIS 1	PLAXIS 2	PLAXIS 4
1a		$R^2 = 0.9987$ Linear Fit	$R^2 = 1$ Linear Fit	$R^2 = 0.9985$ Twisted Plane Fit	$R^2 = 0.9776$ Linear Fit	$R^2 = 0.9868$ Logarithmic Twisted Plane Fit
2a & 2b	$FS_{2a} = 0.8482*FS_{1a} - 0.0513$		$R^2 = 0.9991$ Linear Fit	$R^2 = 0.9985$ Twisted Plane Fit	$R^2 = 0.9869$ Plane Fit	$R^2 = 0.9873$ Logarithmic Twisted Plane Fit
1b	$FS_{1b} = 0.9678*FS_{1a} - 0.0045$	$FS_{1b} = 1.1398*FS_{1b} + 0.0556$		$R^2 = 0.9986$ Twisted Plane Fit	$R^2 = 0.9765$ Linear Fit	$R^2 = 0.987$ Logarithmic Twisted Plane Fit
PLAXIS 1	$FS_{PLX1} = (-0.8961*tanø + 1.2159)*FS_{1a} + (0.5152*tanø + 0.314)$	$FS_{PLX1} = (-0.9768*tanø + 1.3561)*FS_{2a} + (0.5441*tanø + 0.3449)$	$FS_{PLX1} = (-0.8993*tanø + 1.2332)*FS_{1b} + (0.4978*tanø + 0.3335)$		$R^2 = 0.9815$ Linear Fit	$R^2 = 0.9852$ Logarithmic Twisted Plane Fit
PLAXIS 2	$FS_{PLX2} = 1.6326*FS_{1a} + 0.4055$	$FS_{PLX2} = 1.7683*FS_{2a} + 1.708*tanø - 0.561$	$FS_{PLX2} = 1.686*FS_{1b} + 0.4146$	$FS_{PLX2} = (5.7997*tanø - 1.5435)*FS_{PLX1} + (-5.1428*tanø + 2.4977)$		$R^2 = 0.9793$ Logarithmic Twisted Plane Fit
PLAXIS 4	$\ln(FS_{PLX4}) = (-1.9234*tanø + 2.4498)*FS_{1a} + (0.7184*tanø - 1.1875)$	$\ln(FS_{PLX4}) = (-2.1001*tanø + 2.7294)*FS_{2a} + (0.7373*tanø - 1.1046)$	$\ln(FS_{PLX4}) = (-1.9386*tanø + 2.489)*FS_{1b} + (0.6856*tanø - 1.1511)$	$\ln(FS_{PLX4}) = (-0.3999*tanø + 2.1381)*FS_{PLX1} + (-0.0057*tanø - 1.9248)$	$\ln(FS_{PLX4}) = (-1.2509*tanø + 1.5914)*FS_{PLX2} + (0.5123*tanø - 1.3818)$	

5.2.1　Cantilever Wall in Sand

Regression analysis results are presented in table 5.1 for cantilever walls retaining in sand. In cantilever sand models, results that are showing similar properties and fitting to a line are grouped. First group is composed of solution methods 1a, 2a, 1b and PLAXIS 2. The solution data sets which are composed of FS couples picked from this group are fitting to a line, hence, linear fit is applied to these data.

Only exception for the first group is the coupling of 2a & 2b vs PLAXIS 2 solutions, where plane fit is applicable instead of a linear fit.

Second group is composed of PLAXIS 1 and PLAXIS 4 method FS values. PLAXIS 1 solution in analyses fits well into a twisted plane when correlated with limit equilibrium solutions. Data is grouped for each ϕ value in second group, contrary to the first group (see figure 5.4).

Data including PLAXIS 4 solution uses twisted plane fit as well, but the natural logarithm of PLAXIS 4 data is used, as described in section 5.1.4. The outputs are similar to figure 5.6.

Only an exception in PLAXIS 1 vs PLAXIS 2 data is observed. Even though these two analyzes belong to different groups, this data set fits to a plane better compared to twisted plane fit.

5.2.2　Cantilever Wall in Clay

In cantilever clay models, similar to cantilever sand, limit equilibrium methods are suitable for linear fit, and form a group within which, all couples of FS data fit to a line. Group is formed of solution methods 1a, 1b, 2a and 3a. Also, solution procedure PLAXIS 3 is included to this group, since, combination of other solutions with PLAXIS 3 matches a linear fit. Very high R^2 values are obtained within this group. An exception to this first group is due to the pairing of PLAXIS 1 and PLAXIS 3. Any pairs including PLAXIS 1 suits to a plane fit.

Second group is composed of PLAXIS 1 and PLAXIS 2 data sets. These data set uses parabolic fit, which is adjusted manually, and the output data is similar to figure 5.8. Each FS couple's data is grouped for varying c_u values, similar to cantilever sand.

Table 5. 2; Models of cantilever walls retaining undrained clay, regression analyses results with R^2 values and function types

	1a	1b	2a	3a	PLAXIS 1	PLAXIS 2	PLAXIS 3
1a		$R^2 = 0.9992$ Linear Fit	$R^2 = 1$ Linear Fit	$R^2 = 0.9992$ Linear Fit	$R^2 = 0.9994$ Plane Fit	$R^2 = 0.9993$ Parabolic Fit	$R^2 = 0.9859$ Linear Fit
1b	$FS_{1b} = 1.1709*FS_{1a} + 0.0691$		$R^2 = 0.9994$ Linear Fit	$R^2 = 1$ Linear Fit	$R^2 = 0.9997$ Plane Fit	$R^2 = 0.9992$ Parabolic Fit	$R^2 = 0.9881$ Linear Fit
2a	$FS_{2a} = 0.9717*FS_{1a} + 0.0106$	$FS_{2a} = 0.8293*FS_{1b} - 0.0458$		$R^2 = 0.9994$ Linear Fit	$R^2 = 0.9994$ Plane Fit	$R^2 = 0.9947$ Parabolic Fit	$R^2 = 0.9862$ Linear Fit
3a	$FS_{3a}=1.1521*FS_{1a}+0.0638$	$FS_{3a}=0.984*FS_{1b}-0.0042$	$FS_{3a}=1.1858*FS_{2a}+0.051$		$R^2 = 0.9996$ Plane Fit	$R^2 = 0.9973$ Parabolic Fit	$R^2 = 0.9878$ Linear Fit
PLAXIS 1	$FS_{PLX1}=1.12407*FS_{1a}+0.0064*c_u]+0.0342$	$FS_{PLX1}=1.0984*FS_{1b}+0.0049*c_u]+0.0224$	$FS_{PLX1}=1.283*FS_{2a}+0.0062*c_u+0.029$	$FS_{PLX1}=1.1164*FS_{3a}+0.0049*c_u+0.0274$		$R^2 = 0.9965$ Plane Fit	$R^2 = 0.9883$ Plane Fit
PLAXIS 2	$FS_{PLX2}=[-0.1129 FS_{1a}^2+0.7261*FS_{1a}+0.3992-0.0044c_u]/[1.3-0.006c_u]$	$FS_{PLX2}=[-0.0745FS_{1b}^2+0.6219*FS_{1b}+0.3777-0.004c_u]/[1.28-0.0056c_u]$	$FS_{PLX2}=[-0.1044 FS_{2a}^2+0.7135*FS_{2a}+0.3699-0.0038c_u]/[1.25-0.0053c_u]$	$FS_{PLX2}=[-0.0733 FS_{3a}^2+0.593*FS_{3a}+0.3532-0.0043c_u]/[1.2-0.0053c_u]$	$FS_{PLX3}=0.4199*FS_{PLX1}-0.0013*c_u+0.1706$		$R^2 = 0.9922$ Linear Fit
PLAXIS 3	$FS_{PLX3} = 2.66*FS_{3a} - 0.4912$	$FS_{PLX3} = 2.2733*FS_{1b} - 0.6507$	$FS_{PLX3} = 2.7378*FS_{2a} - 0.5207$	$FS_{PLX3} = 2.31*FS_{3a} - 0.6404$	$FS_{PLX3} = 2.0163*FS_{PLX1} - 0.0076*c_u - 0.7851$	$FS_{PLX1} = 4.7348*FS_{PLX2} - 1.6375$	

5.2.3 Strut Supported Problems

Strut supported sand results are in accordance within themselves, except for PLAXIS 3 results. Linear fit is suitable for free earth support method, PLAXIS 1 and PLAXIS 2 solutions and provided satisfying results. PLAXIS 3 results, on the other hand, provided very low R^2 parameters, due to the non-stability of FS results. Table 5.3a presents the results obtained for strut supported sands.

Table 5. 3; Strut supported models, regression analyses results with R^2 parameters and function types, a. Strut supported sand, b. Strut supported clay

	LE	PLX1	PLX2	PLX 3
LE		R^2 = 0.9821 Linear Fit	R^2 = 0.9848 Linear Fit	R^2 = 0.6637 Linear Fit
PLX1	$FS_{PLX1} = 0.3872 \cdot FS_{FES} + 0.9107$		R^2 = 0.961 Linear Fit	R^2 = 0.6825 Linear Fit
PLX2	$FS_{PLX2} = 0.8232 \cdot FS_{FES} + 0.1372$	$FS_{PLX2} = 2.0818 \cdot FS_{PLX1} - 1.729$		R^2 = 0.6445 Linear Fit
PLX3	$FS_{PLX3} = 0.1982 \cdot FS_{FES} + 1.2935$	$FS_{PLX3} = 0.5145 \cdot FS_{PLX1} + 0.8232$	$FS_{PLX3} = 0.2355 \cdot FS_{PLX2} + 1.2687$	

a

	LE	PLX1	PLX2	PLX 3
LE		R^2 = 0.9998 Plane Fit	R^2 = 0.9938 Linear Fit	R^2 = 0.9641 Modified Power Fit
PLX1	$FS_{PLX1} = 1.2846 \cdot FS_{FES} + 0.0044\, c_u - 0.0022$		R^2 = 0.9801 Linear Fit	R^2 = 0.9825 Power Fit
PLX2	$FS_{PLX2} = 0.5218 \cdot FS_{FES} + 0.1296$	$FS_{PLX2} = 0.3504 \cdot FS_{PLX1} + 0.1025$		R^2 = 0.9591 Modified Power Fit
PLX3	$FS_{PLX3} = 1.2683 \cdot (FS_{FES})^{1.6576} + 0.0104 \cdot c_u$	$FS_{PLX3} = 1.0204 \cdot FS_{PLX1}^{1.4411}$	$FS_{PLX3} = 3.3526 \cdot (FS_{PLX2})^{1.8839} + 0.0066 \cdot c_u$	

b

Unlike the strut supported sand results, in clay case, plane and power fits are also used in addition to linear fit. PLAXIS 1 vs. LE provide very high R^2 values (R^2 = 0.9998) by using plane fit. PLAXIS 2 results are well matched with PLAXIS 1 or LE results and hence, linear fit is

used. PLAXIS 3 vs. LE or PLAXIS 2 results are fitted into a plane, and PLAXIS 3 vs. PLAXIS 1 is related by using power fit. Table 5.3b provides the results and fit types used for regression analysis of strut supported clay model's solution methods.

CHAPTER 6

CONCLUSIONS AND SUGGESTIONS

As the solution techniques advance with development of software modeling, although it becomes possible to model much more complex geotechnical problems, the risk of solving for incorrect models in softwares have increased, due to the black box approach of computer softwares' nature. Relating the results of traditional limit equilibrium solutions with finite element modeling is crucial for engineers, because it is possible to estimate the results of one by using the other (ie. by using limit equilibrium's FS values, FS values of finite element modeling can be determined). Such relation can even provide an estimate of complex finite element modeling result with simple limit equilibrium analysis that is used for preliminary design.

In order to obtain these relations, first, limit equilibrium methods used by various manuals are analyzed for different models involving varying retaining heights and soil properties. To explore a wider range of possibilities for correlating finite element modeling and limit equilibrium, a variety of methods were applied to the PLAXIS analyses. These methods relate software outputs with limit equilibrium methods to obtain safety factors. In chapter 3, these methods are provided with the methodology behind them (see Appendix B for the summary chart of methods).

6.1   Research Findings

6.1.1   Individual Analyses

Models used in analyses are divided into four, considering soil parameters (undrained clay, $\phi = 0°$ and drained sand, c = 0 kPa) and considering support method (cantilever and strut supported models). For cantilever sand models, four limit equilibrium and four PLAXIS solution is analyzed for 21 models. In cantilever clay models, seven limit equilibrium and four PLAXIS FS values are obtained for each of 26 models. Similarly, for strut supported

sand and clay cases, one limit equilibrium and three PLAXIS FS values are calculated for each of 36 models. Total of 523 FS values are calculated in the calculations for this thesis.

Results obtained from all of the calculations mentioned above are presented in the 4th chapter. These results show that, limit equilibrium methods provide very close FS values within themselves. Some methods (2c & 3b for cantilever clay and 2b for cantilever sand models) provided exactly the same FS values. The only major difference to be considered within the limit equilibrium data set is due to the simplified approach (i.e. analysis depth + 20% increase in embedment depth = design depth) and this difference can be explained as the difference between analysis and design approaches. Another finding is that, depth of rotational point is almost independent of retained height H and internal friction angle ϕ, and it changes with embedment depth D.

PLAXIS 1 (phi-c reduction method ΣMsf) results provided similar FS values with limit equilibrium methods, and used for regression analyses. These results are the only FS that is provided by PLAXIS to user (considering soil parameters, not structural parameters), and have an important role in assigning FS values not only for relating with limit equilibrium solutions, but also for deriving PLAXIS 4 results. PLAXIS 2 results, as in PLAXIS 1, provided compatible data (especially for sand models) to be used in regression analyses.

It can be said that, general trend for ΣMsf value is close to limit equilibrium calculations. In predicting FS values for models with relatively safer parameters (lower retaining heights and higher soil strength parameters), ΣMsf values are slightly lower than calculated limit equilibrium FS values, due to forming of passive pressures. For relatively critical models where FS values approach to 1, ΣMsf values provide higher values than FS values calculated by limit equilibrium methods'.

Results of PLAXIS 2 provided higher FS values for cantilever sand models, compared to those of PLAXIS 1 and limit equilibrium methods'. Also, results are in well accordance and easily be related to other FS values. For strut supported sand models, PLAXIS 2 matched even better with PLAXIS 1 and limit equilibrium methods.

Some of the methods applied onto the numerical modeling results provided unrealistic FS values. Sand models' PLAXIS 3 method which uses shearing planes to obtain FS values, gives results that are not in accordance with other results and also expectations. The reason for

this can be explained as the cantilever drained sand models' not having a clear failure plane in excavated side of wall. Shearing planes for models could not be determined directly from PLAXIS outputs, therefore they are assigned as $45° + \phi/2$ & $45° - \phi/2$ on retained and excavated side, respectively. On the other hand, PLAXIS 3 outputs of cantilever undrained clay models provided shearing planes with angles close to 45 degrees with horizontal, as expected, and results derived are well matched with other methods' results.

Another important point in developed numerical solutions is outputs of PLAXIS 4. Results can be related to other FS values for sand cases and results are close to those of limit equilibrium and PLAXIS 1, especially in critical cases where FS approaches 1. On the other hand, for clay cases where undrained shear strength is high and retaining height is low compared to other models, PLAXIS 4 results provide very high FS values. This is due to the fact that, clays can sustain unsupported excavations based on their c_u and excavation height.

6.1.2 Regression Analyses

After analyzing all the models with varying parameters, results are selected considering the points mentioned above and used in carrying out regression analyses, as described in chapter 5. This part is the most crucial part for this thesis. Safety factors obtained from each method in all the computations mentioned above are plotted with respect to each other. These results are used in a least squares fitting regression analysis relating each pair of safety factor to each other, and when necessary, to soil strength. Resulting correlations are summarized in tables 5.1, 5.2 & 5.3.

Results showed that, for cantilever sand models, among limit equilibrium FS data sets, it is possible to obtain linear relations. On the other hand, data sets with PLAXIS results required involving planar, twisted planar and logarithmic twisted planar fits. Results are well matched with obtained relations providing high R^2 coefficients.

Similar to cantilever sands', cantilever clay models' limit equilibrium result data sets are suitable for linear fit. Solution combinations of 1a, 1b, 2a and 3a provided R^2 values almost equal to 1. PLAXIS 1 results use plane fit with all other methods. It means that, involving soil strength is required to obtain better relations between limit equilibrium solutions and PLAXIS ΣMsf values.

Data pairs involving limit equilibrium and PLAXIS 3 outputs use linear fits which are independent of soil properties (except for strut supported sand models). This shows that, shearing planes that are selected from PLAXIS outputs for calculating PLAXIS 3 FS values are close to real situation, and hence these FS values are in well accordance with limit equilibrium's FS values.

Strut supported sand model's data pair relations are all formed with linear fit. R^2 values of correlations for these models are high between limit equilibrium solution and PLAXIS solutions, the only exception is PLAXIS 3, since data obtained from PLAXIS 3 have incompatibilities due to assigned shearing planes.

In order to obtain formulation between FS values of methods in strut supported clay models, various fits are used. Plane fit suited to data set of PLAXIS 1 and limit equilibrium method, unlike the sand case. Data sets with PLAXIS 2 uses linear fit as in sand cases, except for data set formed of PLAXIS 2 and PLAXIS 3. Sets with PLAXIS 3 uses either power or modified power fitting.

6.2 Practical Implications

Beside the other relations, one of the most important findings is the relation between limit equilibrium solutions and PLAXIS 1 outputs. Through these relations, the FS value of any limit equilibrium solution can be used together with soil strength in the equations provided for PLAXIS 1, and the ΣMsf value expected to be provided by software can be guessed. This operation can also be done reversely. Most materials (codes, papers, lecture books) provide FS values according to traditional methods, on the other hand, modern engineering practice involves software analyses without a clear definition of FS in the traditional sense. An analysis run on softwares can be related to traditional methods by using the expressions presented in this thesis.

PLAXIS 2 methodology involves the ratio of passive forces obtained from limit equilibrium methods and PLAXIS outputs. An initial design involving limit equilibrium solutions can provide information on what percentage of passive force is mobilized in software model, without running the software model.

6.3   Recommendations for Future Research

Common applications of strut and anchor supports involve multi-level design in order to reduce support loads, embedment depths and bending moments. Retaining walls with multi-level strut supports can be investigated in further studies. Methodologies developed in this thesis can be applied to such cases and results can be used at any stage of design in order to obtain an insight towards the problem.

Models with soil properties that are used can be improved by including additional variable parameters. In this thesis, retained height is variable and embedment depth is kept constant. Systems with varying embedment depths can be analyzed in order to observe the effects of embedment depth to safety factors calculated, and hence relation of these FS values with software analyses can be investigated.

Also, clays with drained parameters can be modelled in further studies. After excavation, undrained shear strength of clays reduce with time, to their drained values. In unloading problems such as excavations, drained parameters play a more critical role in design of retaining walls in most cases.

With introduction of Eurocode 7, partial factors are replacing with overall safety factor concept. Relation between traditional FS and partial factors may be investigated and be useful in correlating these two different approaches.

REFERENCES

- Arcelor Group (2005), *Piling Handbook, 8th Edition,* Arcelor Rails, Piles & Special Sections Company, Luxembourg

- Bahar, M. (2009), *The Comparison of Observed and Calculated Displacements at the Diapragm Wall Type Earth Retaining Structures*, Master's Thesis, Yıldız Technical University, Istanbul

- Batali, L., Popa, H., Thorel, L. (2010), *Retaining Walls in Urban Areas Numerical Modelling, Characteristic Interaction Parameters,* Technical University of Civil Engineering, Bucharest, Romania

- Bolton, M. D. & Powrie, W. (1987), *The Collapse of Diaphragm Walls Retaining Clay,* Géotechnique, 37, (3), 335-353

- Bond, A. & Harris, A. (2008), *Decoding Eurocode 7*, Taylor & Francis Group, London and New York

- Brinkgreve, R. B. J. (1999), *Beyond 2000 in Computational Technics, Ten Years of Plaxis International*, A. A. Balkema, Rotterdam, Netherlands

- Brinkgreve, R. B. J., Al-Khoury, R., Bakker, K. J., Bonnier, P. G., Brand, P. J. W., Broere, W., Burd, H. J., Soltys, G., Vermeer, P. A. (2002), *Plaxis 2D Version 8 Manual*, A. A. Balkema Publishers, Netherlands

- Coduto, D. P. (2001), *Foundation Design, Principles and Practices, 2nd Edition,* Prentice Hall, United States of America

- Day, R. A. (2001), Net Pressure Analysis of Cantilever Sheet Pile Walls, Géotechnique, 47, (2), 231-245

- Ergun, U. (2008), *Deep Excavations,* Department of Civil Engineering, Middle East Technical University, Ankara, Turkey

- Eurpoean Norm (BS EN 1997-1:2004), *Eurocode 7: Geotechnical Design – Part 1: General Rules*, European Committee for Standardization, Brussels

- Hayta, Ö. (2005), *Finite Element Analysis of Tieback Wall Using Plaxis, A Case Study,* Boğaziçi University, Istanbul

- King, G. J. W. (1995), *Analysis of Cantilever Sheet Pile Walls in Cohesionless Soil,* (ASCE) 0733-9410 (1995)121:9 (629) (7 pages), American Society of Civil Engineers, USA

- Larkela, A. (2008), *Modeling of a Pile Group Under Static Lateral Loading,* Master's Thesis, Helsinki University of Technology

- Orr, T. L. L. (2009), *New Irish Geotechnical Standards and Selection of Characteristic Parameter Values,* Geotechnical Society of Ireland, Trinity College, Dublin

- Osmanoğlu, D. (2007), *Analysis of Soil Improvement and Soil Stability for Tunnel Construction by Using Plaxis Software and Finite Elements Method*, Master's Thesis, Istanbul Technical University, Istanbul

- Özberk, B. S. (2009), *Investigation of the Deformations in Anchor Supported Deep Excavations*, Master's Thesis, Yıldız Technical University, Istanbul

- Pappin, J., Endicott, J. & Clark, J., *Deep Excavation in Hong Kong, Design and Construction Control,* Hong Kong University of Science and Technology, Hong Kong

- Potts, D. M. L., Zdravkovic (1999), *Finite Element Analysis in Geotechnical Engineering, Theory*, Thomas Telford Publishing, London, United Kingdom

- Powrie, W. (1996*), Limit Equilibrium Analysis of Embedded Retaining Walls,* Géotechnique, 46, (4), 709-723, University of Southampton

- Powrie, W. (2004), *Soil Mechanics; Concepts and Applications,* Spon Press, New York

- Powrie, W., Gaba, A. R., Simpson, B., Beadman, D. R. (2003), *CIRIA C580, Embedded Retaining Walls – Guidance for Economic Design,* Construction Industry Research and Information Association, London

- Schweiger, H. F. (2005), *Application of FEM to ULS Design (Eurocodes) in Surface and Near Surface Geotechnical Structures*, 11th Int. Conf. Computer Methods and Advances in Geomechanics, Bologna

- Sigström, D., Persson, H. (2010), *Staged Excavation in Soft Clay Supported by a Cantilever Sheet Pile Wall -Numerical Analysis & Field Measurements of the Effect of Using a Wailing Beam,* Master's Thesis, Chalmers University of Technology, Göteborg, Sweden

- Smith, C., *Practical Application of Geotechnical Limit Analysis in Limit State Design,* The University of Sheffield, United Kingdom

- Smith, G. N. & Smith, I. G. N. (1998), *Elements of Soil Mechanics, Seventh Edition,* Blackwell Science Ltd., Oxford, United Kingdom

- Smith, I. G. N. & Abebe, A*., Pile Foundation Design: A Student Guide,* School of the Built Environment, Napier University, Edinburgh

- State of California Department of Transportation (1995), *California Trenching and Shoring Manual*, California

- United States Army Corps of Engineers (1994), *Engineering and Design, Design of Sheet Pile Walls,* Department of the Army U. S. Army Corps of Engineers, Washington, DC

- United States Department of Transportation (1984), *U.S.S. Steel Sheet Piling Design Manual,* U. S. Department of Transportation

- Verruijt, A. (2010), *Soil Mechanics,* Delft University of Technology

"For every complex problem, there is a solution that is simple, neat, and wrong."

- H. L. Mencken

APPENDIX A

GRAPHS OBTAINED FROM ANALYSIS RESULTS
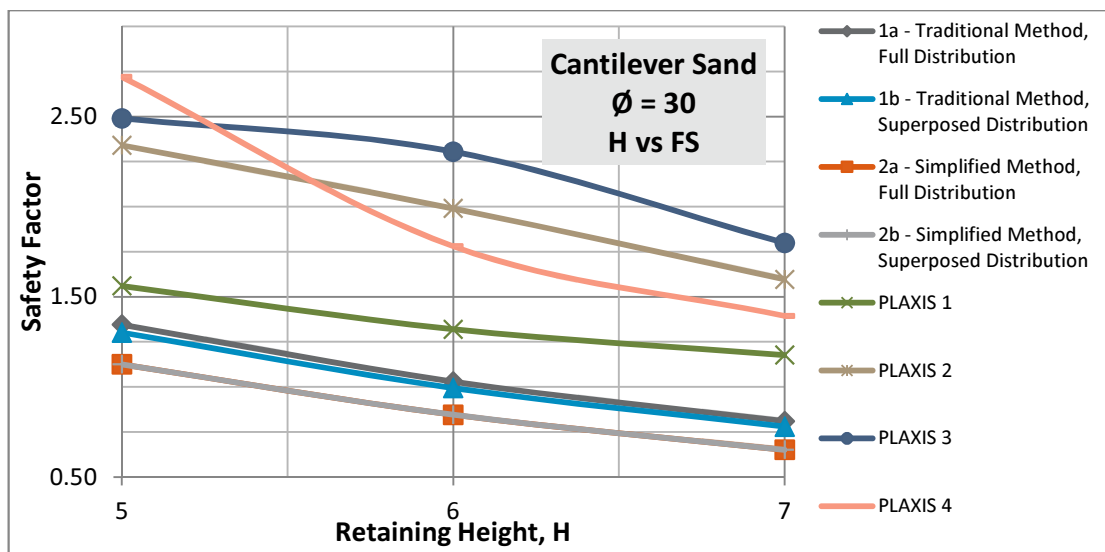
Figure A. 1; Cantilever wall retaining sand, ϕ=30 H vs FS graph
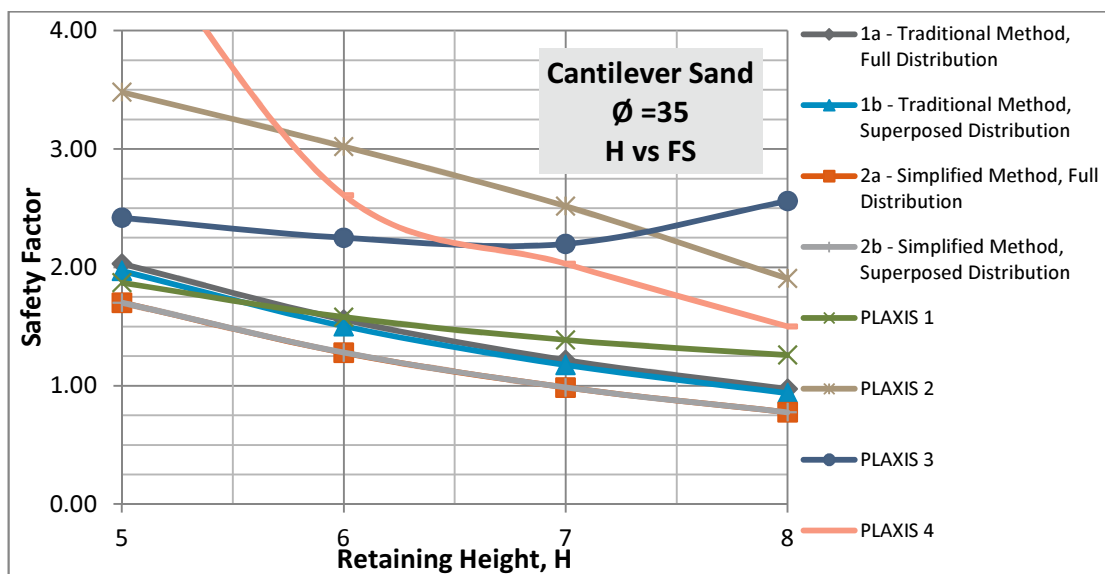
Figure A. 2; Cantilever wall retaining sand, ϕ=35 H vs FS graph
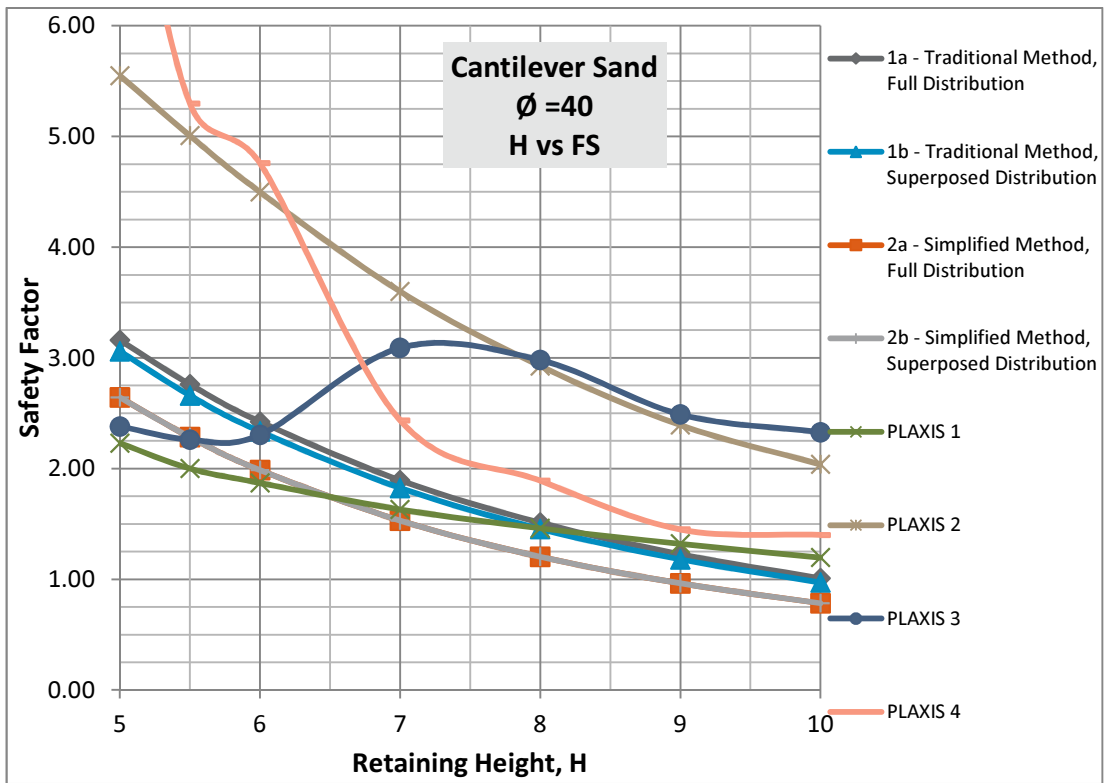
Figure A. 3; Cantilever wall retaining sand, ϕ=40, H vs FS graph
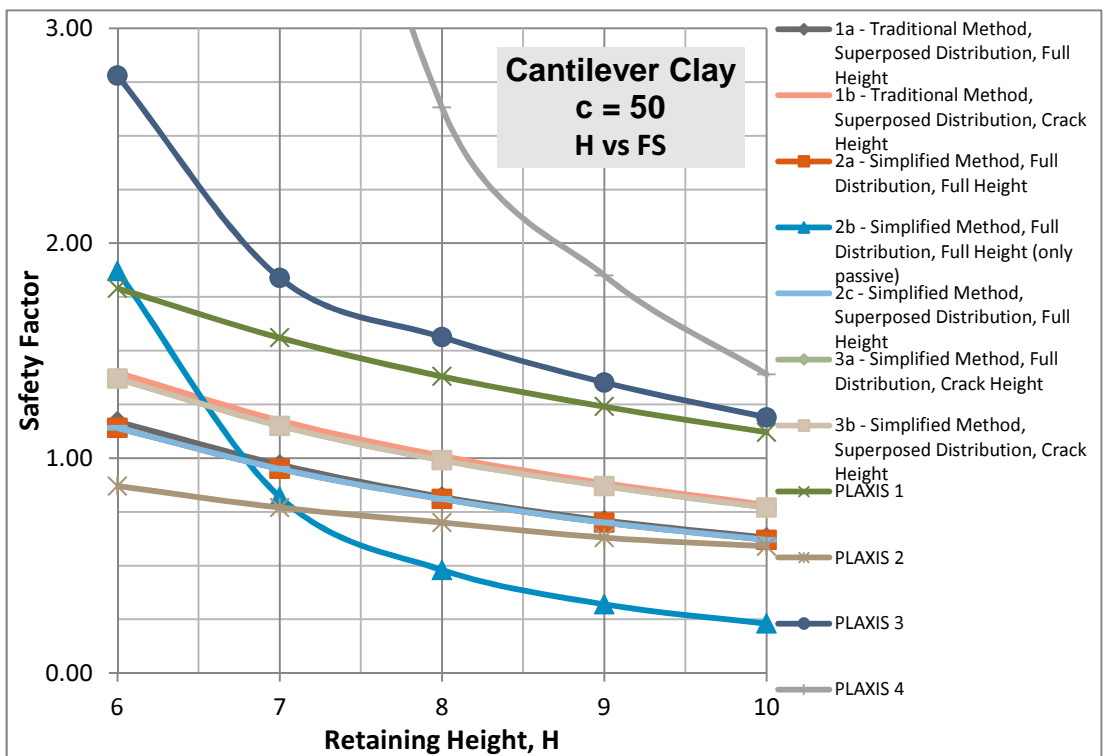
Figure A. 4; Cantilever wall retaining undrained clay, c=50kPa, H vs FS graph
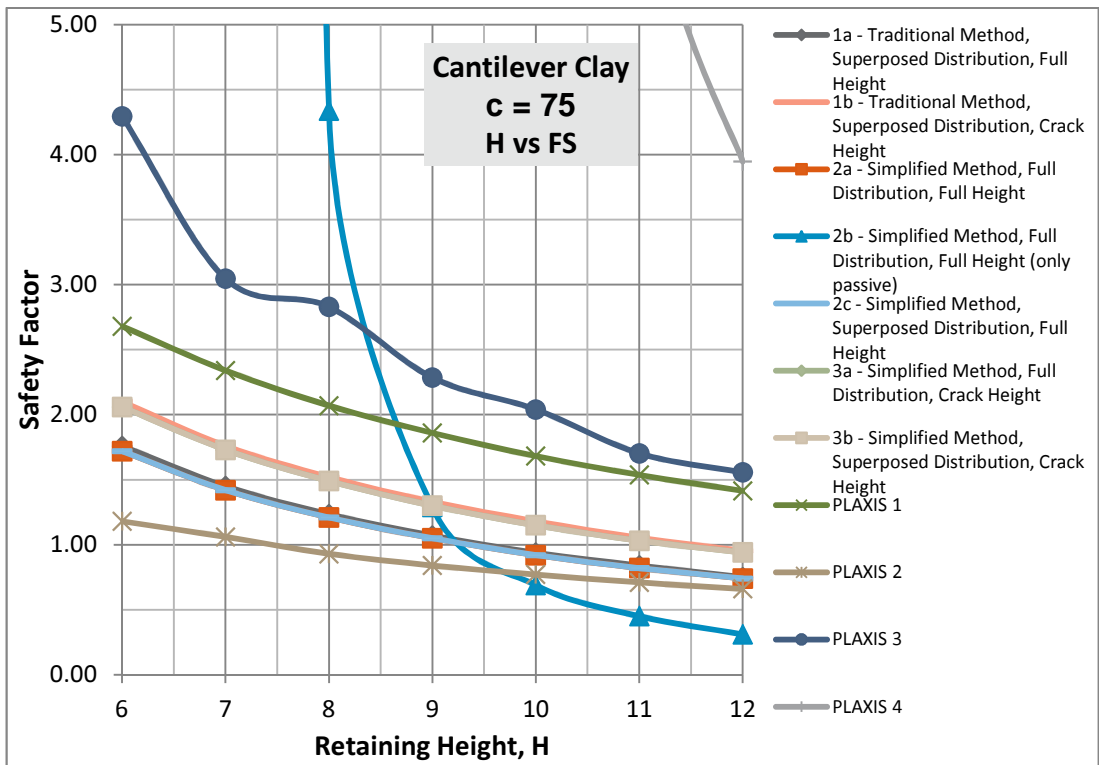
Figure A. 5; Cantilever wall retaining undrained clay, c=75kPa H vs FS graph
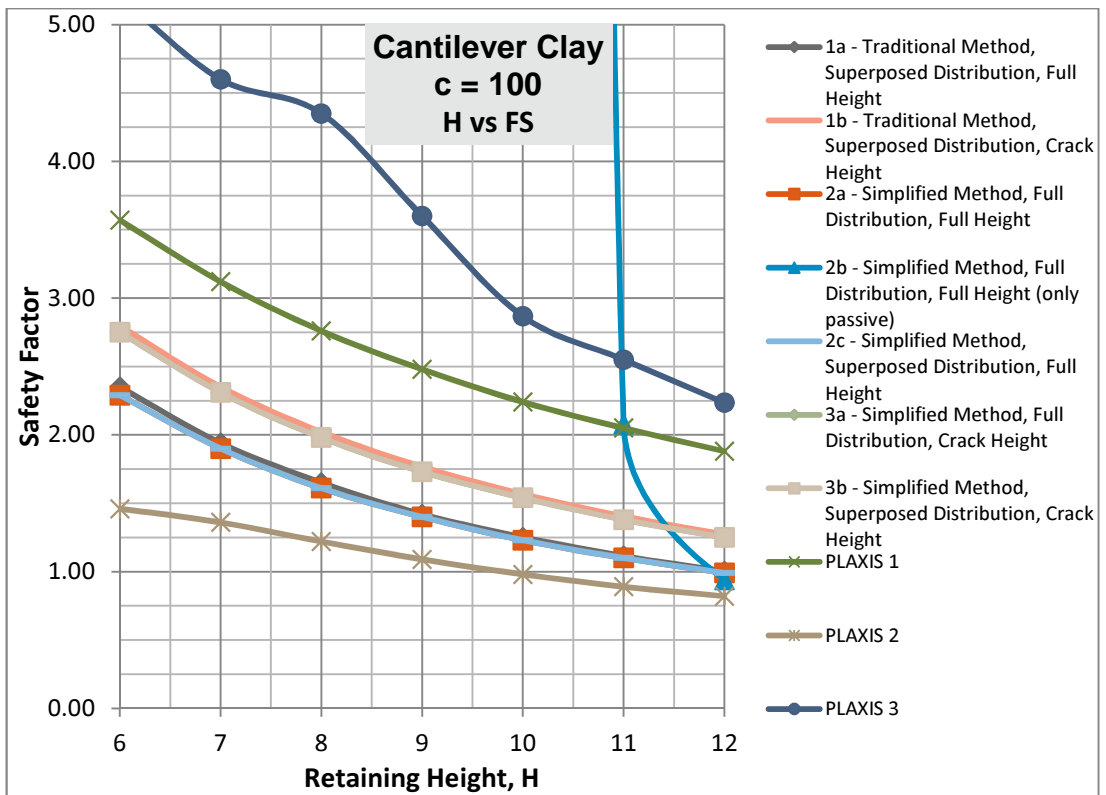
Figure A. 6; Cantilever wall retaining undrained clay, c=100kPa H vs FS graph

109
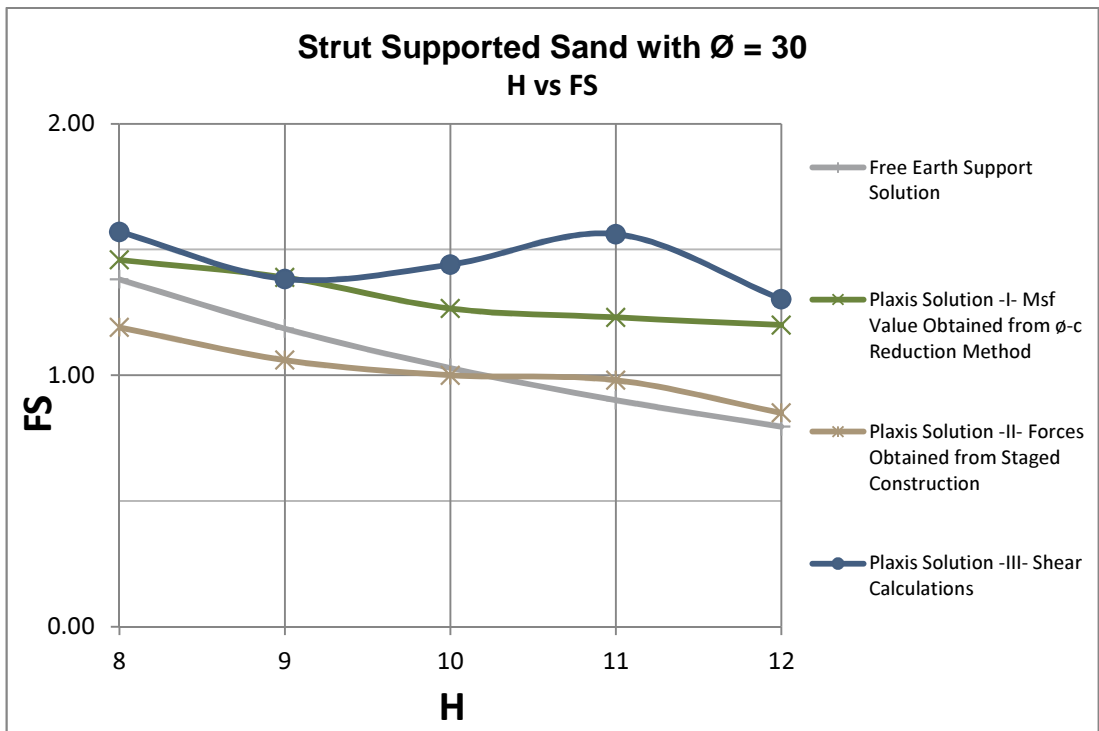
Figure A. 7; Strut supported wall retaining sand, ϕ=30 H vs FS graph
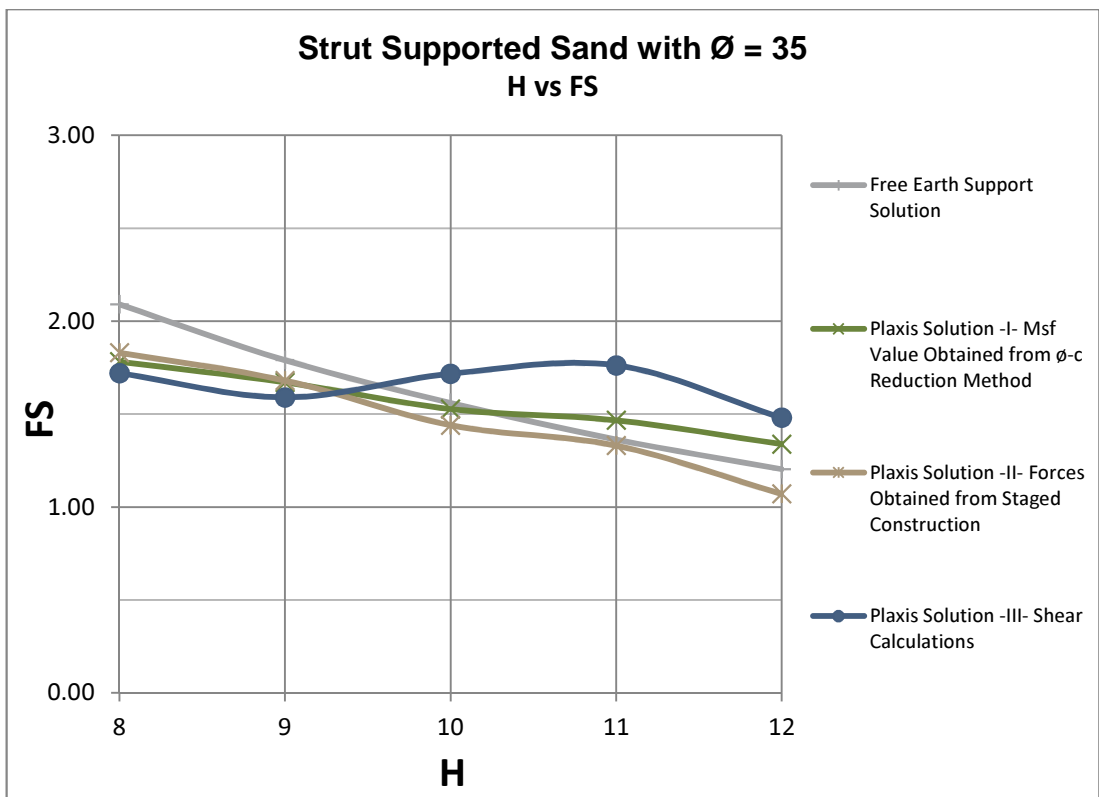
Figure A. 8; Strut supported wall retaining sand, ϕ=35 H vs FS graph

110
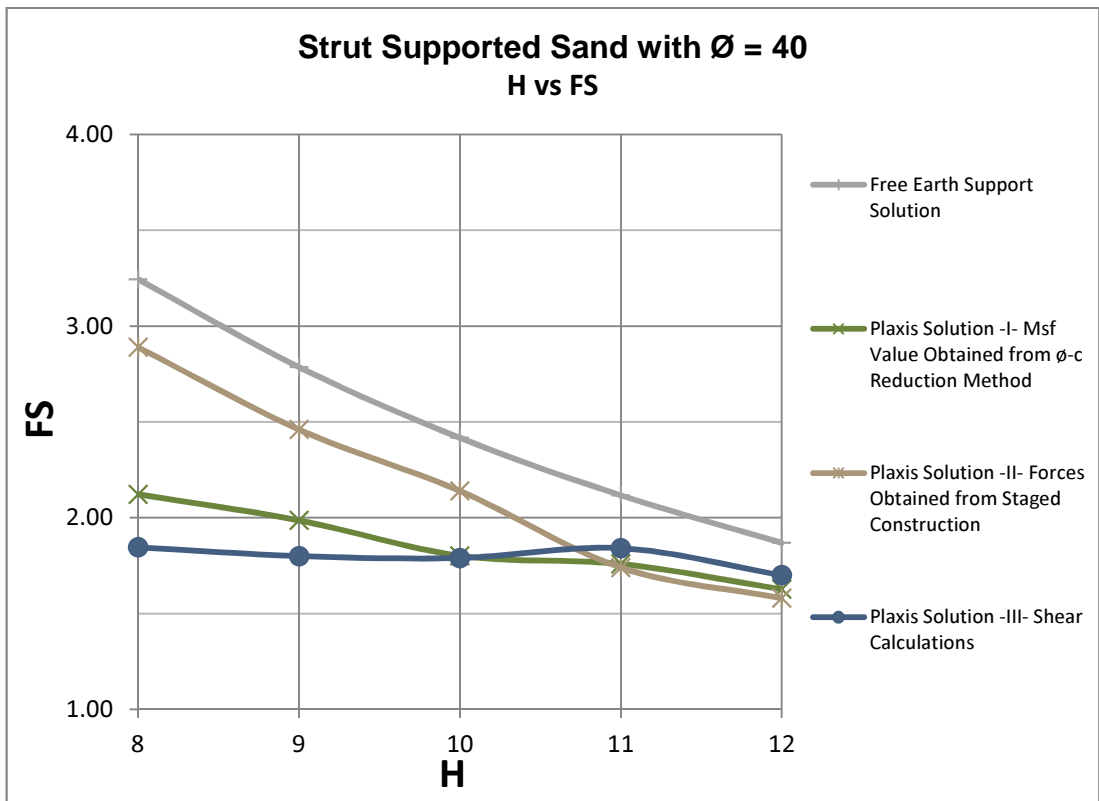
Figure A. 9; Strut supported wall retaining sand, ϕ=40 H vs FS graph
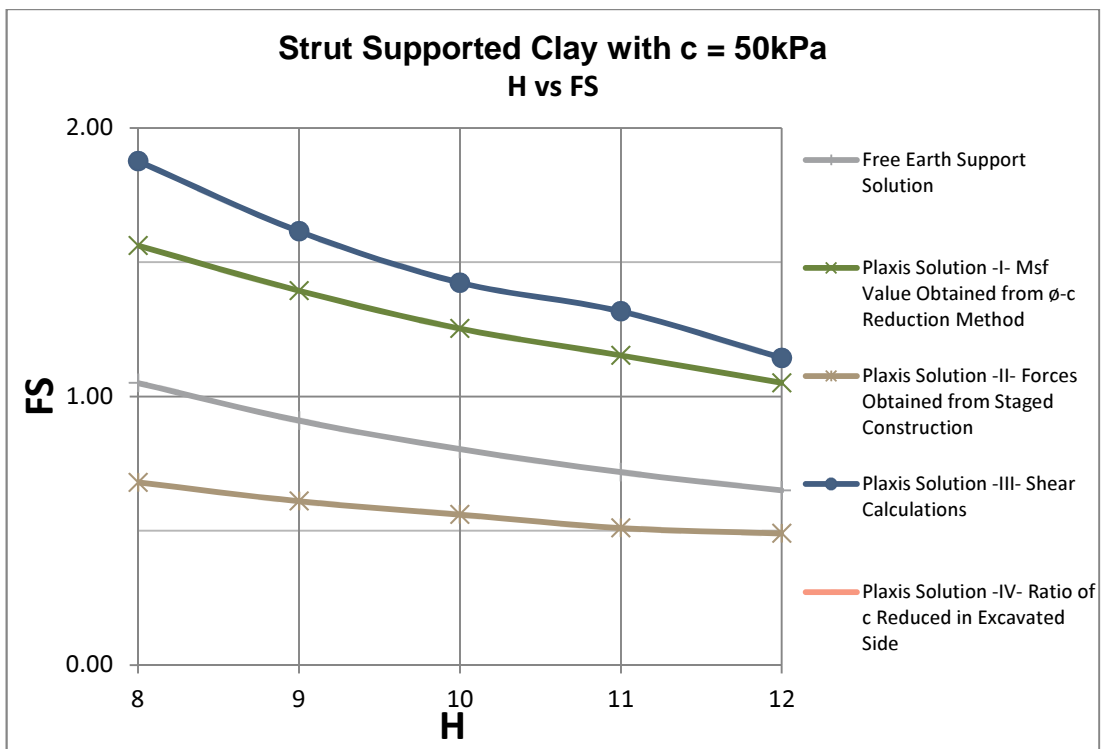
Figure A. 10; Strut supported wall retaining undrained clay, c=50kPa H vs FS graph
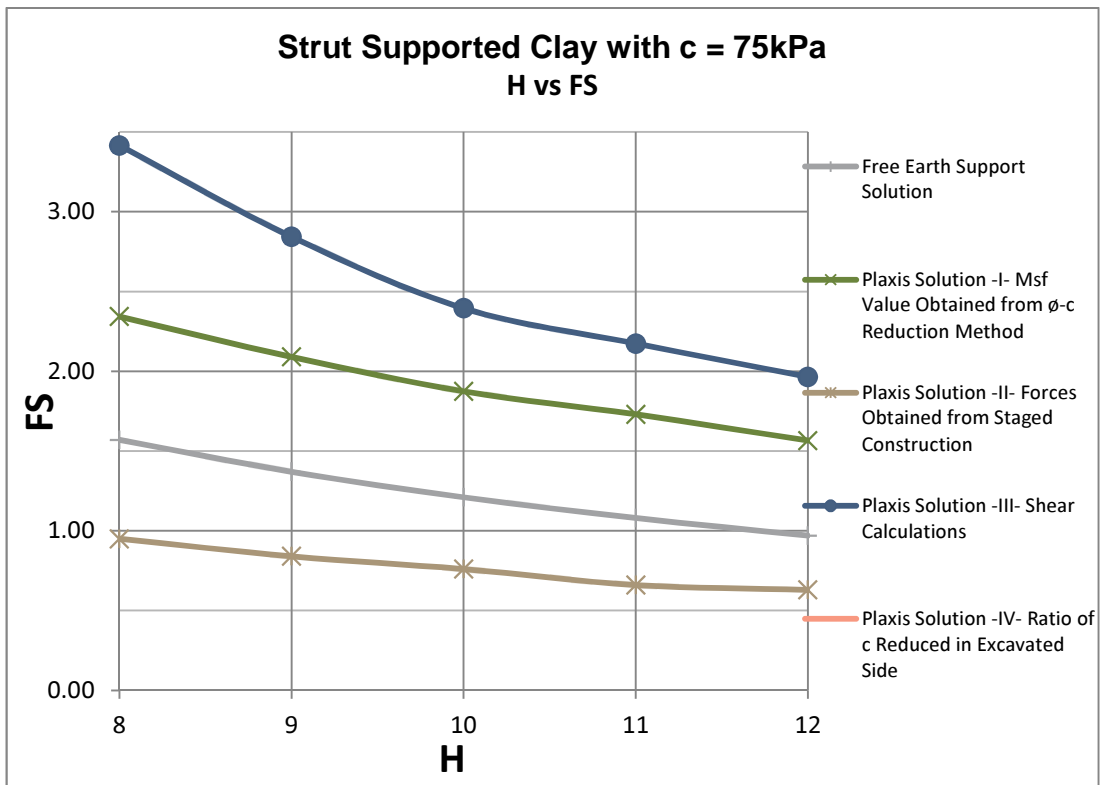
Figure A. 11; Strut supported wall retaining undrained clay c=75kPa H vs FS graph
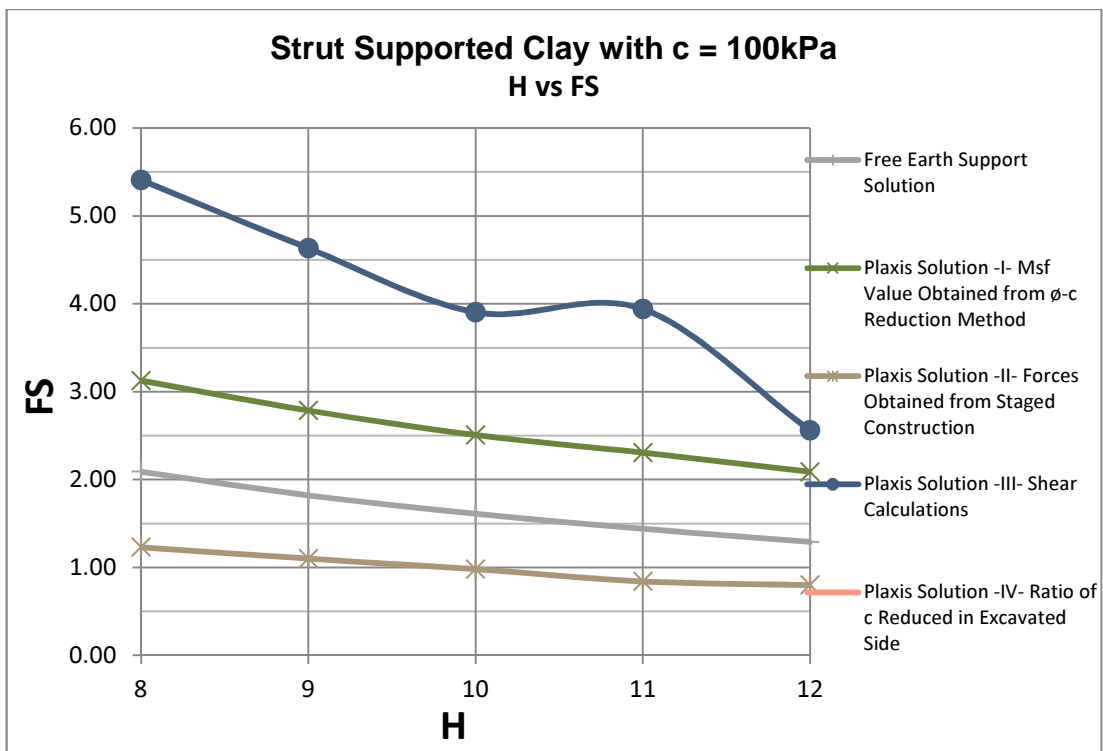
Figure A. 12; Strut supported wall retaining undrained clay c=100kPa H vs FS graph
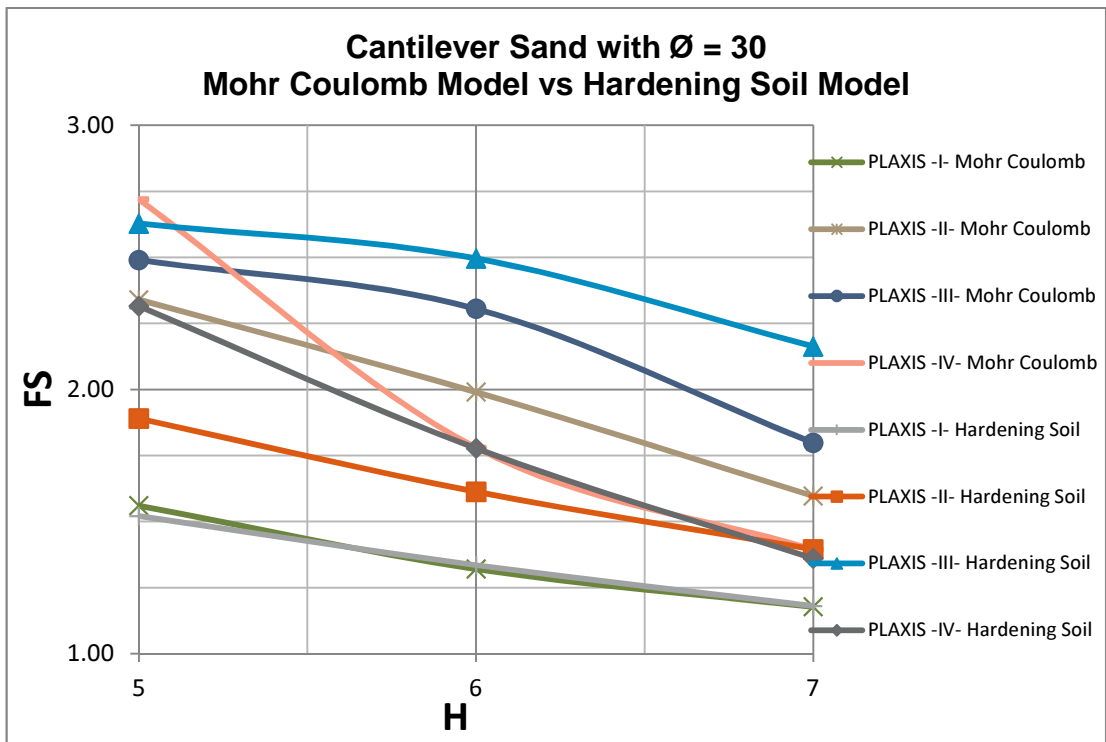
Figure A. 13; Cantilever wall retaining sand φ=30 Mohr Coulomb vs hardening soil model comparison
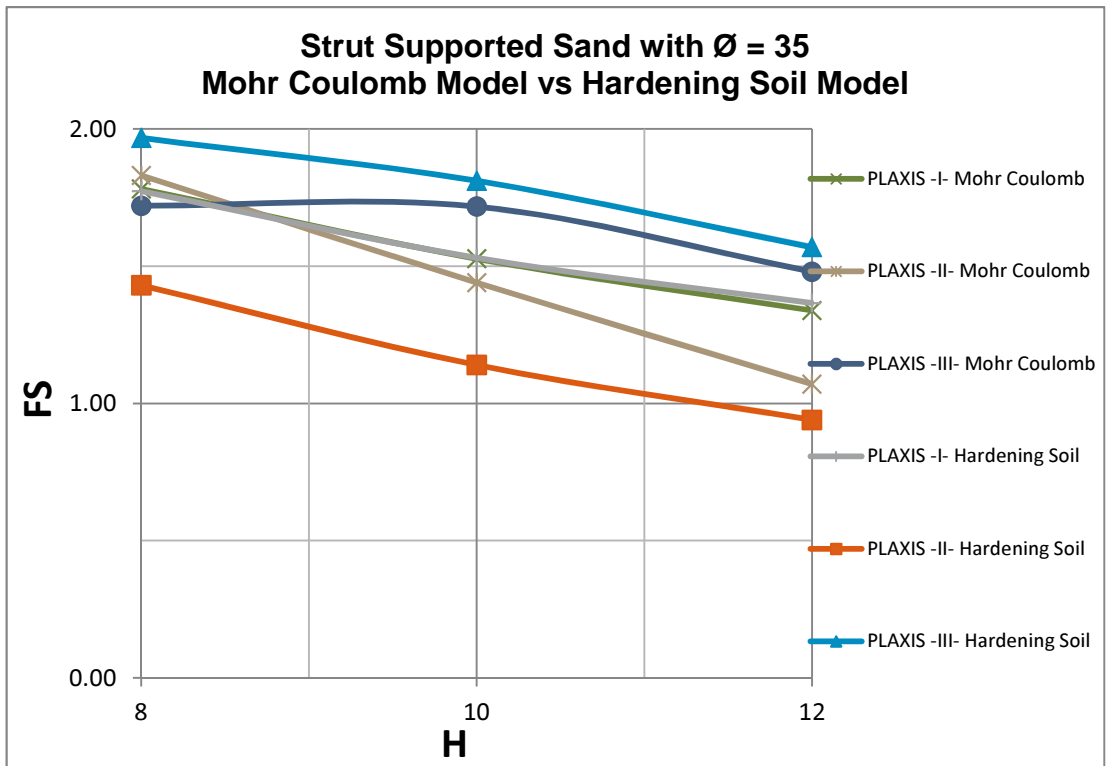
Figure A. 14; Strut supported wall retaining sand φ=35 Mohr Coulomb vs hardening soil model comparison
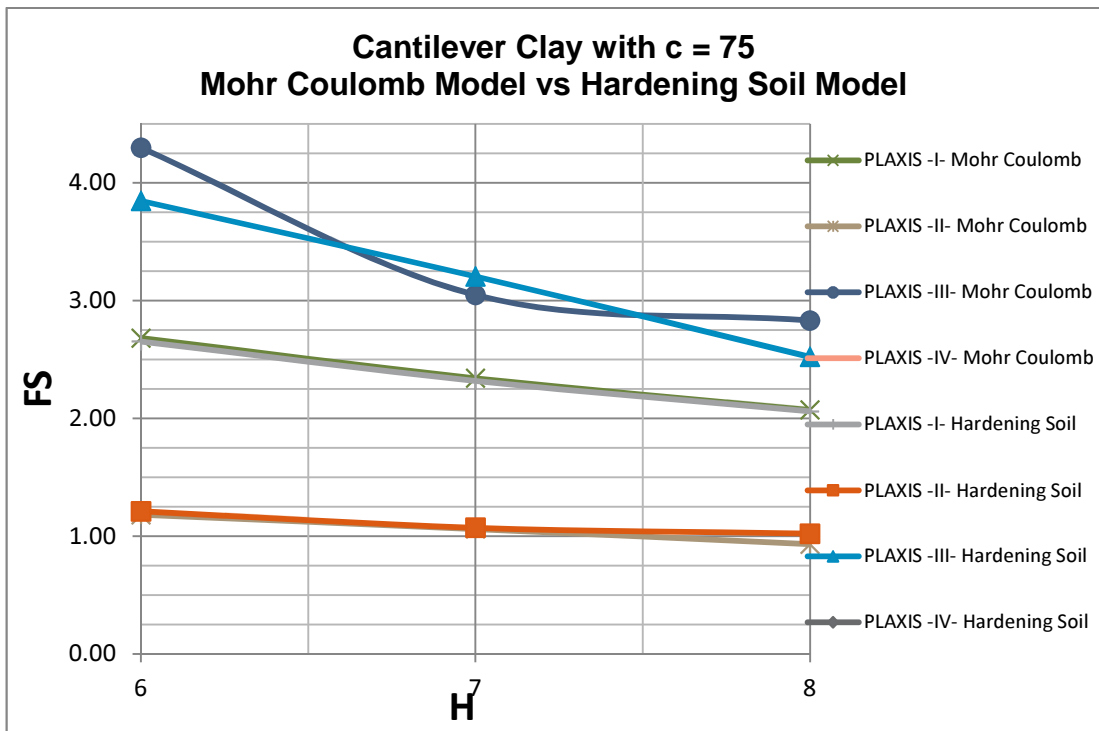
Figure A. 15; Cantilever wall retaining undrained clay c=75kPa Mohr Coulomb vs hardening soil model comparison
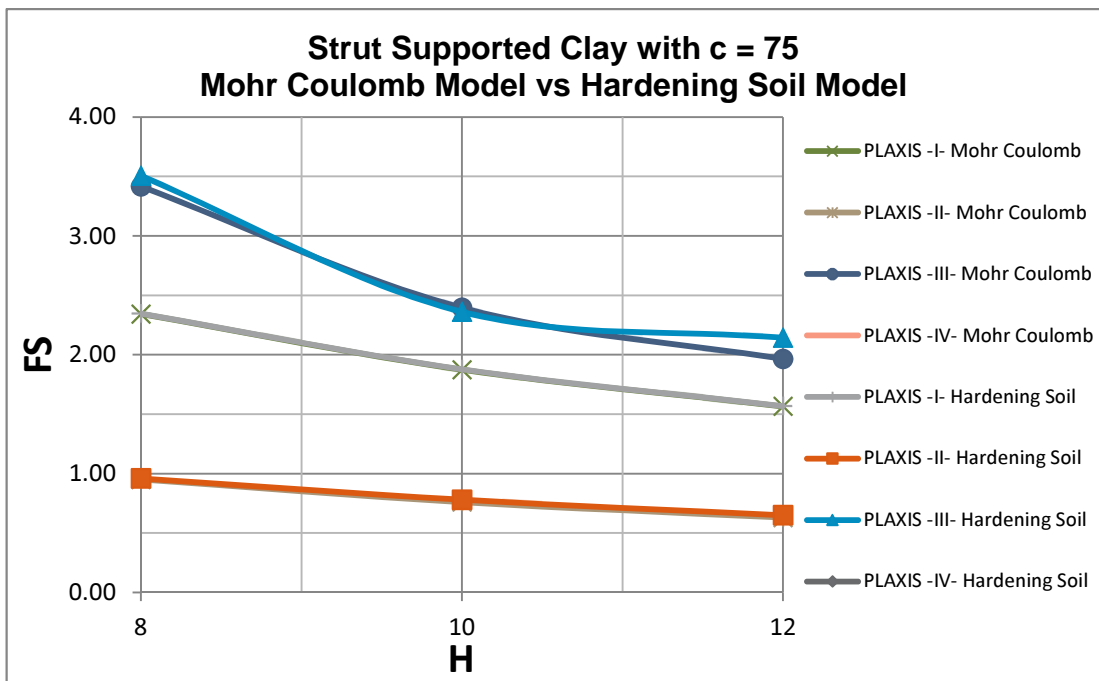
Figure A. 16; Strut supported wall retaining undrained clay c=75kPa Mohr Coulomb vs hardening soil model comparison

APPENDIX B

LATERAL EARTH PRESSURE DIAGRAMS

1a - Traditional Method with Full Pressure Distribution
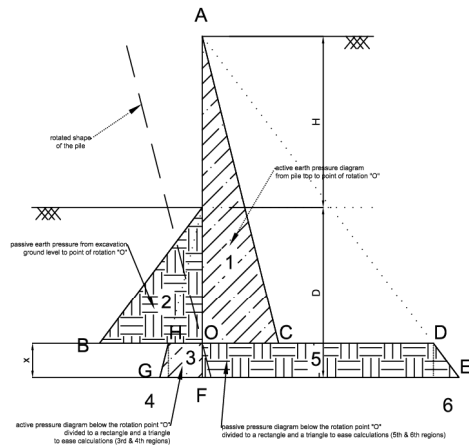
1b - Traditional Method with Full Pressure Distribution
(California Trenching & Shoring Manual)
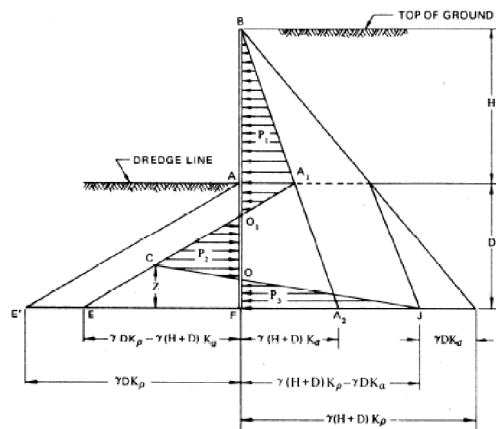
2a - Simplified Method With Full Pressure Distribution
(California Trenching & Shoring Manual)

2b - Simplified Method with Superimposed Pressure Distribution
(Ryner, 2001)

Figure B. 1; Lateral earth pressure diagrams of cantilever walls retaining sand
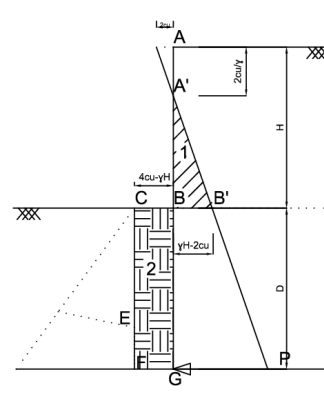
Figure B. 2; Lateral earth pressure diagrams of cantilever walls retaining undrained clay

Sand with One Level Strut Pressure Diagram,
Free Earth Support Method
(U.S. Army Corps of Engineers)
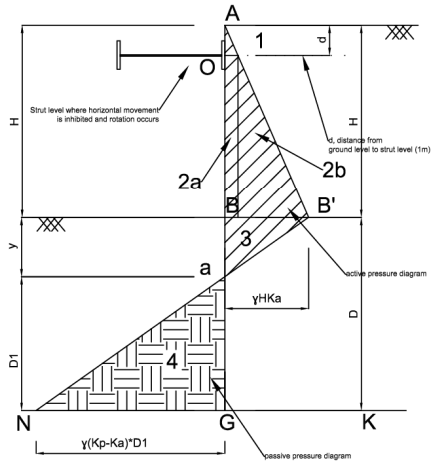
Clay with One Level Strut Pressure Diagram,
Free Earth Support Method
(USS Steel Sheet Piling Design Manual)
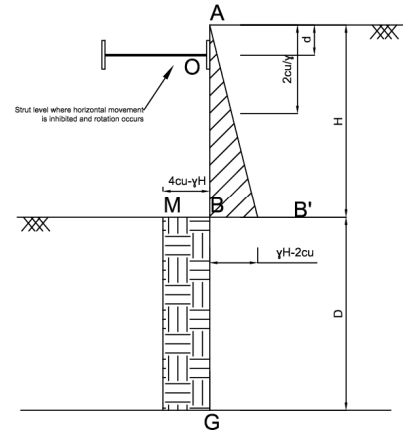
Figure B. 3; Lateral earth pressure diagrams of strut supported walls

APPENDIX C

SELECTED REGRESSION ANALYSIS GRAPHS
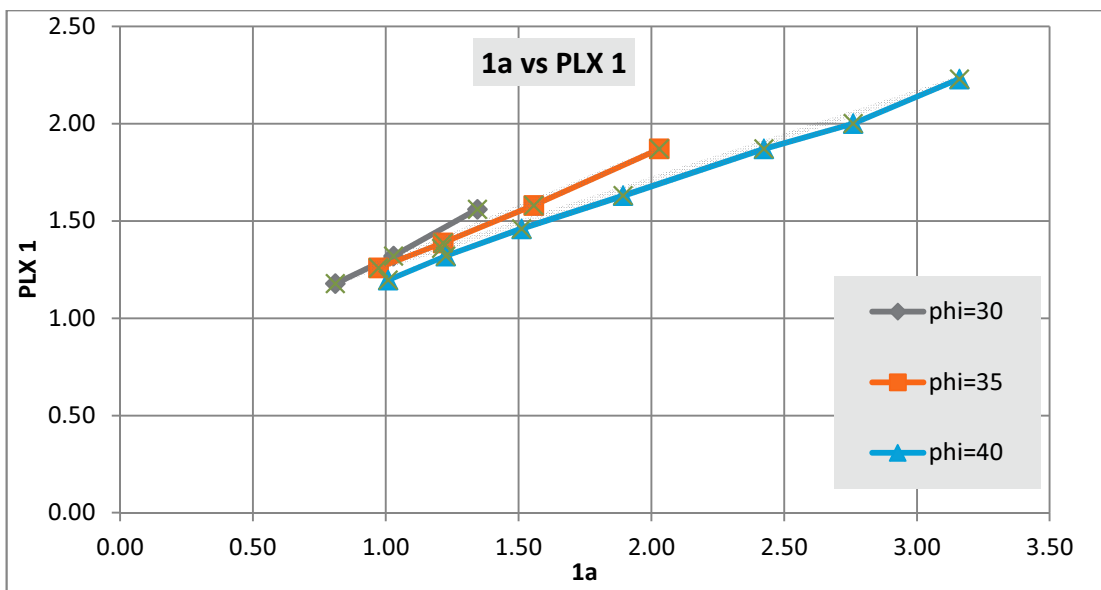
Figure C. 1; Cantilever wall retaining sand, FS $_{LE\,1a}$ vs FS $_{PLX1}$
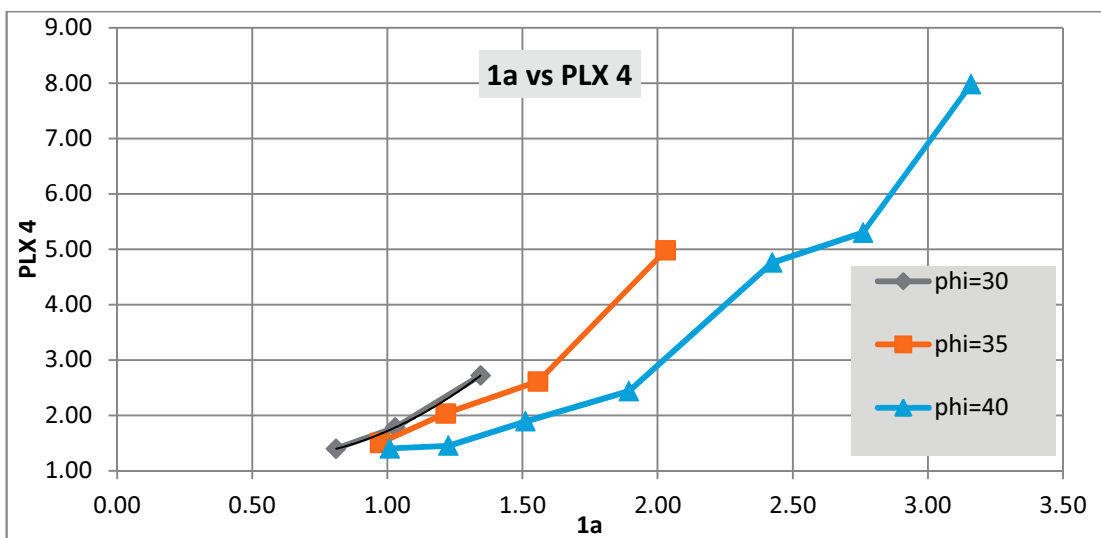
Figure C. 2; Cantilever wall retaining sand, FS $_{LE\,1a}$ vs FS $_{PLX4}$
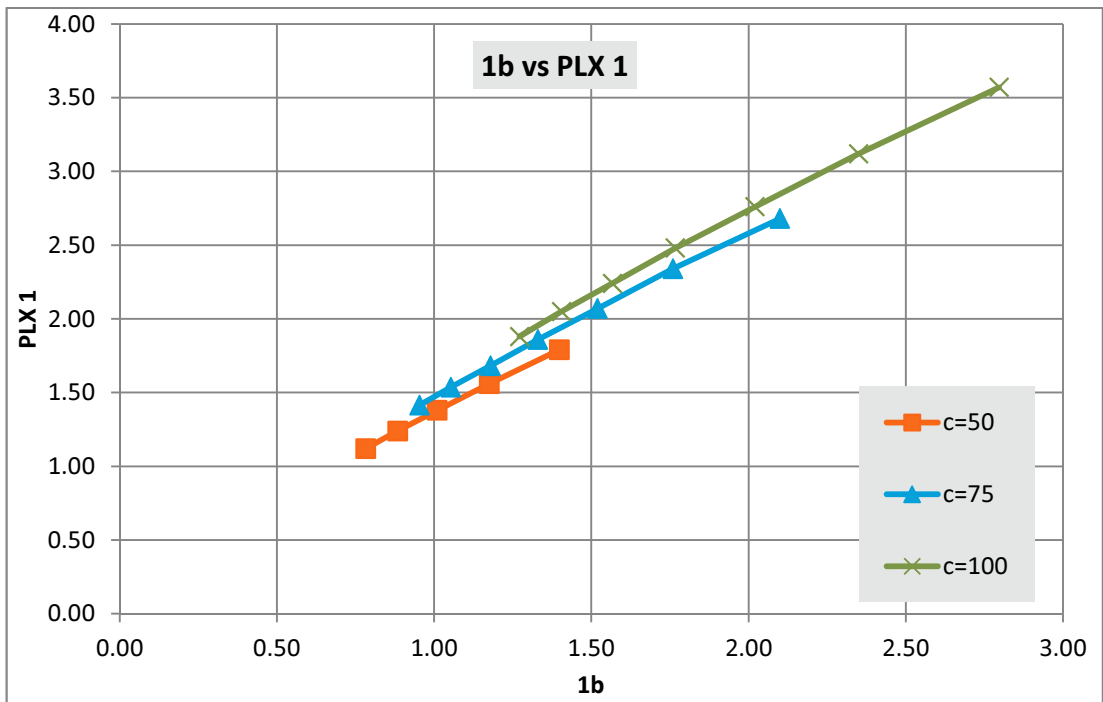
Figure C. 3; Cantilever wall retaining undrained clay, FS $_{LE\ 1b}$ vs FS $_{PLX1}$
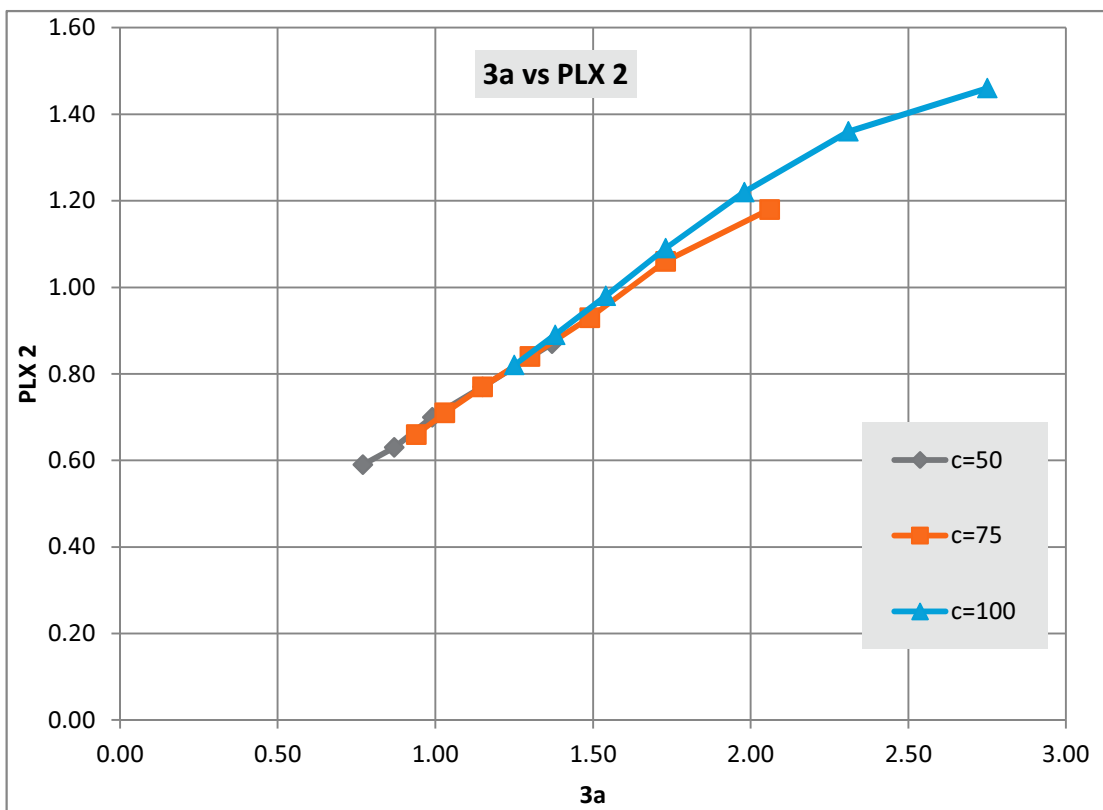
Figure C. 4; Cantilever wall retaining undrained clay, FS $_{LE\ 3a}$ vs FS $_{PLX2}$
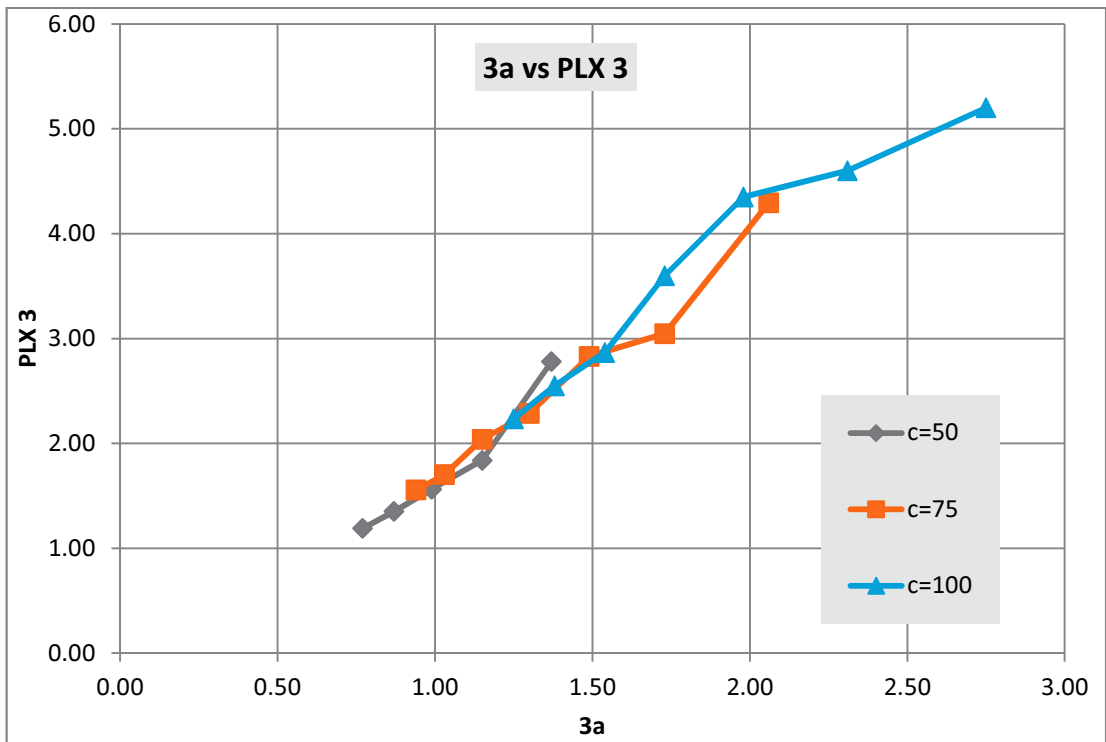
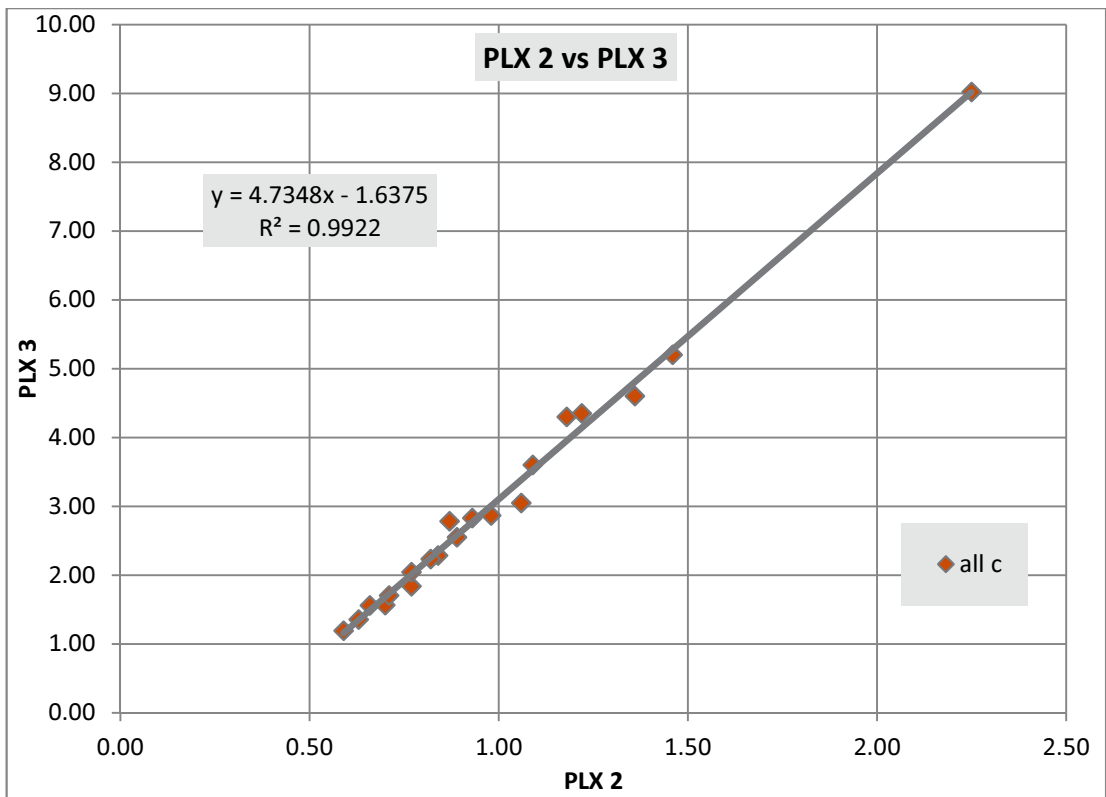Figure C. 5; Cantilever wall retaining undrained clay, FS $_{LE\ 3a}$ vs FS $_{PLX3}$

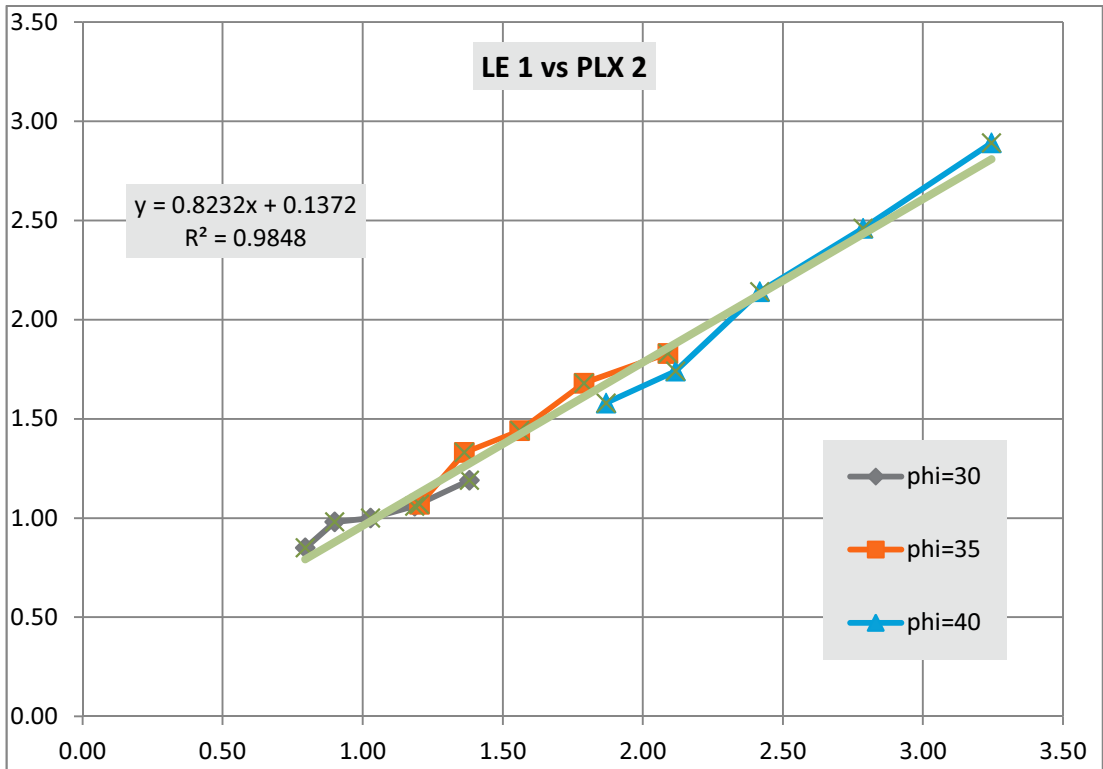Figure C. 6; Cantilever wall retaining undrained clay, FS $_{PLX2}$ vs FS $_{PLX3}$

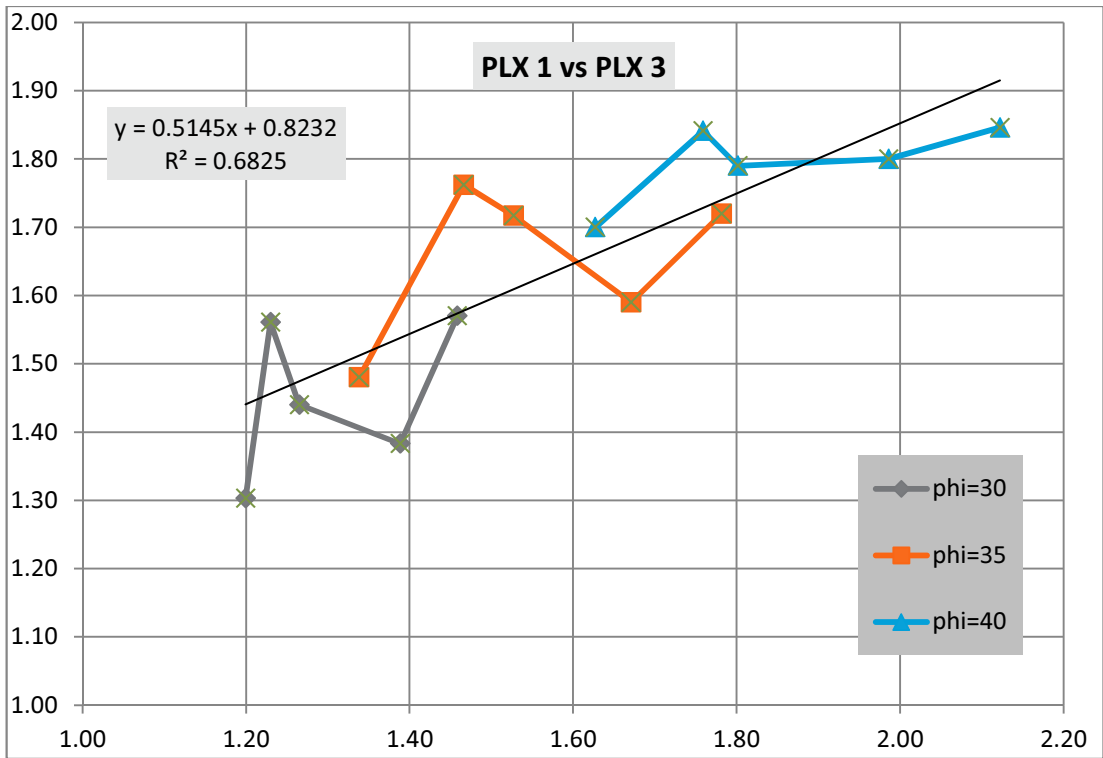Figure C. 7; Strut supported wall retaining sand, FS $_{LE\,1}$ vs FS $_{PLX2}$

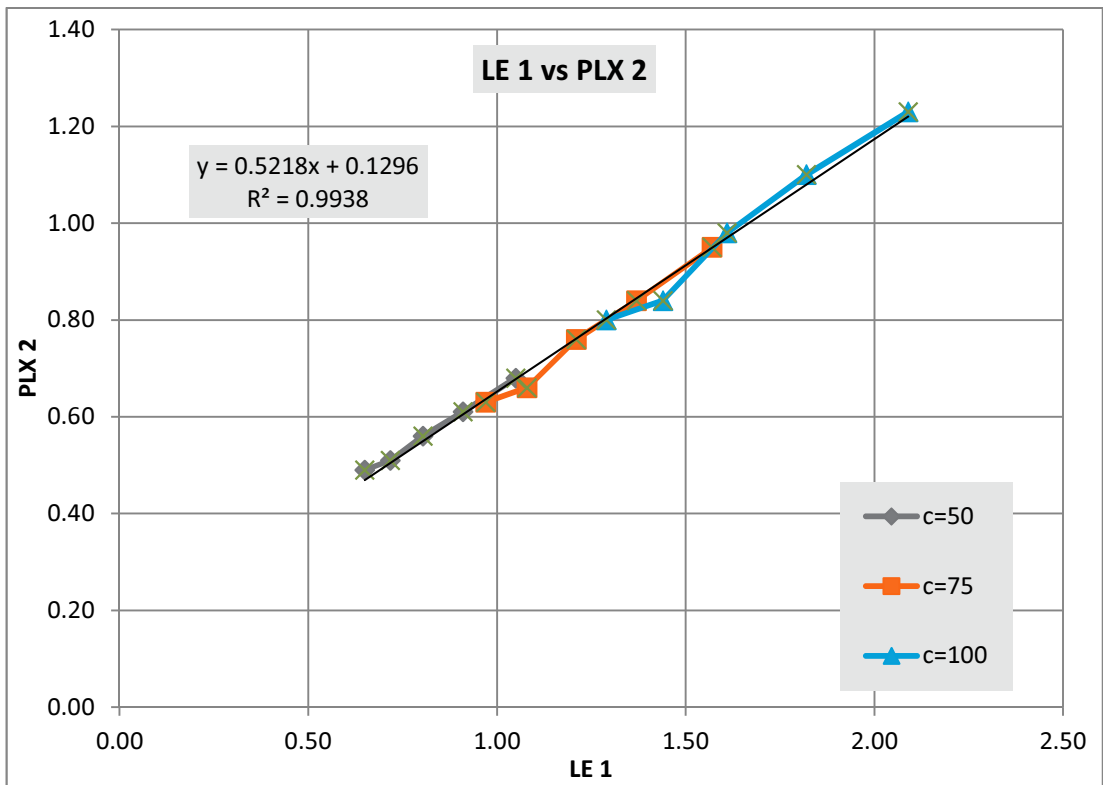Figure C. 8; Strut supported wall retaining sand, FS $_{PLX1}$ vs FS $_{PLX3}$

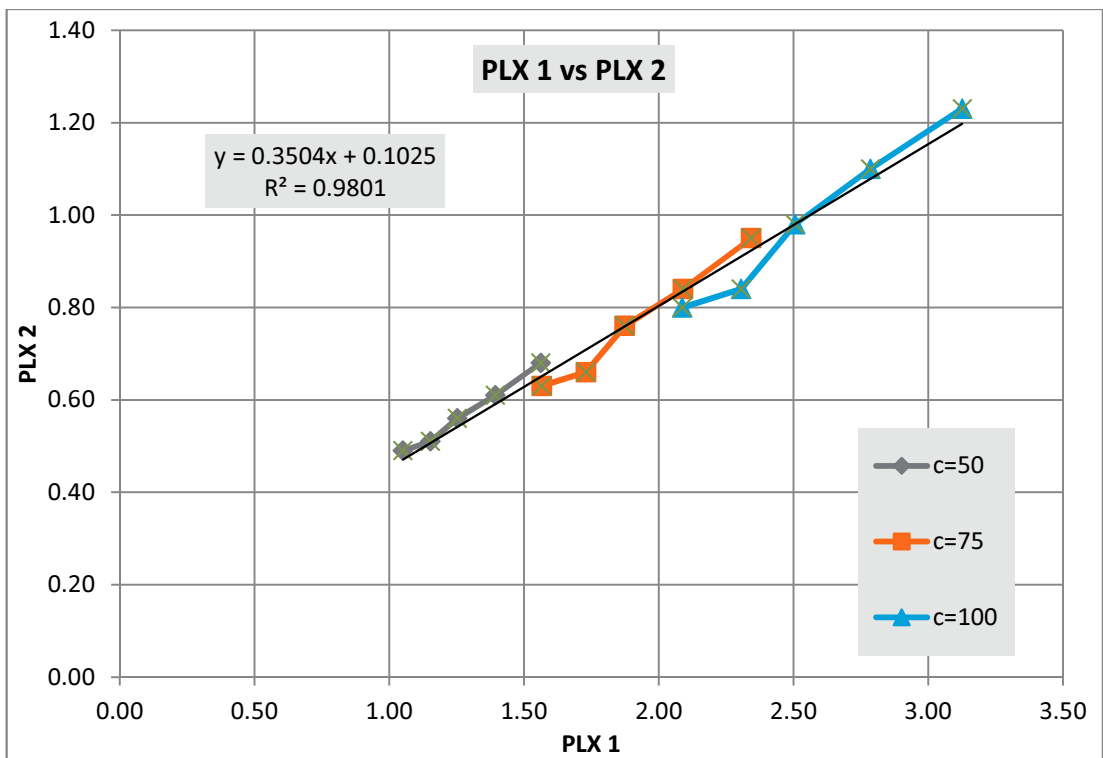Figure C. 9; Strut supported wall retaining undrained clay, FS $_{PLX1}$ vs FS $_{PLX2}$

Figure C. 10; Strut supported wall retaining undrained clay, FS $_{PLX1}$ vs FS $_{PLX2}$